

## INFORMATION TO USERS

This manuscript has been reproduced from the microfilm master. UMI films the text directly from the original or copy submitted. Thus, some thesis and dissertation copies are in typewriter face, while others may be from any type of computer printer.

The quality of this reproduction is dependent upon the quality of the copy submitted. Broken or indistinct print, colored or poor quality illustrations and photographs, print bleedthrough, substandard margins, and improper alignment can adversely affect reproduction.

In the unlikely event that the author did not send UMI a complete manuscript and there are missing pages, these will be noted. Also, if unauthorized copyright material had to be removed, a note will indicate the deletion.

Oversize materials (e.g., maps, drawings, charts) are reproduced by sectioning the original, beginning at the upper left-hand corner and continuing from left to right in equal sections with small overlaps.

ProQuest Information and Learning  
300 North Zeeb Road, Ann Arbor, MI 48106-1346 USA  
800-521-0600

UMI<sup>®</sup>



## **NOTE TO USERS**

**Page(s) not included in the original manuscript are unavailable from the author or university. The manuscript was microfilmed as received.**

**58**

**This reproduction is the best copy available.**

**UMI<sup>®</sup>**



**University of Alberta**

**Structural History of the Humber Arm Allochthon in the Corner Brook Area,  
Western Newfoundland**

by

**James C. Bradley**



**A thesis submitted to the Faculty of Graduate Studies and Research in partial  
fulfillment of the**

**requirements for the degree of Master of Science**

**Department of Earth and Atmospheric Sciences**

**Edmonton, Alberta  
Fall 2005**



Library and  
Archives Canada

Bibliothèque et  
Archives Canada

0-494-09130-4

Published Heritage  
Branch

Direction du  
Patrimoine de l'édition

395 Wellington Street  
Ottawa ON K1A 0N4  
Canada

395, rue Wellington  
Ottawa ON K1A 0N4  
Canada

*Your file* *Voire référence*

*ISBN:*

*Our file* *Notre référence*

*ISBN:*

**NOTICE:**

The author has granted a non-exclusive license allowing Library and Archives Canada to reproduce, publish, archive, preserve, conserve, communicate to the public by telecommunication or on the Internet, loan, distribute and sell theses worldwide, for commercial or non-commercial purposes, in microform, paper, electronic and/or any other formats.

The author retains copyright ownership and moral rights in this thesis. Neither the thesis nor substantial extracts from it may be printed or otherwise reproduced without the author's permission.

**AVIS:**

L'auteur a accordé une licence non exclusive permettant à la Bibliothèque et Archives Canada de reproduire, publier, archiver, sauvegarder, conserver, transmettre au public par télécommunication ou par l'Internet, prêter, distribuer et vendre des thèses partout dans le monde, à des fins commerciales ou autres, sur support microforme, papier, électronique et/ou autres formats.

L'auteur conserve la propriété du droit d'auteur et des droits moraux qui protège cette thèse. Ni la thèse ni des extraits substantiels de celle-ci ne doivent être imprimés ou autrement reproduits sans son autorisation.

---

In compliance with the Canadian Privacy Act some supporting forms may have been removed from this thesis.

Conformément à la loi canadienne sur la protection de la vie privée, quelques formulaires secondaires ont été enlevés de cette thèse.

While these forms may be included in the document page count, their removal does not represent any loss of content from the thesis.

Bien que ces formulaires aient inclus dans la pagination, il n'y aura aucun contenu manquant.

  
**Canada**

## **Abstract**

The Humber Arm Allochthon was initially emplaced in the external Humber Zone of the Appalachian Orogen during the Early Ordovician, Taconian Orogeny, and further emplaced during the Devonian, Acadian Orogeny.

Sedimentary units were deposited during Precambrian rifting, Cambrian-Ordovician passive margin development, and at the onset of foreland basin deposition (the Curling, Northern Head, Pinchgut Lake, Goose Tickle and Table Head Groups) were mapped at 1:50,000 scale.

Five generations of structures are recognized based on overprinting criteria, mapping, and Argon isotopic dating techniques. D1 structures are dominantly west-directed thrusts and folds. D2 structures are east-directed folds and thrusts, age 455 Ma, and are interpreted as a loading event responsible for the creation of foreland accommodation space in the Late Ordovician. D3 structures are ductile and brittle normal sense faults, age 440 Ma, and associated with an Early Silurian foreland unconformity. D4 structures are open folds with steeply dipping axial surfaces. D5 is manifested as shallowly dipping east-west crenulation lineations.

## **Acknowledgements**

Contained in this thesis is the support of many individuals to whom I owe thanks. In particular I would like to thank my supervisor, Dr John Waldron, who provided a project, support, guidance, expertise, funding, and endless revisions. His excitement at finding and understanding new things, both in the field and in the office, are contagious and I've benefited greatly from that influence.

Thanks to my field assistants/ co-workers from three field seasons. Countless confused hours were spent waist deep in water in pouring rain with Amber Henry. Shane Krepekevich and Jocelyn Tanton both put in their time trudging, and "quadding" up brooks, logging roads, and moose paths. Lastly, Ken Wallace kept me safe even if the Newfoundland Constabulary weren't convinced.

Funding for this project was provided by the NATMAP Geological Bridges in Eastern Canada project by a Geological Society of Canada Contribution as well as a NSERC discovery grant to Dr. John Waldron. Thanks to the Department of EAS at the university of Alberta for providing TA funding the duration of my thesis.

Thanks to the residence at Sir Wilfred Grenfell College; it is a very fine field camp location and everyone there helped in many ways. Thanks to Glen Pennel, who provided dory rides, boating expertise, equipment storage, and the odd lobster.

Thanks to Dr. Peter Reynolds and Keith Taylor for running the argon geochronology analyses and providing their expertise. Thanks to Valery Companytsev who provided GIS support at the University of Alberta.

Dr. Tom Calon, Dr. Elliot Burden, and Chris Buchanan provided many hours of discussions and field comparisons. Thanks to Peter Cawood and Ian Knight for, unfortunately, few conversations but many hours spent poring over their maps.

Finally, thanks to Jennifer for sticking with me through this whole procedure and providing her continual support.

# Table of Contents

Chapter 1: Introduction .....	1
1.1 Regional Geology .....	1
1.2 Methods.....	3
1.3 Regional Stratigraphic Framework.....	5
1.3.1 Passive Margin .....	5
1.3.2 Foreland Basins .....	5
1.3.3 Humber Arm Allochthon .....	7
1.4 Structure .....	8
1.5 Objective .....	10
Chapter 2: Map Units and Stratigraphy.....	16
2.1 Humber Arm Supergroup.....	16
2.1.1 Stratigraphic History of the Humber Arm Supergroup .....	16
2.1.2 Curling Group.....	17
2.1.2.1 Summerside formation .....	18
2.1.2.2 Irishtown formation.....	19
2.1.2.3 Blow Me Down Brook formation .....	22
2.1.3 Northern Head Group .....	23
2.1.3.2 Middle Arm Point formation .....	24
2.2 Shelf and related units.....	25
2.2.1 Shelf Succession .....	25
2.2.2 Table Head Group.....	26
2.3 Pinchgut Lake and Goose Tickle Groups .....	27

2.3.1	The Pinchgut Lake Group .....	27
2.3.2	Goose Tickle Group.....	29
2.3.2.1	Eagle Island formation .....	30
2.3.2.2	Whale Back formation.....	31
2.4	The Bay of Islands Complex and igneous units.....	32
2.5	Mélange and broken formation .....	33
2.6	Stratigraphic successions .....	33
<b>Chapter 3: Structure of the Corner Brook Map Area.....</b>		<b>39</b>
3.1	Introduction .....	39
3.2	Syn-sedimentary structures .....	39
3.2.1	Outcrop.....	39
3.3	D1 Structures.....	41
3.3.1	Outcrop Scale Structures.....	42
3.3.2	Map-Scale D1 structures.....	45
3.4	D2 Structures.....	47
3.4.1	Outcrop-scale structures.....	47
3.4.2	Thin-section scale structures .....	49
3.4.3	Map Scale.....	50
3.4.4	Overprinting .....	51
3.5	Late Structures.....	52
3.5.1	Crenulation Fabrics.....	52
3.5.2	Folds and cleavage.....	53
3.5.3	Shear zones and faults.....	53

3.5.4 Overprinting .....	57
Chapter 4: Isotopic Dating.....	78
4.1 Introduction .....	78
4.1.1 Argon/ Argon method.....	78
4.1.2 Rhenium Osmium.....	79
4.2 Argon dating methodology .....	80
4.3 Sample descriptions & results .....	81
4.3.1 DW170A .....	82
4.3.2 DW065A .....	83
4.3.3 JA083A .....	84
4.3.4 JA083B.....	85
4.3.5 JA023B.....	86
4.3.6 JA082A .....	87
4.3.7 GQ112A .....	88
4.3.8 HV002A .....	89
4.3.9 HV123A .....	90
4.3.10 HV134A .....	92
4.3.11 HY056A .....	93
4.3.12 HQ092A .....	94
4.4 Conclusion.....	95
Chapter 5: Discussion.....	101
5.1 Introduction .....	101
5.2 Basement, Rift, and clastic passive margin units .....	102

5.2.1	Clastic units in the Humber Arm Allochthon.....	102
5.2.1.1	Summerside formation .....	102
5.2.1.2	Irishtown formation.....	103
5.2.1.3	Blow Me Down Brook formation .....	104
5.2.1.4	Relationships between the Curling Group units .....	105
5.3	Carbonate passive margin .....	107
5.3.1	Northern Head Group .....	107
5.3.2	Pinchgut Lake Group .....	108
5.4	Taconian Orogeny .....	109
5.4.1	Taconian Stratigraphy .....	109
5.4.2	Taconian Deformation .....	111
5.4.2.1	Fluids and fabric development.....	111
5.4.2.2	Volcanic blocks within mélangé.....	112
5.5	Post Taconian History.....	113
5.5.1	D2 deformation.....	113
5.5.1.1	Variability of D2 structures .....	114
5.5.1.2	Isotopic Dates .....	116
5.5.1.3	Margin/ foreland basin significance.....	116
5.5.2	D3 .....	117
5.5.3	D4 and D5 structures .....	118
Chapter 6: Conclusions .....		128
6.1	Geologic History.....	128
6.2	Future research .....	129

<b>References .....</b>	<b>132</b>
<b>Appendix A.....</b>	<b>142</b>

## List of Figures

- Figure 1.1** Map of the lithotectonic zones of the Canadian Maritime Appalachians.
- Figure 1.2** Map of the Humber Arm Allochthon showing major lithologic units.
- Figure 1.3** The Corner Brook map area, showing major tectonic boundaries and important locations.
- Figure 1.4** History of the stratigraphic nomenclature in the Bay of Islands Area.
- Figure 1.5** Stratigraphic columns showing the relationship between the successions of the Humber Arm Allochthon.
- Figure 2.1** Contrasting measured stratigraphic sections of the Irishtown formation.
- Figure 2.2** Ternary diagrams showing the distribution of point counting results from the three formations of the Curling Group.
- Figure 2.3** Measured section of Blow Me Down Brook formation.
- Figure 2.4** Comparison between the carbonate slope units from different structural positions.
- Figure 3.1** Illustrations showing soft sediment deformation.
- Figure 3.2** Outcrop scale F1 isoclinal folds.
- Figure 3.3** Thin section photos showing mica crystals in bed parallel orientations.
- Figure 3.4** F1 west-vergent fold with axial planar S1 dissolution cleavage and cross-cutting S2 slaty cleavage.
- Figure 3.5** Thin section photos of pressure solution cleavage and the relationship to S2 oriented micas.
- Figure 3.6** Stereonets showing the distribution of F2 fold axes measurements on curved fold hinges.
- Figure 3.7** Sigma structure showing reverse kinematics along the S2 foliation.
- Figure 3.8** Thin section photos showing tectonic mica and chlorite development parallel to S2.
- Figure 3.9** Thin section photos showing S2 fabric characterized by a discrete crenulation.
- Figure 3.10** Equal area stereoplots showing the change in orientation of S2 foliation and L2 lineation across the map area.
- Figure 3.11** Map and cross section of the Watsons Brook Area.
- Figure 3.12** Map and cross section of the Feeder Brook Area.
- Figure 3.13** Equal area stereoplots of bedding and S1 fabrics across the map area.
- Figure 3.14** Equal area stereoplots of L3 to L5 lineations, and a population of S2 poles folded gently about an F4 fold.
- Figure 3.15** Photo and sketch of S3 shear surfaces deforming L2 lineations showing normal-sense kinematics.
- Figure 3.16** A late east-dipping fault in Little Feeder Brook and the associated kink fold.
- Figure 3.17** Kinematic and dynamic analyses of faults measured at location O.
- Figure 3.18** Block diagrams showing a possible sequence of events responsible for the map pattern near location U.
- Figure 3.19** D3 normal-sense, ductile structures overprinted by D5 slickenfibres.
- Figure 4.1** Argon samples location map.
- Figure 4.2** Spectra acquired from argon analyses

- Figure 4.3** Summary of the argon analyses results.
- Figure 5.1** Models showing the potential for facies differences as a result of sedimentary architecture versus thrust stack transportation.
- Figure 5.2** Model for structural stacking of units before and after D1 deformation.
- Figure 5.3** Graben and rift model for the deposition of the Summerside and the Blow Me Down Brook formations.
- Figure 5.4** Time-Stratigraphic chart of the Early to middle Paleozoic Laurentian margin.
- Figure 5.5** Map of the major thrust sheets and subdivision between the east and west Humber Arm Allochthon.
- Figure 5.6** Diagram to show F1 folds preserved from transposition into S2, in the HW above the Crow Hill fault.
- Figure 5.7** Model of the structural history of the Humber Arm Allochthon
- Figure 5.8** Seismic line showing deformed Late Ordovician to Devonian sediments indicate that later thrusting occurred along the roof thrust of the triangle zone during the Devonian.

## **Inserts**

**Insert 1**      Geology of the Corner Brook area: stations and bedding orientations

**Insert 2**      Geology of the Corner Brook area: structural features

**Insert 3**      Natural Scale Structural Cross Sections V-Z of the Corner Brook Area

# Chapter 1: Introduction

The Humber Zone of the Western Newfoundland Appalachians records the eastern margin of the post-Grenville Laurentian Continent from the late Proterozoic to the middle Paleozoic. During this time period, the eastern Laurentian margin was constructed through a cycle of rift and passive margin processes and then destroyed through a series of orogenic events. These orogenic events are attributed to the collision of the eastern Laurentian margin with other continental crustal plates. The history of orogenesis is recorded in the stratigraphy of the Paleozoic foreland basins, which are primarily observed in seismic profiles beneath the Gulf of St. Lawrence, as well as an isotopic record, preserved in the igneous and highly metamorphosed units towards the hinterland of the orogen. However, there is a disparity in the timing of the events recorded by the two datasets. The Bay of Islands area is geographically positioned between the foreland basins and the hinterland. This study examines the structural history of the Bay of Islands area in an effort to reconcile differences between the timing of orogenic events recorded in the foreland and hinterland of the Paleozoic Appalachian Orogen. Structural and stratigraphic features of several generations of structures represented in the Bay of Islands area will be incorporated using fieldwork-based techniques, analyses of orientation data, and Argon-Argon dating.

## 1.1 Regional Geology

*The Paleozoic Appalachian Orogen* extends through the Maritime Provinces of Canada, Southern Quebec, and the eastern United States. It has been divided into five zones, named the Humber, Dunnage, Gander Avalon, and Meguma (figure 1.1, Williams

1979). The Humber Zone consists of the deformed continental margin of Laurentia and the Dunnage Zone represents the oceanic floor of the Iapetus Ocean. The Gander, Avalon, and Meguma Zones represent terranes accreted during orogeny (Williams 1995).

***The Humber Zone*** is the furthest westward of the Appalachian zones. Its western boundary represents the limit of Appalachian orogenic deformation (e.g. Williams 1995). The Humber zone is subdivided into internal and external parts (figure 1.1), which are differentiated based on grade of metamorphism. The external Humber Zone, which contains the area of this study, experienced little or no metamorphism, in contrast with high-grade metamorphism and intense deformation found in the internal zone. The external zone includes Grenville crystalline basement, Paleozoic carbonate and siliciclastic sedimentary rocks and allochthonous structural slices. The external Humber Zone records the Cambrian-Ordovician margin of the Laurentian continent from construction to destruction. The external zone includes rocks originally deposited in both on- and off-shelf locations.

***The Humber Arm Allochthon*** is composed of structurally transported sedimentary rocks and ophiolitic igneous rocks, which overlie the Laurentian margin carbonates (Fig 1.2). The sedimentary rocks within the allochthon include both clastic and carbonate facies and constitute the Humber Arm Supergroup (Williams 1975). Tectonically above the Humber Arm Supergroup and still within the allochthon are igneous rocks of the Bay of Islands Complex. This complex contains the igneous rocks of the Skinner Cove Formation and a complete ophiolite sequence in the Blow Me Down Mountain massif (Suhr and Cawood 1993). The most current map published on the Bay

of Islands area of the Humber Arm Allochthon is at a scale of 1:250,000 (Williams and Cawood, 1989).

## **1.2 Methods**

Mapping was carried out over three summer field seasons of two months each from July 2001 to August 2003, on the 1:50,000 topographic sheets 12 A/13, 12 B/16, 12 G/1, and 12 H/4. Most of the map area (figure 1.3) was accessible within a single day traverse from highways or logging roads. A new network of logging roads was in the process of being built and conveniently increased access inland and created outcrop. Access to the area was dominantly by four-wheel drive vehicle, although visits to type sections along the coast and on islands within the Bay of Islands were accomplished by boat.

Much of the previous work was restricted to the shores of the Humber Arm and the Bay of Islands, and within the city limits of Corner Brook, so mapping during 2001-2003 was mainly directed at inland exposures, in an effort to cover an entire 1:50,000 map sheet and to provide a three dimensional understanding of the structure within the allochthon. Inland exposure is very poor. Outcrops were found in brooks, in ditches along logging roads, and occasionally on hilltops formed by competent units in the area. Mapping during 2001 and 2002 was almost exclusively at 1:50,000 scale. During the 2004 season, detailed mapping was undertaken of two areas at a scale of 1:5,000 (figure 1.3, insert 1).

During all mapping, Global Positioning System (GPS) was used almost exclusively for locating observations and measurements within the map area. A complete set of air photos was collected to cover the area and was dominantly used for geological

interpretation. Measurements were taken using right hand rule (RHR) on planes and trend and plunge (TP) on linear data.

Over three field seasons ArcView 3.2, ArcGIS 8.1, and ArcGIS 8.2 were used in successive field seasons for geographic data management. Microsoft Excel was initially used for measurement and data recording. However, because of its superior interface with ArcGIS, Microsoft Access was used for entry and management of data collected in the field.

Data was compiled from several sources as Dr. John Waldron made available field data from several previous years of mapping. These archival data were in several formats: AutoCAD-based Fieldlog database format, Excel spreadsheets with either station numbering or UTM coordinates attached, and finally air photo overlays and associated notebook entries. Some of the earliest planar data assimilated into the database required conversion from 180° azimuth and quadrant notation into right hand rule before inclusion.

The age of deformation is largely unconstrained in this area. Therefore, in an effort to produce isotopic ages for structures within the Humber Arm Allochthon, samples were analyzed using the Argon-Argon isotopic dating method in collaboration with Dr. P. Reynolds (Dalhousie University). The Argon analyses were successful and the resulting dates provide useful constraints on the deformation history.

## **1.3 Regional Stratigraphic Framework**

### **1.3.1 Passive Margin**

On-shelf units in the Humber Zone include those deposited in rift, passive margin and foreland basin settings.

The Late Proterozoic to Early Cambrian Labrador Group was deposited directly on Grenville basement and represents clastic and minor carbonate deposition during rifting and early passive margin development (James et al 1988). Stratigraphically above the Labrador Group, *the carbonate shelf units*, in stratigraphic order, are the Port au Port and the St. George Groups. The Port Au Port Group spans the Middle to Upper Cambrian and represents a high-energy narrow carbonate platform (James et al 1988). The St. George Group is Lower to lower Middle Ordovician and represents a wide, low energy, rimmed platform (James et al 1988). Loading of the continental margin early in the Taconian orogeny resulted in a migrating fore-bulge, causing uplift, sub-aerial exposure, and erosion of the carbonate platform. The resulting feature is called the St. George unconformity and it marks the top of the St. George Group and the base of the Table Head Group. This is interpreted as the transition from passive margin to foreland basin accumulation (Williams and Hiscott 1987).

### **1.3.2 Foreland Basins**

Stratigraphically above the passive margin shelf units are three successions of *foreland basin units*. These units are, in stratigraphic order: first, the Table Head Group and Goose Tickle Group; second, the Long Point Group; and third the Clam Bank and Red Island Road Formations. The uppermost part of the Table Head Group is the only

one of these units that is present in the Corner Brook map area (figure 1.3) and it defines the eastern boundary of mapping. The Late Ordovician and younger foreland basin units are observed in outcrop on Port Au Port Peninsula (Quinn 1999) and they are observed in the roof of a triangle zone in offshore industry seismic lines (Stockmal and Waldron 1993, Waldron and Stockmal 1994, Waldron et al 1998).

The foreland basin units are critical in interpreting the structural history of the Laurentian margin as each succession is interpreted as the depositional response to an increase in accommodation space in the basin. Foreland basin accommodation space is dominantly a function of hinterland loading in the orogen. Therefore, the three separate foreland successions observed on the shelf are interpreted as the result of three loading events within the orogen to the east of the area in this study.

The base of the *Table Head Group*, the St. George unconformity (Knight et al 1991), is interpreted as the result of a migrating peripheral bulge, and is interpreted as the end of passive margin shelf deposition and the beginning of foreland basin deposition (Williams and Hiscott 1987).

*The Goose Tickle Group* (figure 1.4) is a dominantly clastic Ordovician unit overlying the Table Head Group in on-shelf depositional settings. However, the Goose Tickle Group also contains units within the Humber Arm Allochthon and near Pinchgut Lake. Quinn (1996) interpreted the Goose Tickle Group in autochthonous settings as a flysch deposited during foreland basin formation.

*The Long Point Group* is a thick foreland basin unit composed of the Lourdes, Winterhouse, and Misty Point Formations (Quinn et al 1999). The Lourdes Formation is carbonate dominated, and the subsequent two formations are clastic and interpreted as

easterly-derived. The Long Point Group has an approximate thickness of greater than 1 km and was deposited entirely during the Late Ordovician (Quinn et al 1999).

*The Clam Bank and Red Island Road Formations* are Latest Silurian to Devonian clastic flysch units associated with the Acadian Orogeny (Hibbard 1994). These formations are interpreted as the third foreland basin succession present on the margin of Laurentia and are separated from the Late Ordovician Long Point Group by a disconformity interpreted from the absence of Llandovery, Wenlock, and Ludlow sediments (Quinn et al 1999).

### **1.3.3 Humber Arm Allochthon**

The Humber Arm Allochthon is composed of transported rocks deposited in a deep-water environment (Stevens 1965). These rocks are time correlative to the Labrador, Port au Port, and St. George Groups, which are on-shelf units (Stevens 1970, James and Stevens 1986, James et al 1988, Botsford 1988). Some of the formations have been formally defined and others have not, due to their tectonized nature and limited outcrop. The sedimentary units involved in this study are the Northern Head Group, Curling Group, Pinchgut Lake Group, and portions of the Goose Tickle Group.

*The Curling Group* is the lowest stratigraphic unit in the map area (figure 1.3, insert 1, figure 1.4) and is composed of siliciclastic rocks (Stevens 1965). It includes three formations in the map area: the Summerside formation, the Irishtown formation, and the Blow Me Down Brook formation.

Botsford (1988) and Boyce et al. (1992) examined *the Northern Head Group*, a dominantly carbonate package that stratigraphically overlies the Curling Group (figure

1.4). The Northern Head Group is composed of the Cooks Brook and Middle Arm Point formations (figure 1.5).

*The Pinchgut Lake Group* (figure 1.4) is lithologically very similar to the Cooks Brook formation. It is found to the west of the platform units in structural slices of varying thickness (Knight, 1996b).

*The Goose Tickle Group*, as mentioned previously, is also represented in the allochthonous units (figure 1.4). In the map area, the Goose Tickle Group includes the Eagle Island formation and the Whale Back formation. The Whale Back overlies the Pinchgut Lake Group and the Eagle Island formation overlies the Northern Head Group (figure 1.4).

*The Bay of Islands Complex* contains the Blow Me Down Mountain massif and associated igneous units that exist in a position structurally above the sedimentary units of the allochthon. The Blow Me Down Mountain massif exists on the western edge of the map area (figure 1.3) and marks the boundary of mapping. Cawood and Suhr (1992) and Suhr and Cawood (1993) discuss time of formation, time and process of obduction, and structure of the massif.

## **1.4 Structure**

At least three generations of structures can be observed throughout the map area. The structures observed include: D0 syn-sedimentary features; early D1 folds and thrusts; penetrative tight F2 folds; and later D3+ brittle and ductile structures seen at outcrop scale, and represented by crenulation lineations, small faults and joints, and brittle or ductile shear zones (Waldron 1985, Waldron and Palmer 2000, Waldron et al 2003, Henry 2001).

*D0* structures include load, dewatering, and slump structures. In some instances, folds resulting from soft sediment slumping are difficult to distinguish from tectonic folds.

*D1* structures include recumbent isoclinal folds and major thrusts (figure 1.5). This first generation of structures is interpreted to be associated with the emplacement of the allochthon (Cawood and Suhr 1992, Waldron 1985, Waldron et al 1988, 2003).

Mélange is interpreted as a *D1* structure that occurs at tectonic contacts between major structural slices, often identified by the juxtaposition of stratigraphic successions (figure 1.5). Mélange is dominantly black shale that displays very irregular and anastomosing cleavage, often described as scaly (Waldron et al 1988). Mélange characteristically contains blocks of several lithologies characteristic of different formations, within the black scaly shale matrix.

*D2* structures are dominantly east-vergent folds that are upright to overturned. These folds occur throughout the map area and can be observed refolding *F1* folds. Smaller wavelength folds and strongly curved fold hinges are observed in the east portion of the map area.

Several generations of later structures, *D3* through *D5*, have been identified, including faults, folds, shear planes, and crenulation fabrics. More than one generation of crenulation lineations can be observed on *S1* or *S2* slaty cleavage surfaces. Carbonate units characteristically show strong folds but poor cleavage; complex fold interference patterns are observed and interpreted as products of post-*S2* deformation.

## **1.5 Objective**

This study focuses on an area that transects the Humber Arm Supergroup, extending from the east contact with the margin carbonates to the west contact with the Blow Me Down Mountain massif (figure 1.2). The objective of this study is to determine the geological history of the Humber Arm Allochthon in the Bay of Islands area after its initial emplacement in the Middle Ordovician. The structures observed in this area, in an intermediate position between the foreland basins and hinterland, will provide an important connection between the two separate histories of orogenic activity. This relationship is critical to develop our understanding of the development of the Appalachian Orogeny and its effect on the development of the Laurentian margin.

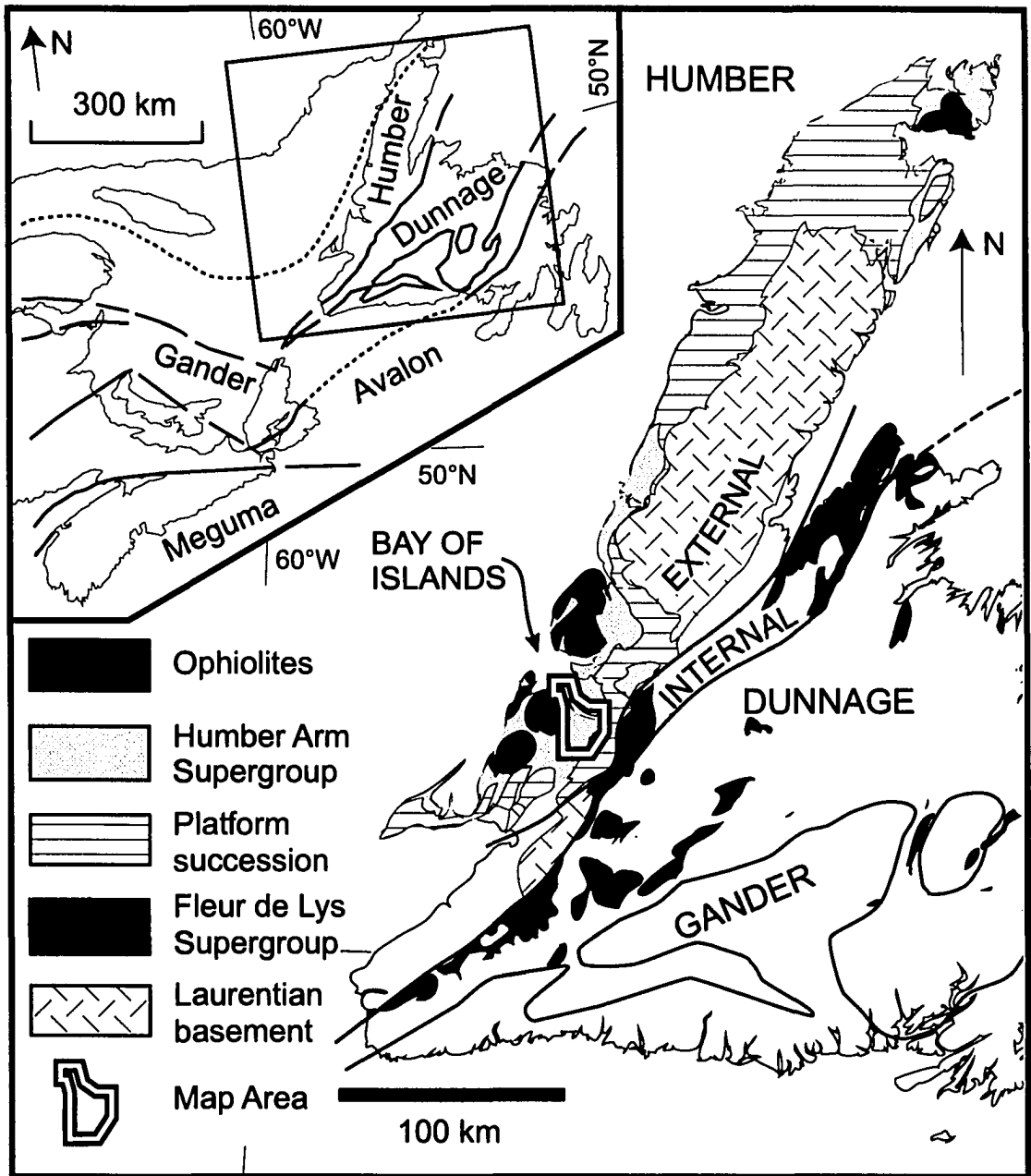
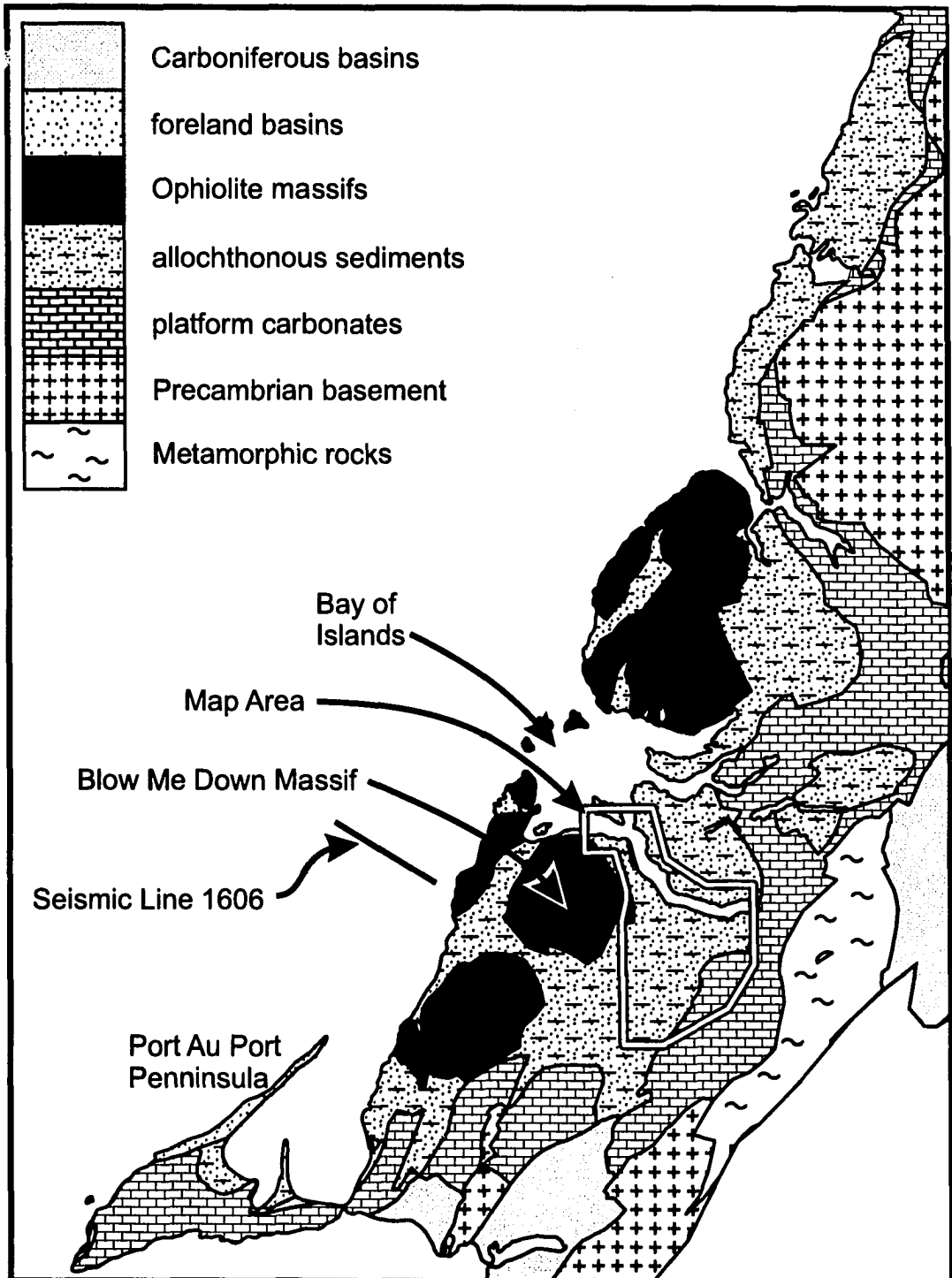


Figure 1.1  
 Map of the lithotectonic zones of the Canadian Appalachians. Western Newfoundland Appalachians showing the zonal subdivisions and the Corner Brook map area.

Figure 1.2  
 Map of the Humber Arm Allochthon showing the coverage of major lithological units.



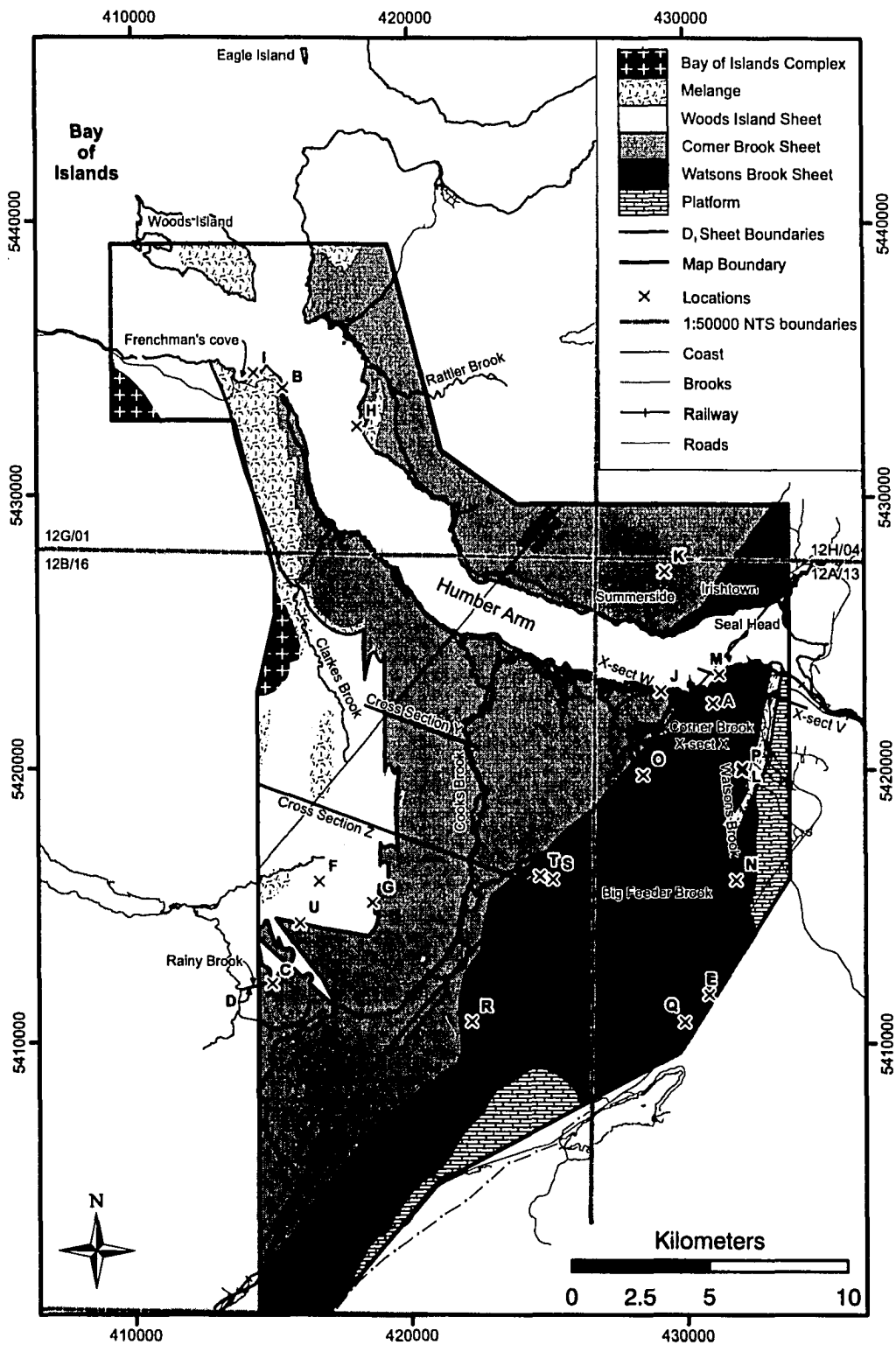


Figure 1.3  
 The Corner Brook Map Area showing major tectonic boundaries and important locations.

Stevens 1965		Lilly 1963, Bruckner 1965	Stevens 1970	Waldron 1985	Botsford 1988	Williams and Cawood 1989	This Study		
		Humber Arm Volcanics	Bay of Islands Igneous Complex	Bay of Islands Igneous Complex	Bay of Islands Igneous Complex	Bay of Islands Igneous Complex		Bay of Islands Igneous Complex	
Woods Island formation		Blow Me Down Brook formation	Blow Me Down Brook formation	"Western" sandstones	Eagle Island formation	Blow Me Down Brook fm.		Blow Me Down Brook fm.	
Transition zone				Easterly derived flysch		Eagle Island formation	Eagle Island formation	Whale Back Formation	Goose Tickle Gp.
Middle Arm Point fm.		Middle Arm Point fm.	Middle Arm Point fm.	Middle Arm Point fm.	Middle Arm Point Fm.	Middle Arm Point Fm.	Northern Head Gp	Middle Arm Point Fm.	Pinchgut Lake Group
Cooks formation		Cooks Brook formation	Cooks Brook formation	Cooks Brook formation	Cooks Brook Formation	Cooks Brook Formation		Cooks Brook Formation	
Transition zone		Irishtown formation	Irishtown Formation	Irishtown Formation	Irishtown Formation	Irishtown Formation	Curling Group	Irishtown Formation	Curling Group
Meadows formation									
Summerside formation		Summerside formation	Summerside formation	Summerside formation	Summerside formation	Summerside formation	Curling Group	Summerside formation	
		Summerside formation	Summerside formation	Summerside formation	Summerside formation	Summerside formation		Curling Group	Summerside formation
Tectonic contact at base of all formations									

Figure 1.4 (Table adapted from Botsford 1988)

History of the stratigraphic nomenclature in the Humber Arm Allochthon in the Bay of Islands area and the stratigraphic names used in this study. Note the inclusion of both the Whale Back Formation and the Eagle Island Formation in the Goose Tickle Group.

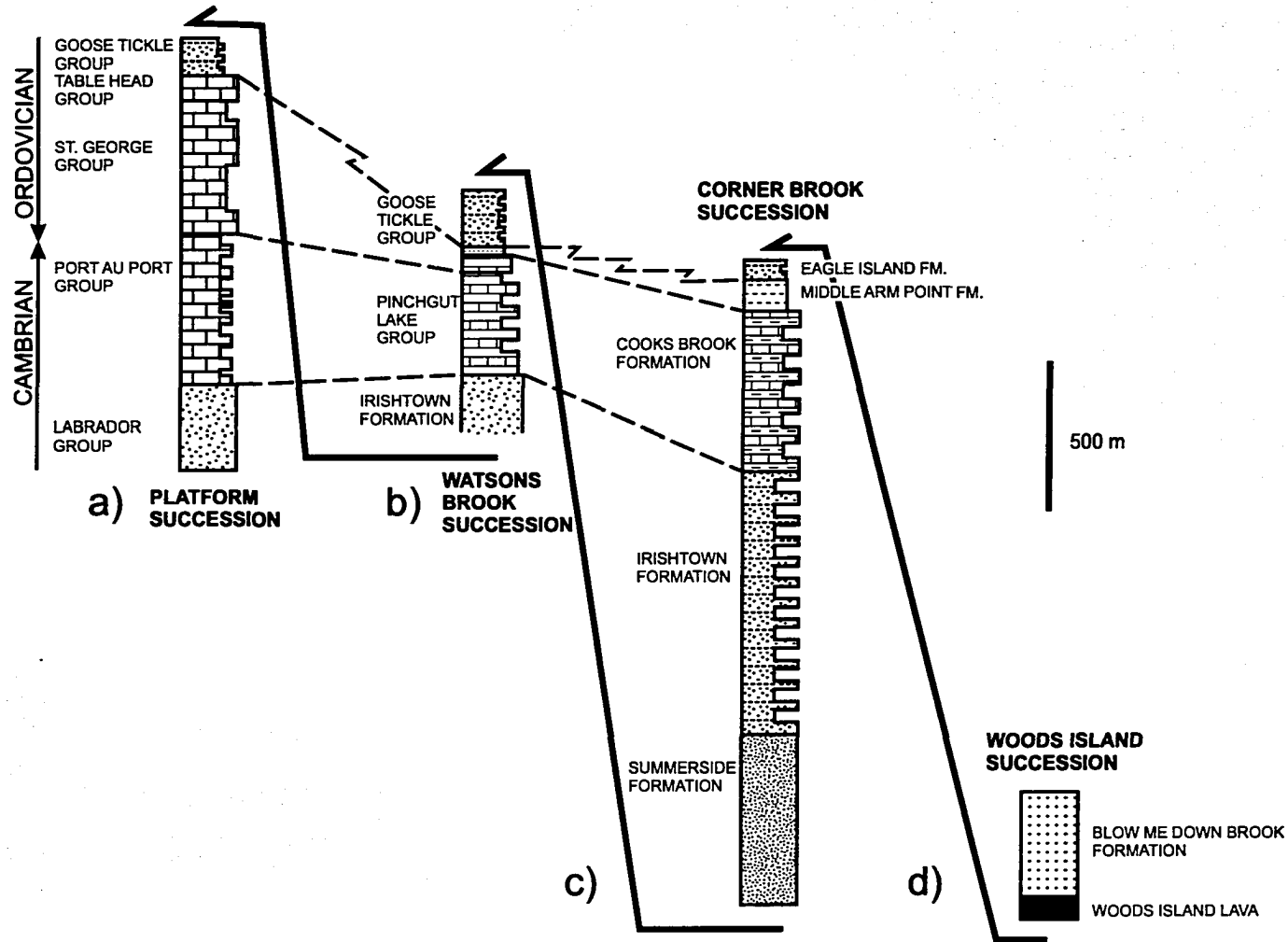


Figure 1.5  
 Stratigraphic columns showing the relationship between the successions of the Humber Arm Allochthon (adapted from Waldron et al 2003). This diagram also shows the trajectories of D1 thrusts responsible for the stacking order of the stratigraphic successions. melange is commonly observed between these successions, and is interpreted as a structure associated with thrusting.

## **Chapter 2: Map Units and Stratigraphy**

### **2.1 *Humber Arm Supergroup***

The stratigraphic definitions of the sedimentary rocks of the Humber Arm Supergroup have had a convoluted history. Due to their tectonized nature, few of the formations within the Humber Arm Supergroup are formally defined. This chapter includes a review of the history of the stratigraphic definitions, formation-specific observations made during the current study, and the definitions of each of the map units that are used in this study.

#### **2.1.1 Stratigraphic History of the Humber Arm Supergroup**

Works by Stevens (1965, 1970), Lilly (1965), and Bruckner (1966) contain the earliest definitions that led to the currently used stratigraphic nomenclature (figure 1.4). Stevens (1965, 1970) defined the Humber Arm Supergroup to include all the sedimentary rocks of the Humber Arm Allochthon. The deep-water sedimentary rocks in the vicinity of the Bay of Islands were all included in the Curling Group. Stevens (1970) recognized that there were lithologically distinct components within his Curling Group: a lower, Cambrian siliciclastic succession, a middle limestone-dominated succession and an upper, Ordovician siliciclastic flysch succession. The formations included in the Curling Group by Stevens (1970) were: the lower, siliciclastic Summerside and Irishtown formations; the middle, calcareous Cooks Brook and Middle Arm Point formation; the upper siliciclastics were assigned to the Blow Me Down Brook formation.

Based on observed differences between the rocks at Blow Me Down Brook and the Ordovician flysch units, Waldron (1985) and Quinn (1985, 1988) suggested that Stevens had included two distinct units in his Blow Me Down Brook formation. One of these sits stratigraphically on top of the Middle Arm Point formation, contains graptolites, and was referred to as “easterly-derived flysch” by Waldron (1985). The second unit was thought to contain no fossils, is tectonically bounded, and was referred to as “western sandstones” by Waldron (1985).

Botsford (1988) restricted Stevens (1970) Curling Group to contain only the lower, siliciclastic Summerside and Irishtown Formations, and introduced the Northern Head group, to include the carbonate Cooks Brook and Middle Arm Point Formations. Botsford (1988) also proposed the name Eagle Island formation for Waldron’s (1985) easterly-derived flysch.

Subsequently, Lindholm and Casey (1989, 1990) assigned a Cambrian age to the rocks at Blow Me Down Brook (Waldron’s (1985) western sandstones) after the discovery of a specific morphology of the *Oldhamia* trace fossil. They proposed that the name Blow Me Down Brook be restricted to this Cambrian unit.

The nomenclature used in this study for the stratigraphy of the Humber Arm Allochthon is shown in figure 1.4.

### **2.1.2 Curling Group**

The Curling Group is the lowest stratigraphic unit in the Corner Brook map area (figure 1.3, 1.5) and is composed of siliciclastic rocks. The formations included in the Curling Group are the Summerside, Irishtown, and Blow Me Down Brook formations.

### **2.1.2.1 *Summerside formation***

The Summerside formation is a stratigraphic unit that outcrops in the eastern portion of the map area (figure 1.3, insert 1). The Summerside formation has been informally described and measured by Palmer et al (2001). The bottom contact is observed to be everywhere tectonic. It is stratigraphically overlain by the Irishtown formation.

#### ***Lithology***

The Summerside formation contains red and green slates and arkosic sandstone beds, commonly greater than one metre thick and poorly sorted. Sandstone beds typically weather tan to white. Isolated carbonate-cemented “pods” can be found. Coarser beds are sometimes observed with sedimentary structures similar to the classic Bouma (1963) sequence. However, most of the sandstone beds are more than 1 m thick and massive. In thin section, Summerside sandstones are commonly well sorted, very fine to very coarse, and subangular. Summerside formation sandstones are differentiated from other Curling Group sandstones by a higher proportion of feldspar (Tanton 2003). The mudrocks vary from slate to phyllite. Muscovite and chlorite are observed in thin section both as detrital fragments and within the tectonic fabric. Some tectonic crystallization of mica and chlorite is interpreted to have occurred.

#### ***Age***

No fossils have been found in the Summerside formation; age constraints are established by the dating of detrital zircons and the stratigraphic relationship with the overlying Irishtown formation. Cawood and Nemchin (2001) examined detrital zircons

in the Summerside formation and found a youngest age, and therefore maximum limit of deposition, of  $580 \pm 12$  Ma. The upper age is bounded by the overlying, Irishtown formation, which contains Early Cambrian fossils.

### *Environment*

Lithology and sedimentary structures indicate that the depositional environment of the Summerside formation is deep-water and turbidite-dominated (Stevens 1970). Palmer et al (2001) propose that the Summerside formation was mainly deposited under oxidizing conditions.

#### **2.1.2.2 *Irishtown formation***

The Irishtown formation is observed in several tectonic slices throughout the map area (figure 1.3, 1.5). The initial name proposed by Stevens (1965) was the Meadows formation. The name was later changed to the Irishtown formation (Lilly 1965, Bruckner 1966). It was most recently examined in Waldron and Palmer (2000), and a composite measured section was produced in Palmer et al (2001). The Irishtown formation stratigraphically overlies the Summerside formation and underlies the Northern Head Group.

### *Field characteristics*

Lithologies found in the Irishtown formation are light coloured very quartzose sandstones, grey to black shales and slates, and conglomerates. Approximate relative abundances of lithologies over the entire formation are: shale and slate > 70%, sandstone  $\approx$  25%, and conglomerate < 5%. Irishtown sandstones are very well lithified and often informally termed quartzite. Quartz veining is abundant within the sandstone beds.

The thickness of Irishtown sandstone beds ranges from centimetres to many metres. The sandstone beds greater than 1 m thick are commonly massive and conglomerate beds greater than one metre often show rough graded bedding. Sandstone beds thinner than 50 cm commonly show abundant and well-preserved sedimentary structures, such as load and scour bottom structures, cross bedding, and grading.

No complete measurable sections through the entire Irishtown formation are observed within the map area due to the sporadic outcrop. Additionally, formational thickness is very difficult to determine due to structural complexity. Palmer et al (2001) show a composite section of the formation based on several measured sections in large coastal exposures west of Summerside formation and between Corner Brook and Cooks Brook. These sections show a proportion of at least 50% black shale and slate present in the Irishtown formation, including intervals up to 100 m thick of tectonized shale.

A section of Irishtown was measured in Rainy Brook, near the western boundary of mapping (section b, figure 2.1), that shows a thinly bedded facies of the Irishtown formation. The sandstones included in the sections by Palmer et al. are massive, and thickly bedded sandstones, which is distinct from the fine to medium bedded sandstone containing abundant sedimentary structures observed in Rainy Brook (section b, figure 2.1). These structures include: cross bedding, parallel laminations, flute casts, load casts, and convolute laminations.

The coarsest occurrences of the Irishtown formation are restricted to exposures near the eastern boundary of mapping. This coarse facies is composed of thickly bedded pebble to boulder conglomerates. In Corner Brook, there is a large section of very coarse Irishtown formation exposed at locality A (figure 1.3, insert 1). Its composition is 90%

conglomerate with clasts of sandstone, mudstone, limestone, quartz, and feldspar. Sporadic occurrences of this very coarse facies of the Irishtown formation have been interpreted as lenticular domains, possibly the result of channel fill (Palmer et al. 2001). However, due to the systematic decrease in clast size and bed thickness across the area, a tectonic interpretation has been favoured in this study as will be discussed in chapter 5.

### *Petrography*

Sand grains in the Irishtown sandstones are usually well sorted and very well rounded; feldspar and lithic grains are rare. Detrital mica grains are rare, although mica is observed in tectonic fabrics. A matrix is composed of smaller quartz grains and lesser amounts of mud and clay minerals. Carbonate cement is occasionally found in the Irishtown sandstones and tends to occur with greater frequency near the top of the Irishtown formation. Tanton (2003) produced a ternary QFL plot based on point counting of Irishtown samples, which resulted in a cluster within 10% of the quartz vertex. This is compared to the clast composition of the Summerside and Blow Me Down Brook formations in figure 2.2.

### *Age*

Stevens (1965) found Early Cambrian trilobites Austinvillia? sp. and Pagetides sp. through examination of clasts from Irishtown conglomerate beds. In addition, palynological results by Palmer et al (2001) support an Early Cambrian age.

### *Environment*

The depositional environment of the Irishtown formation is interpreted as being deep-water and turbiditic (Stevens 1965). Palmer et al (2001) provide a more specific

environmental interpretation that characterizes the Irishtown formation as a mud-dominated channelized submarine fan environment.

### **2.1.2.3 *Blow Me Down Brook formation***

*The Blow Me Down Brook formation* is observed in the western portions of the map area. It is tectonically bounded except for one location on Woods Island where it is interpreted to sit stratigraphically above extrusive volcanics (figure 1.5) (Palmer et al 2001).

#### ***Lithology***

The Blow Me Down Brook formation consists of interbedded very thick arkosic sandstones, pebble and granule conglomerates, and mudrocks of various colours.

Sections exist, such as Woods Island (figure 1.3), that consist of >95% sandstone. Inland exposures show higher proportions of shale and mudstone (figure 2.3). There are instances (locality C: figure 1.3, insert 1) where 30-50 m sections of massive red-purple slate or massive black poorly cleaved mudstone are observed. One to five metre sandstone beds occur in sections up to 50 m thick.

#### ***Age***

The age of the Blow Me Down Brook formation is thought to be Early Cambrian due to the presence of the trace fossil *Oldhamia curvata* (Lindholm and Casey 1989, 1990).

## *Environment*

The depositional environment of the Blow Me Down Brook formation is deep marine, with deposition of sandstones likely caused by high-energy gravity flow deposits in a submarine fan (Palmer et al 2001). The association with the lavas near the base has traditionally led to the interpretation that it is a rift-related unit.

### **2.1.3 Northern Head Group**

Botsford (1988) and Boyce et al. (1992) defined the Northern Head Group, which stratigraphically overlies the Curling Group and contains the Cooks Brook and Middle Arm Point formations. It is dominated by carbonate and shale redeposited through debris flows and turbidity currents. Botsford (1988) provides several type sections through the Northern Head Group that are very similar to the Northern Head Group observed during mapping, except at a few locations on the west side of the map area such as Rainy Brook (location D, figure 1.3, insert 1), where a much thinner Cooks Brook formation, and much thicker Middle Arm Point formation are observed (figure 2.4).

#### **2.1.3.1 *Cooks Brook formation***

##### *Lithology*

There is significant variation in lithology in the Cooks Brook formation. The dominant lithologies are thin-bedded calc-arenite interbedded with grey to black shale and limestone conglomerate. Sections of black mudrocks occur up to 30 m thick. Also, rare sections of green siliceous mudstone are observed, commonly near the top of the formation. The most diagnostic lithology in the Cooks Brook formation is limestone

conglomerate, which occurs in beds up to 10 m thick. Clasts range from 1 cm to approximately 1m in diameter and are normally platy/tabular.

### *Age*

Trilobites and graptolites have been found in the Cooks Brook formation and define the age as late Middle Cambrian to Early Ordovician (late Tremadocian) (Botsford 1988, Boyce et al. 1992).

### *Environment*

Williams (1975) interpreted this portion of the stratigraphy as a condensed slope section due to the formation of a carbonate bank to the west. Botsford's environmental interpretation was that the group formed as a base-of-slope sediment apron (1988).

#### **2.1.3.2 Middle Arm Point formation**

### *Lithology*

Botsford (1988) measured coastal exposures of the Middle Arm Point formation, which show a total stratigraphic thickness of approximately 100 m.

The Middle Arm Point formation is composed of black, green, and minor red siliceous mudstone, thinly bedded silty dolostone, and thinly bedded limestone. Chert beds also occur near the top of the formation and are generally red or green in colour. The intensity of bioturbation is significantly higher in the Middle Arm Point formation than the Cooks Brook formation.

Coastal exposures have significant quantities of red and green siliceous mudstone. The quantity of thinly bedded dolostone and limestone decreases towards the top of the

Middle Arm Point formation. In coastal outcrops, dolomitic layers are easy to distinguish from limestone of the Cooks Brook formation due to their slightly yellow weathering and higher prominence. Dolomitic layers in inland outcrops of the Middle Arm Point formation are often very distinctive. Outside of brook outcrops the dolomitic beds are commonly observed as dark brown, very porous, and soft, described in the field as “rotten dolomite”. These beds have no reaction with dilute hydrochloric acid, as a result of prior dissolution of calcareous material. This is interpreted as a result of soil-related processes of weathering inland and is a distinctive characteristic of weathered dolomite layers.

### *Age*

The Middle Arm Point formation is shown to have a Tremadoc to Arenig (Early Ordovician) age based on graptolite occurrences (Botsford 1988).

### *Environment*

The Middle Arm Point formation is very similar to the fine-grained portions of the Cooks Brook formation. Deposition of most of the Middle Arm Point formation occurred in a sediment-starved slope environment similar to the Cooks Brook formation (Botsford 1988), but lacking sources of coarse, shelf and slope derived carbonate.

## **2.2 Shelf and related units**

### **2.2.1 Shelf Succession**

The Humber zone includes units deposited in rift, passive margin, and foreland basin tectonic settings. Shelf and related units represent the carbonate dominated eastern

Laurentian shelf margin from Early Cambrian rifting (James et al 1988) to margin submergence and the end of carbonate deposition in the Middle Ordovician. The shelf units, in stratigraphic order, are the Labrador, the Port au Port, the St. George, and Table Head Groups. These groups, commonly described as autochthonous, are shallow marine equivalents of the deep-water allochthonous units described in the Humber Arm Supergroup. These units are observed at depth beneath the Gulf of St. Lawrence in offshore industry seismic lines and in one onland lithoprobe seismic line through the Bay of Islands area (Waldron et al 1998). The onland survey in the area of the allochthon does not resolve the subsurface structure of the area, although Waldron et al (1998) interpreted the existence of several blocks of dismembered platform succession units at depth. The shelf and related units in the Bay of Islands area also have a tectonized nature in outcrop and therefore are not likely to be truly autochthonous.

### **2.2.2 Table Head Group**

The Table Head Group was deposited during the early stages of the Taconian Orogeny and represents rapid subsidence prior to the failure of the carbonate production rate to keep up to shelf subsidence rate, which resulted in a transition to flysch sedimentation (Klappa et al. 1980).

The Table Head Group consists of the Table Point Formation, the Cape Cormorant Formation, and the Table Cove Formation (Stenzel et al 1990). The lowest formation of the Table Head Group, the Table Point Formation is the common unit composing the eastern boundary of mapping. There is a possibility that tectonically disrupted mud rocks and carbonates found in the *mélange* are derived from the Table Cove Formation.

## ***Lithology***

The Table Point Formation is carbonate dominated and mainly composed of thick-bedded or massive grey limestone with interbedded dolostone. The Table Point limestones are generally bioturbated bioclastic wackestones and packstones, lime mudstones, and peloidal grainstones (Klappa et al 1980).

## ***Age***

The Table Head Group is Middle to late Ordovician (early Llanvirn) and has relatively good fossil age control, including graptolites and brachiopods. The Table Head Group is up to 300 m thick in places and, based on observations at Table Point and at Port au Choix, is thought to span less than one graptolite zone (zone 9: *Hallograptus etheridgei* zone; Whittington and Kindle 1963, Williams et al 1987).

## ***Environment***

The Table Head Group is characterized by very rapid carbonate deposition, as shown by the thick carbonate bank, up to 300 m, and the short duration of deposition. The lower Table Point Formation of the Table Head Group records a transition from peritidal to subtidal carbonate accumulation (James et al 1988). The upper Table Point Formation records complete inundation of the margin and subtidal carbonate deposition.

## ***2.3 Pinchgut Lake and Goose Tickle Groups***

### ***2.3.1 The Pinchgut Lake Group***

Originally named the Pinchgut group by Williams and Cawood (1986), the thick-bedded limestone conglomerate and silty to sandy ribbon limestone is found to the west

of the platform units in structural slices of varying thickness (Knight 1996b, insert 1). Williams and Cawood (1986) observed that their Pinchgut group was tectonically associated with a unit of grey-green sandstone and slate, which they called the Whale Back formation (figure 1.4). Cawood and Van Gool (1998) observed that the Whale Back formation was, in fact, in stratigraphic contact with the Pinchgut group, and referred to the entire package of carbonates and clastics as the Pinchgut formation. Knight (1996b) named the carbonate-rich unit the Pinchgut Lake Group, and based on similarities to the Flysch sandstone overlying the Table Head Group, correlated the clastic unit to the Goose Tickle Group.

Williams (1989) shows the Pinchgut Lake Group as an equivalent to the nearby Cooks Brook formation. Knight interpreted the Pinchgut Lake Group as off-shelf deeper water deposit time equivalent to the Port au Port and St. George groups (1996a).

During the course of this study it was re-affirmed that the carbonate unit shares both stratigraphic and structural contacts with the overlying clastics as mentioned by Cawood and Van Gool (1998). The terminology used here names the carbonate unit the Pinchgut Lake Group, and the overlying clastics are termed the Whale Back formation, a subdivision of the Goose Tickle Group (figure 1.4).

### ***Lithology***

Rock types in the group include ribbon limestone, mudstone, phyllitic slate, oolitic limestone and limestone conglomerate. Knight (1996b) measured lithostratigraphic sections and estimated a minimum thickness of 225 m for the Pinchgut Lake Group, but the extensive folding and faulting in the area make accurate thickness estimates impossible (figure 2.4).

### *Age*

The age of the Pinchgut Lake Group is unknown, due to a lack of fossil control. Williams and Cawood (1986) and Cawood and van Gool (1998) suggest that the Pinchgut Lake Group is correlative to the Weasel group or the Cooks Brook formation based on lithology and similar structural positions. Based on this correlation, the age of the Pinchgut Lake Group likely begins in the Late Middle to early Late Cambrian and extends into the Early Ordovician (Arenig).

### *Environment*

Knight interpreted the Pinchgut Lake Group as off-shelf deeper water deposits, time equivalent to the Port au Port and St. George groups (1996a).

### **2.3.2 Goose Tickle Group**

The name Goose Tickle Group has been regionally applied to the clastic stratigraphic cover of the carbonate shelf units. Here the Goose Tickle Group is extended to include closely similar lithologies that overlie slope units of the Northern Head Group and Pinchgut Lake Group. Quinn (1996) interpreted the Goose Tickle Group as flysch deposited during foreland basin formation. Previous stratigraphic classification includes the American Tickle Formation, the Mainland formation, and the Black Cove Formation in the Goose Tickle Group. The Eagle Island formation is a unit of coarse clastics overlying the slope-deposited Northern Head Group and is also interpreted as a flysch unit (Stevens 1970, Quinn 1988, Botsford 1988). It is treated here as a formation belonging to the Goose Tickle Group. Additionally, as mentioned in 2.3.1, following

Knight (1996b), the clastic package overlying the Pinchgut Lake Group assigned to the Whale Back formation of the Goose Tickle Group.

### **2.3.2.1 *Eagle Island formation***

The Eagle Island formation occurs in relatively limited areas on the west side of the map area (figure 1.3, insert 1) and is distinguished from the Whale Back formation and the rest of the Goose Tickle Group primarily by its stratigraphic position overlying the Northern Head Group. However, lithological differences are noted as well. Botsford informally proposed the Eagle Island formation name and a type section at Middle Arm Point (1988).

#### *Lithology*

Complete sections of the Eagle Island formation are difficult to identify because the top of the formation is tectonic in every instance. Botsford measured an approximate thickness of 203 m at the type section at Middle Arm Point. The Eagle Island formation consists of a high proportion of coarse-grained lithic sandstone, conglomerate, and a small proportion of red or green siliceous mudstone. These lithologies are interbedded in thin to thick beds. Sandstone beds thinner than 50 cm commonly show grading and sedimentary structures suggesting turbidite deposition. Sand is observed both slumped and injected downward into the underlying sediment in distinctive soft sediment dykes near the bottom of the formation. Heavy minerals, such as zircon and chromite, interpreted as ophiolite debris, are found in the Eagle Island sandstone (Botsford 1988).

## *Age*

Deposition of the Eagle Island formation began in the middle Arenig (I.v. victoriae Zone, Bostford 1988) and is thought to have ceased by the Middle Ordovician.

## *Environment*

The slumps and sandstone injection are indicative of tectonic instability (Bostford 1988). The main lithologies of massive sandstone, medium-bedded normally-graded sandstone, and parallel or ripple laminated siltstone. Medium bedded portions of the formation exhibit partial Bouma sequences. Deposition is interpreted to be in a submarine fan environment. The depositional style and the existence of ophiolite debris suggest the Eagle Island sandstone is a flysch deposit, and records an introduction of debris into the basin due to erosion of the advancing Taconian allochthons.

### **2.3.2.2 *Whale Back formation***

The Whale Back formation is the part of the Ordovician Goose Tickle Group that overlies the Pinchgut Lake Group. It is present in the eastern parts of the map area (insert1) and the formation is in stratigraphic or tectonic contact with the Pinchgut Lake Group in almost all observed instances. It is composed of: poorly sorted sandstone beds; grey, green, or black shales; and rare carbonate beds.

## *Lithology*

The Whale Back formation contains several lithologies: green and black shales, green lithic and arkosic sandstones, minor ribbon limestone and dolostone, and rare thin-bedded conglomerate (Knight 1996b). The sandstones are quite characteristic in the

Whale Back formation. They are typically greenish in colour, cleaved and very poorly sorted with angular clasts. Thicknesses of sandstone beds range from laminae to one to two metres.

### *Age*

The Whale Back formation in the map area has had no paleontological work completed on it. Additionally, the highly tectonized nature of the sandstones and slates probably make it a poor candidate for biostratigraphic work. It is interpreted to be a similar age to the rest of the Goose Tickle Group, which is Early to Middle Ordovician based on graptolite evidence (Quinn 1988).

### *Environment*

Like other units of the Goose Tickle Group, the Whale Back formation is interpreted as foreland flysch deposited during the Taconian Orogeny (Quinn 1988, 1995).

## **2.4 *The Bay of Islands Complex and igneous units***

The Bay of Islands Complex contains the Blow Me Down Mountain massif and associated igneous units that exist in a position structurally above the sedimentary units of the allochthon. The Blow Me Down Mountain massif outcrops on the western edge of the map area (figure 1.3, insert 1) and marks the boundary of mapping. Cawood and Suhr (1992) and Suhr and Cawood (1993) discuss time of formation, time and process of obduction, and structure of the massif. The Fox Island volcanics are extrusive mafic flows, including pillows, and are a unit found outside the map area in the Humber Arm Allochthon and have been interpreted as late Precambrian and rift related (Williams

1975, 1985). Lava found on Woods Island (figure 1.3) has been suggested as a correlative to the Fox Island volcanics (Williams 1975, Waldron and Palmer 2000).

## **2.5 *Mélange and broken formation***

Mélange occurs at tectonic contacts between major structural slices in the Bay of Islands area (figure 1.3, 1.5), and is treated as a distinct unit. Mélange in this area is dominantly black shale that displays very irregular and anastomosing cleavage, often described as scaly (Waldron et al 1988). The common definition, and the one which is used here, requires that mélange units contain competent blocks of lithologies characteristic of different formations. In the Bay of Islands area these distinctive blocks can be of widely ranging sizes but always occur within a black scaly shale matrix. Boulder sized blocks of extrusive igneous rock are infrequently observed throughout the mélange zones in the map area, most often observed near the Bay of Islands Complex. The mélange zone directly in contact with the Blow Me Down Mountain massif contains 10-15 percent igneous material; with of block sizes up to 40 m. However, there are areas not associated with the massif where very large blocks of volcanic material are also present, such as the south-eastern flank of Crow Hill (figure 1.3, insert 1). Outcrops that resemble mélange but which do not contain lithologies characteristic of multiple formations are here referred to as broken formation.

## **2.6 *Stratigraphic successions***

Stratigraphic units are important in differentiating tectonic relationships in the map area, as will be described in Chapter 3. Terminology used here follows that of Waldron et al (2003), where four *successions* have been defined to include all the

sedimentary units of the Humber Arm Allochthon. These are tectonically bounded and separated based on distinct depositional environment on the margin of Laurentia. They are the Platform succession, which is the Port au Port, St. George, and Table head Groups; the Watsons Brook succession, which is the Irishtown formation, Pinchgut Lake Group, and Whale Back formation; the Corner Brook succession, which is the Summerside, Irishtown, Cooks Brook, Middle Arm Point, and the Eagle Island Formations; and the Woods Island succession, which is the Blow Me Down Brook formation and the Woods Island volcanics (figure 1.5).

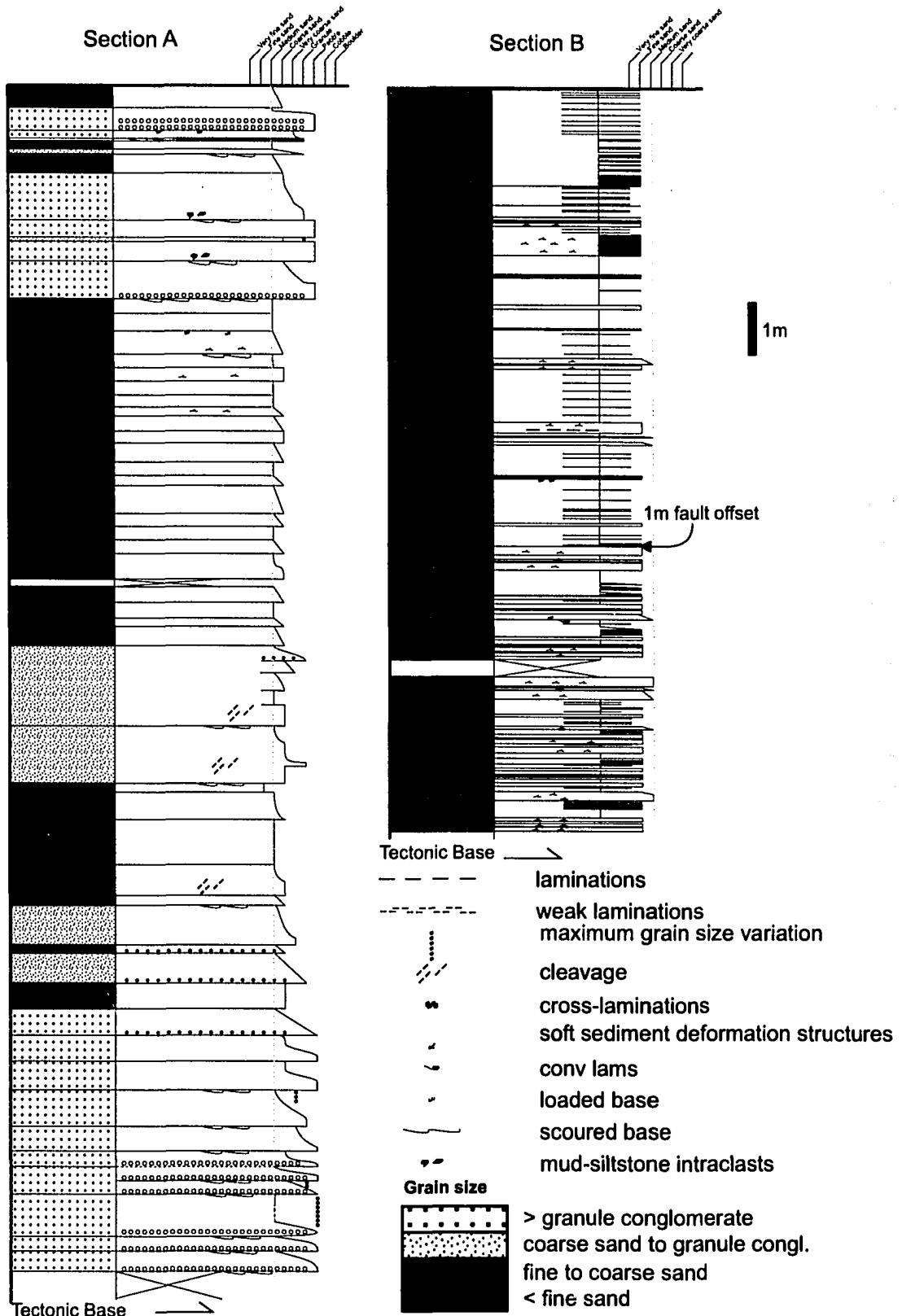


**Figure 2.1**  
 Contrasting measured stratigraphic sections of the Irishtown formation at Localities A and B (Insert 1, figure 1.3).

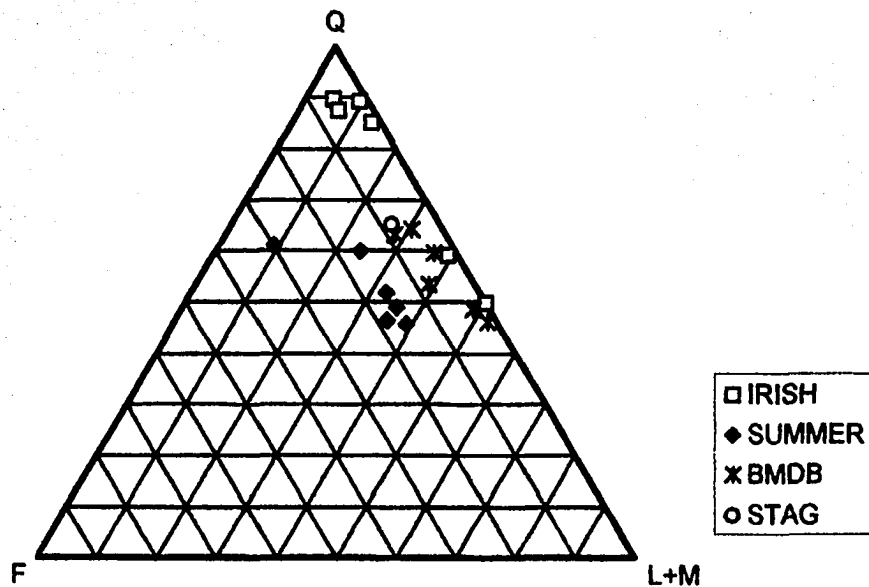
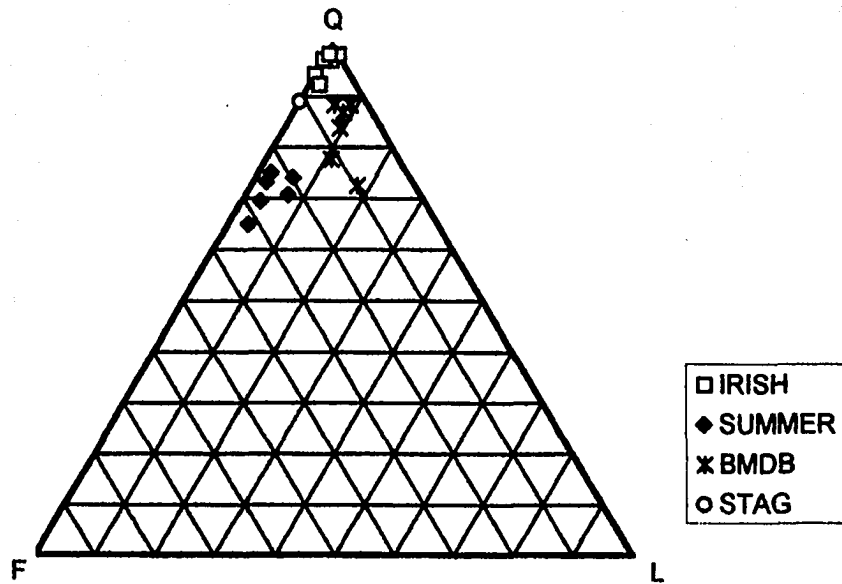
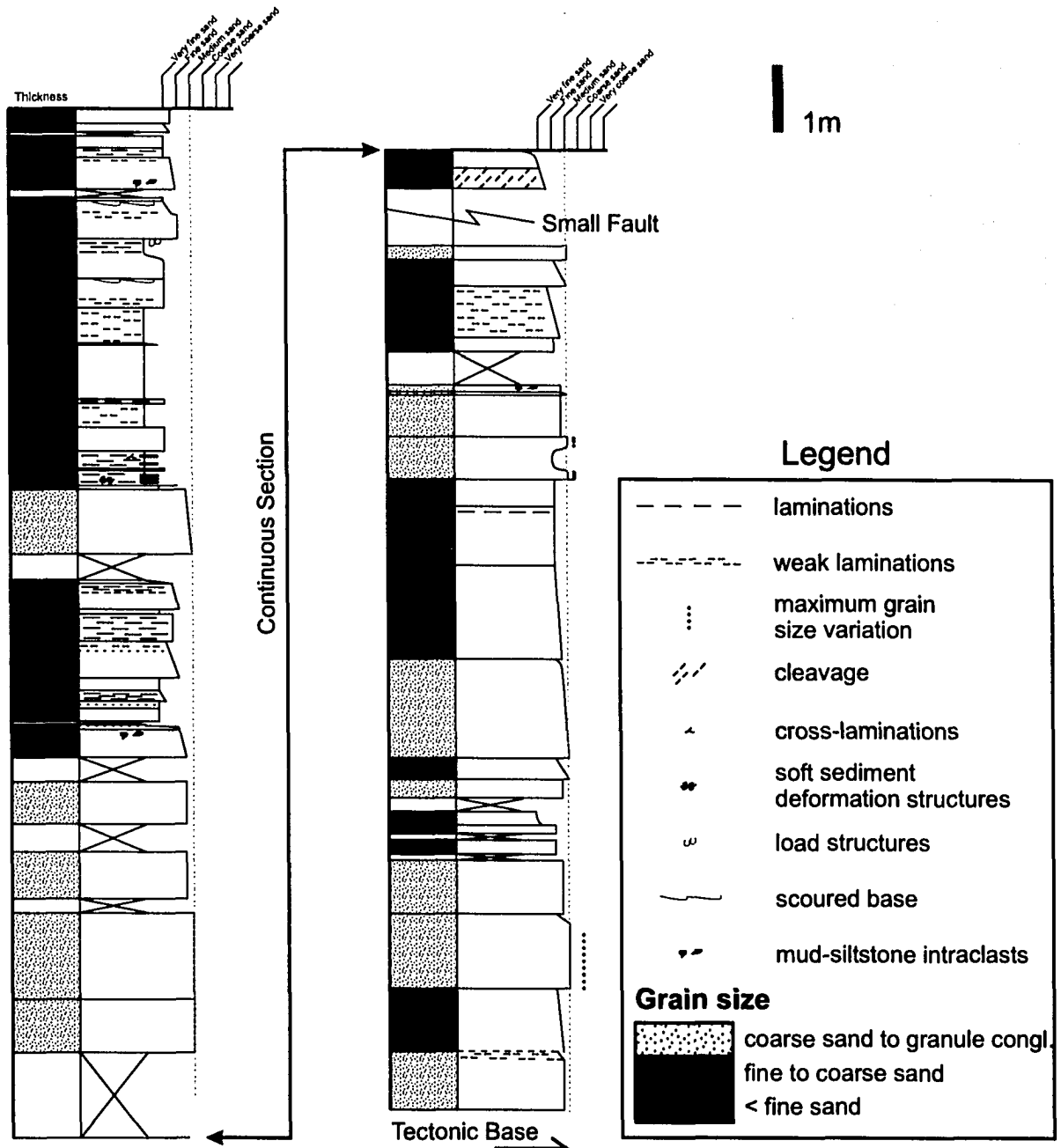
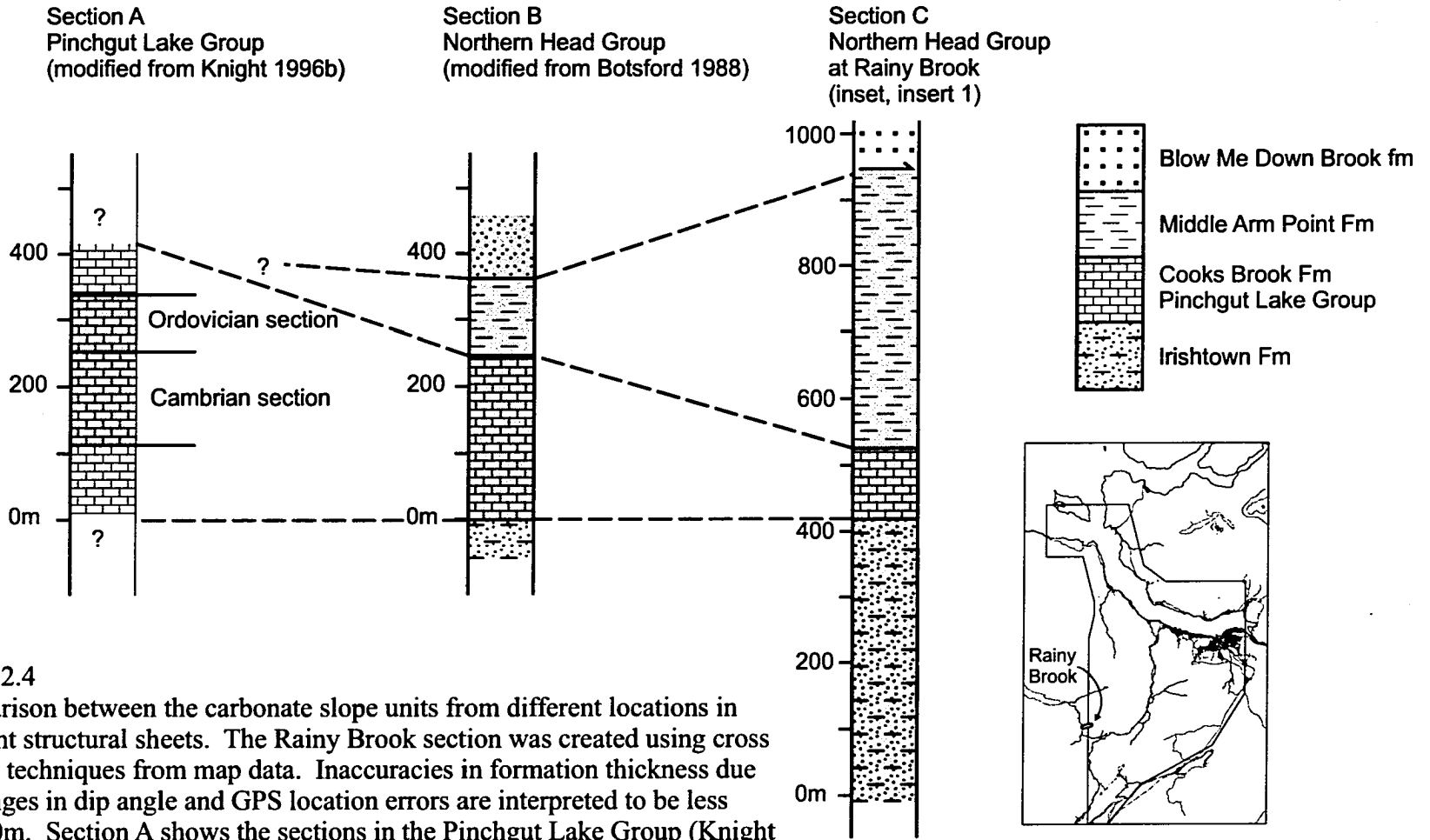


Figure 2.2 Ternary diagrams showing the distribution of point counting results, illustrating the petrographic distinction between the three formations within the Curling group (Tanton 2001). Q is quartz grains, F is feldspar grains, L is lithic fragments and M is matrix.



**Figure 2.3**  
 Measured section of Blow Me Down Brook formation (location C, insert 1). This is an example of an inland exposure showing a higher proportion of fine-grained lithologies than sections measured in coastal exposures (e.g. Palmer et al 2001, Buchanan 2004)



**Figure 2.4**  
 Comparison between the carbonate slope units from different locations in different structural sheets. The Rainy Brook section was created using cross section techniques from map data. Inaccuracies in formation thickness due to changes in dip angle and GPS location errors are interpreted to be less than 50m. Section A shows the sections in the Pinchgut Lake Group (Knight 1996b). The full thickness of the group is indeterminate. Shading shows the minimum measured thicknesses in each section. Inset shows map area and the location of Rainy Brook.

## **Chapter 3: Structure of the Corner Brook Map Area**

### **3.1 *Introduction***

The structural history of the Corner Brook area is complex and many types of structures are present, including multiple fabrics and folds. In cases where these structures were observed overprinting one another, the relative timing could be determined. Such overprinting relationships were recorded at all outcrops where they were identifiable, resulting in the classification of structures into generations D1 through D5. Later structures are less penetrative, and therefore occurrences of overprinting are more sporadic. Observed structures each display characteristic styles that are commonly associated with a specific generation. For example, S1 fabrics are commonly scaly and S2 are slaty or crenulation fabrics. In cases where structures were observed in outcrops without overprinting criteria, the generation of the structure was inferred for mapping purposes based on the style of deformation observed.

### **3.2 *Syn-sedimentary structures***

Syn-sedimentary structures (designated D0) are common in the Northern Head, Pinchgut Lake, and Curling Groups. Syn-sedimentary structures observed in outcrop include slump, dewatering, and load/ remobilization structures.

#### **3.2.1 *Outcrop***

Folds interpreted as syn-sedimentary occur in the ribbon-laminated limestones of the Cooks Brook formation and Pinchgut Lake Group. At outcrop scale these occur in various irregular orientations, and are never associated with a penetrative tectonic fabric.

Zones in Clarks Brook and Cooks Brook (figure 1.3, insert 1) are characterized by bedding in limestone which changes in character across a span of several metres, from undeformed and ribbon-laminated, to boudinaged and folded but traceable, and finally to completely untraceable conglomerate composed of folded and boudinaged platy limestone fragments (figure 3.1). Folds in multiple orientations commonly have thickened hinges. These folds are interpreted to be a result of soft sediment deformation, such as slumping due to slope failure in non-lithified to semi-lithified substrate (figure 3.1). This type of soft-sediment deformation is consistent with the interpretation that these units were deposited in a slope environment.

Limestone concretions, superficially resembling boudins, occur at the Pinchgut Lake Group type sections (locality E, Knight 1996b) and in numerous locations in the Cooks Brook formation along Cooks Brook (figure 1.3, insert 1). Planar laminae can be seen cross-cutting concretion boundaries, leading to the interpretation that the concretions are diagenetic. There are also rare occurrences of carbonate concretions in thinly bedded Irishtown sandstones and Summerside sandstones.

Convolute laminations and sheet structures are common in the Curling Group clastic units (Summerside, Irishtown and Blow Me Down Brook formations). For example, convolute lamination occurs in the Blow Me Down Brook formation at locality F (figure 1.3, insert 1). The intensity of the convolutions increases closer to the bed bottoms. Convolute lamination was also observed in thin sections of fine to very fine-grained sandstones. Sheet structures (Laird 1970) are common in massive sandstone beds in the Irishtown formation such as those at locality G (figure 1.3, insert 1). The sheet structures are irregularly planar zones of whiter, better sorted sandstone, best seen

in faces perpendicular to bedding. Fine linear traces of clean white quartz sandstone occur where planar sheet structures intersect the outcrop surface. These sheets can be up to 1 cm thick and are usually more resistant to erosion. This creates a ripple-like effect observed on weathered bed or outcrop surfaces (figure 3.1). These structures typically branch downwards; so well exposed instances can be used as an indicator of way up on individual beds.

Sandstone dykes, or sandstone injection structures, are observed at locality H (figure 1.3, insert 1) near Rattler Brook (insert1), at the stratigraphic boundary between the Middle Arm Point formation and the overlying Eagle Island formation. Sandstone dykes are formed by the overlying coarse unlithified, or liquefied, Eagle Island sandstone injecting down into the shale at the top of the Middle Arm Point formation. Stevens (1965) and Botsford (1988) both document sedimentary dykes at this stratigraphic boundary. Botsford refers to this zone as the “slump and injection interval of the Eagle Island formation” (1988).

### **3.3 *D1 Structures***

Structures identifiable as D1 include: *mélange*, cleavage, folds, and faults. D1 structures are interpreted as products of a combination of extreme progressive brittle and ductile shear. Although occasional overprinting relationships between these structures were observed, they have been grouped into a single generation of “early deformation” due to the difficulty of determining relative timing and/ or relationships between them. Most importantly, it can be shown that each of these structures is overprinted by D2 structures.

### 3.3.1 Outcrop Scale Structures

#### *Mélange and broken formation*

D1 “mélange-style” structures are the most difficult to interpret of all of the structures in the Bay of Islands area. Mélange is characterized by scaly black shale with anastomosing cleavage that contains blocks of more competent lithologies ranging in size from millimetres to tens of metres in diameter. A typical outcrop of mélange occurs structurally above the Middle Arm Point formation near Frenchmans Cove (locality I, insert1). This belt of mélange contains blocks of various lithologies, including calc-arenite, arkosic to arenitic sandstone, abundant vein quartz and dismembered pillows of mafic volcanics with interstitial chert fragments. The calc-arenite is likely from the Cooks Brook formation or the Pinchgut Lake Group, both of which are present in nearby slices; the sandstones are from either the Irishtown or the Summerside Formations, parts of the Corner Brook Sheet; and the volcanic rocks are of unknown origin. Cleavage in mélange is scaly and anastomosing, defining the boundary of lenticular fragments of less disrupted rock. The lenticular domains can be composed of more competent lithologies, fragments of boudinaged quartz veins, or simply mudstone. Linear features, such as crenulation, and slickenstriae, are common on the irregular and often polished surfaces of the scaly fabric. Shaly portions of these types of outcrops are usually extremely friable. Colours are commonly black but can vary to silver/ grey and or green depending on the protolith shales.

The use of the term *mélange* in this study has been restricted to localities where competent blocks from multiple formations are found in single outcrops. Mélange-like scaly fabrics and blocks are observed at other locations, where lithologies from only one

formation can be identified. These cases are characterized as *broken formation*. On the map (figure 1.3, insert 1 and 2) areas composed of broken formation are given formation classification according to the competent lithology composing the blocks.

Scaly cleavage commonly occurs in accretionary wedges and is a fabric developed during faulting at low confining pressures and low temperature, often associated with underconsolidated sediments (sediments that are partially supported by sedimentary fabric and partially by excess fluid pressure (Moore et al 1986)). Moore et al (1986) interpret each polished and striated cleavage plane as a small temporary slip surface, or fault, that ceased to be active when there was an increase in the coefficient of friction, either due to a decrease in pore pressure or reorientation of the slip plane relative to the stress field. Progressive deformation results in a rough foliation defined by the scaly fabric that occurs sub-parallel to the orientation of the shear surface. Based on extensional features, veins, and scaly fabric in the *mélange* of the Bay of Islands area, Waldron et al (1988) invoke a brittle accretionary wedge model to interpret the emplacement of the Humber Arm Allochthon, inferring that tectonic dewatering of the underlying muddy sediments increased pore pressures facilitating brittle fracture and allochthon emplacement.

### ***Folds***

True isoclinal folds (F1) with an interlimb angle of zero degrees are observed in the map area. They occur in beds with thicknesses of centimetres to several metres (figure 3.2). Observed F1 fold wavelengths range from a few centimetres to a maximum of four metres. In most instances these folds are reclined, gently inclined to recumbent, and west-vergent (Waldron 1985, Waldron and Palmer 2000, Cawood and van Gool

1998). F1 folds are typically parallel, or class 1B (Ramsay 1967) in competent lithologies as shown in figure 3.2. Incompetent lithologies, such as shale and mudstone, exhibit ductile behaviour and form class 3 folds, or in the case of true isoclinal folds are removed completely. In many cases F1 isoclinal folds can be traced across an outcrop and observed overprinted by F2 folds and S2 cleavage. Examples occur at the base of Crow Hill (location J), and Eagle Island (figure 1.2). In general, F1 folds are found more commonly towards the western edge of the map area.

### *Cleavage*

S1 cleavage is dominantly bed-parallel and is distinguished from simple compactional fissility in locations where it occurs axial planar to isoclinal F1 fold hinges. This S1 fabric is typically crenulated by S2 and/ or later crenulation cleavage. Bed-parallel fabric is observed in thin sections and is defined by grains of micas, mostly muscovite and chlorite, oriented parallel to bedding. This is interpreted as a product of tectonic reorientation or even crystal growth during D1 deformation (figure 3.3). In contrast, mica grains that are clearly detrital within the compositionally immature sandstones are haphazardly oriented.

Another type of S1 cleavage is a spaced foliation defined by alternating bands of quartz-rich and quartz-poor material that occurs exclusively in the Summerside formation, and is observed at Crow Hill, Watsons Brook, and at outcrops near Summerside (figure 1.3, insert 1). In hand specimen, this cleavage typically occurs as alternating bands of colour or a rough weathered-out foliation. In cases where F1 folds and spaced cleavage are present in a single outcrop, the dissolution cleavage is axial

planar to the folds. This occurs at locality K, where there is an F1 fold with spaced axial planar S1 cleavage that is overprinted by S2 slaty cleavage (figure 3.4).

A thin section was cut from a sample of a sandstone bed taken from locality L that shows this cleavage. In thin section, quartz grains appear dissolved and truncated near and within the boundaries of the quartz poor-portion of the rock, indicating that this spaced cleavage is likely a dissolution cleavage (figure 3.5). This sample has dissolution bands with spacing of 1-2 cm; the band thickness is irregular but averages 2-3 mm. In thin section, the mineralogy of the clasts in the entire rock is approximately 80 percent quartz and 20 percent feldspar with an average size of 0.15 to 0.2 mm in diameter. The quartz rich bands are composed of approximately 80 percent clasts. The quartz poor bands contain between 5 and 10 percent clasts; the remainder appears to be very fine-grained micas and clays. Chlorite crosscuts earlier grain boundaries primarily in the fine-grained portions of the rock and is interpreted as developing late. Muscovite is present and takes the form of small, unoriented, grains (< 0.01 mm) and larger (0.1 to 0.2 mm) aggregate crystals that have a preferred orientation. Within these sandstone beds the muscovite orientation cross cuts the orientation of the S1 dissolution bands and is interpreted as an S2 foliation (figure 3.5). Significant quartz dissolution occurred in the development of the S1 dissolution cleavage, which would have resulted in silica rich fluids. Silica removed from this structurally low location is tentatively interpreted as a source for the abundant quartz veins that occur in *mélange* zones.

### **3.3.2 Map-Scale D1 structures**

The Corner Brook map area has been divided into four domains based on tectonically bounded stratigraphic successions. The terminology that will be used here

follows that published by Waldron et al (2003). The first categorization is based on stratigraphic relationships resulting in a grouping of four *successions* (figure 2.4). The four stratigraphic successions described in Chapter 2 (the Platform succession, the Watsons Brook succession, the Corner Brook succession, and the Woods Island succession) are tectonically bounded and each composes a single *sheet* (figure 1.3). Tectonic contacts within sheets are not considered sheet boundaries because they do not separate successions.

Mélange is observed in broad bands in the map area and can be geographically related to major thrust boundaries, such as those structurally above the Corner Brook sheet and above the Woods Island sheet (figure 1.3, insert 1). The belt above the Woods Island sheet contains exotic blocks large enough to appear at 1:50,000 map scale, observed at Frenchmans Cove, Clarks Brook and Knights Brook. These blocks consist of mafic volcanics of unknown origin, including pillow lavas, and competent sedimentary lithologies. Mélange is interpreted as a product of westward thrusting responsible for emplacement of the Bay of Islands Complex.

Typical sections with almost 100 percent exposure occur on the Coast of the Humber Arm near Frenchman's Cove and on Woods Island. Buchanan (2004) provides a detailed structural analysis of the fabrics and their relationships within the mélange that surrounds the Bay of Islands Complex.

Facing direction of bedding on S2 provides evidence for larger than outcrop-scale F1 folds. For example, in locations that have good sedimentary way-up indicators and good S2 fabric, bedding that faces downward on S2 cleavage planes is occasionally

observed. A downward facing bed on an F2 fold limb requires an F1 fold to have overturned bedding prior to F2 folding (figure 3.2).

### **3.4 D2 Structures**

Folding, penetrative slaty cleavage, and crenulation cleavage are common D2 structures. Throughout the map area penetrative S2 cleavage is typically axial planar to open to tight, upright to overturned F2 folds. Overturned folds dominate F2 geometries near Corner Brook and the eastern boundary of mapping; upright folds are commonly observed near the western boundary of the map area. D2 structures are the most consistent and penetrative structures in the map area and consistently overprint D1 structures.

#### **3.4.1 Outcrop-scale structures**

##### ***Folds***

F2 folds are upright to overturned, with interlimb angles ranging from open to tight. In most of the fine-grained lithologies in the area, these folds have an associated S2 axial-planar cleavage. The S2 cleavage is usually manifested as a slaty or crenulation cleavage. The F2 asymmetry is east vergent (Insert 3, Bosworth 1985, Cawood and Van Gool 1998).

One of the largest single-outcrop F2 folds occurs on Seal Head at a position very close to the eastern contact of the Humber Arm Supergroup with the carbonate platform units (location M, figure 1.3, insert 1). This slightly overturned syncline of competent Irishtown formation can be traced for almost one kilometre through Corner Brook. The

axial plane, and axial planar S2 cleavage, of this fold dip gently to moderately west (38 to 50 degrees dip) and strike approximately north-south.

At locality N the Pinchgut Lake Group is observed in close proximity to the contact with the platform units. F2 folds in the less competent lithologies of the Pinchgut Lake group have similar axial plane orientations to the Seal Head Syncline, but tend to have tighter interlimb angles and curvilinear fold hinges that ultimately result in both north and south plunging fold axes. Measurements taken on curved fold hinges at localities N and O are shown on equal-area projections shown in figure 3.6.

Overprinting of F2 folds on F1 folds is interpreted from refolded folds observed in many locations, such as Eagle Island (figure 1.2) and near Corner Brook (locality I, figure 1.3, insert 1). These locations both show isoclinal F1 folds being refolded by F2 (figure 3.2). F1 isoclinal folds are more common further west, where relationships of F2 folds overprinting F1 folds are also more commonly observed.

### *Cleavage*

In outcrops containing only black slates, bed-parallel S1 fabrics appear very similar to slaty S2 fabric. In the absence of overprinting relationships, if the two cannot be distinguished, the generation of the cleavage is classified as unknown, or indeterminate, for mapping purposes.

At locality K (figure 1.3, insert 1), slaty S2 cleavage is observed crosscutting an F1 fold and S1 fabric. Additionally, in samples taken from location L (figure 1.3, insert 1), thin sections cut perpendicular to the dissolution cleavage show development of S2 crosscutting the earlier S1 dissolution zones (figure 3.5). Slaty S2 fabrics are occasionally observed overprinting S1 scaly mélangé-like, and slaty, fabrics. This

overprinting usually results in the development of L2 crenulation lineations on both planar and scaly S1 fabrics.

Crenulation lineations are common in locations where there is S1 bed-parallel cleavage and S2 crenulation cleavage. The crenulation cleavage is interpreted as a D2 structure because it both overprints the S1 fabrics and usually has an axial planar relationship to F2 folds.

Near the eastern edge of the map area shear-sense indicators were observed indicating that that shearing had occurred parallel to S2. Sigma structures indicate reverse sense of shear (figure 3.7). These structures suggest significant eastward thrusting during D2 deformation.

### **3.4.2 Thin-section scale structures**

Structures observed in thin section include the fabrics such as S2 crenulation cleavage and slaty cleavage. Micro-folds (F2) are also common and fold S1 and bedding. Well-developed slaty S2 cleavage observed in thin section is characterized by mica and chlorite alignment (figure 3.8). Single crystals are rarely greater than 1 mm in length. The S2 fabric in thin section was most prevalent in very fine mud-rocks. In less well-developed instances of S2, in thin section, bulk extinction of mud occurred in parallelism with the S2 fabric, leading to the interpretation that reorientation had occurred during D2 but not recrystallization. In coarser rock such as siltstone and sandstone, strain shadows surrounding competent clasts were commonly the location of mica and chlorite crystallization.

Both simple and discrete crenulation fabrics are observed, in some cases within single thin sections. Simple crenulation is identified where S1 oriented minerals are

showing the initial stages of transposition into the S2 fabric orientation, generally in diffuse zones and the earlier fabric continues uninterrupted (zonal crenulation of Gray 1977). Similar to observations made in outcrop, in instances where the S1 fabric was well developed, this S2 fabric was typically observed as a crenulation of S1 (figure 3.3).

A locally developed discrete crenulation fabric was observed in locations along Watsons Brook (location P, figure 3.9) and in slates of the Summerside formation, and identified in thin section. Discrete crenulation involves little deformation of the earlier fabric; crenulation planes are sharp and truncate the earlier fabric. This fabric occurs in laminated green shale in the Pinchgut Lake Group where it offsets fine black shale laminae. In subhorizontal outcrop in the field, horizontal separations resulting from dissolution are asymmetric and have magnitudes of several millimetres. The asymmetry of the dissolution planes was also examined in oriented thin section and were found in specific instances, to have a component of reverse displacement (figure 3.9).

### **3.4.3 Map Scale**

The strike of S2 fabric is consistent through the area, commonly ranging from 170° to 220°. The dip of the S2 fabric is less consistent: it ranges from gently to moderately west in the easternmost map area, to vertical or even steeply eastward in the westernmost parts of the map area. This range is illustrated in the equal area projections in figure 3.10 and is apparent in cross section Z (insert 3). The envelope of bedding and D1 thrusts is subhorizontal; therefore the area-wide change in orientation of S2 fabrics and folds show increasingly east-vergent geometry to the east.

F2 folds have a pronounced effect on the map pattern at 1:50,000 scale. Fold closures have been interpreted based on the observed outcrop pattern. The map pattern

near the platform contact with the Pinchgut sheet requires closures to the northeast and southwest on single folds, consistent with fold hinges that plunge in opposite directions, as observed in single outcrops, as described above.

Several major tectonic contacts, commonly interpreted as D1 thrusts, dip to the west. An example of this is the Crow Hill fault (figure 1.3, insert 1), which is well defined and dips moderately westward. Westward-vergence of D1 thrusts indicates that thrusts formed during D1 would dip east. The west-dipping attitude of tectonic contacts, such as the one at Crow Hill, has been explained as a product of F2 folding (e.g. Waldron et al 2003).

Watsons Brook was mapped at a scale of 1:5000 (figure 3.11). The detailed map and cross sections of Watsons Brook show discrete zones where S1 and S2 are parallel. Except for these discrete zones of parallelism, the rest of Watsons Brook has a consistent map relationship between S1 and S2 cleavage, with S1 striking 15 to 30 degrees counter clockwise from S2. S2 cleavage along Watsons Brook has a very consistent orientation. Parallelism between S2 and S1 can be attributed to F2 folds, which, near the eastern edge of the map area, occasionally display a single very sheared and attenuated limb; this rotates earlier structures into parallelism with S2 (figure 3.11). This characteristic is also apparent in the Little Feeder Book cross section where the steep limbs of F2 folds are commonly shear surfaces close in orientation to the S2 fabric (figure 3.12).

#### **3.4.4 Overprinting**

The poles to S1 fabrics, illustrated on equal area projections from the entire map area, (figure 3.13) have variable orientations that are roughly distributed along a subvertical E-W girdle. Near the eastern map boundary, the S1 fabric has a similar

orientation to the S2 fabrics, interpreted as a result of transposition of the S1 fabrics into the S2 orientation in areas of most intense D2 deformation. This increase in intensity also resulted in tighter folds, curved fold hinges, and tighter S2 pole clusters (figure 3.10, 3.13).

Later deformation, discussed below, is inferred to have reactivated S2 fabrics and, in some cases, caused further transposition of S1 into the S2 planes.

### **3.5 *Late Structures***

In many outcrops one or more structures are present that post-date D2. These later structures are only locally developed, making overprinting relationships between them difficult to distinguish.

#### **3.5.1 Crenulation Fabrics**

Crenulations lineations are common throughout the area. They are frequently observed on both S1 and S2 foliations. Crenulation lineations that occur on S2 cleavages are interpreted as later than the S2 fabric. These crenulations are typically present on well-developed slaty cleavage, particularly in the Irishtown formation. In many instances two distinct crenulation lineations were observed on the S2 cleavage, indicating the existence of at least two generations of structures later than D2.

Over the entire mapped area, two clusters of crenulation lineations later than L2 lie in a girdle corresponding to the mean S2 cleavage (figure 3.14). One cluster trends west-northwest and has a variable plunge. The second cluster has a shallow plunge and trends south-southwest. In cases where both lineations are visible on a single plane, there

are very rare instances where it is possible to determine that the south-southwest lineation overprints the west-northwest lineation.

### **3.5.2 Folds and Cleavage**

Upright, open, subhorizontal folds that deform bedding, S1, and S2, were observed throughout the map area with a large concentration in the Cooks Brook formation near Cooks Brook. The axial planes strike approximately WNW- ESE (figure 3.14). Axial planar spaced cleavage is occasionally developed with these late folds. This spaced, subvertical cleavage occurs sporadically throughout the map area with or without associated folds.

In the area of Watsons Brook, there is a girdle distribution of S2 poles on an equal area projection (figure 3.14), which is interpreted as a result of late folding with a steeply west-plunging fold axis.

### **3.5.3 Shear zones and faults**

Instances of shear and fault surfaces in the map area are common, typically sub-parallel to the S2 foliation. However, most late faults are recessive due to preferential erosion in the tectonically disrupted, often shale-dominated, fault zones. Therefore, kinematic indicators are rarely preserved. In instances where fault motion is recorded, it is primarily by quartz and calcite slickenfibres or slickenstriae in the plane of the fault. Kinematic indicators on shear and fault surfaces can have conflicting senses. In rare instances, faults develop with associated conjugate kink folds. The magnitude of displacement on these late shear zones and faults is only observed at outcrop scale where it is relatively minor.

### *Normal kinematics*

Ductile normal-sense shear zones occur near the contact with the Platform sheet at location Q and in Watsons Brook, sub-parallel to the S2 foliation. At outcrop scale these are discrete zones that display drag of earlier structures into planar zones of shear (figure 3.15) less than one centimetre thick.

At location Q these normal shear zones are penetrative in the outcrop and deform L2 (figure 3.15). Displacement of individual shears was not determined, but it appears to be small. At location R distinct and similarly oriented normal-sense sigma structures are observed nucleating on quartz pebbles in an Irishtown conglomerate.

The detailed map of the Watsons Brook area (figure 3.11) shows where bedding, S1, and S2 are parallel. As described in section 3.4.3, this is partly attributable to shearing along attenuated F2 limbs. However, as shown in figure 3.15, D1 and D2 structures are also rotated into parallelism within normal ductile shear zones.

With increasing distance to the west in the map area, the style of deformation is more brittle, with less late ductile deformation and more occurrences of steep brittle faults. Some of these steep faults have dip-slip indicators of fault displacement, usually quartz slickenfibres. Typical examples of these are seen at the boundary between the Watsons Brook and Corner Brook Sheets in the Little Feeder Brook area (insert 3).

Thick quartz veins are observed at location S with strong dip-slip slickenfibres that are clearly indicative of brittle dip-slip faulting. Across this fault, there is a major change in lithology from Irishtown formation of the Corner Brook succession in the west to Pinchgut Lake Group of the Watsons Brook succession in the east. A significant amount of normal displacement is required to bring Irishtown formation from the Corner

Brook succession down to the structural level of the Watsons Brook succession. The bedding and early foliations indicate reverse kinematics. However, this is interpreted as a reactivated S2 shear surface or steep fold limb, due to the normal displacement required for juxtaposition of the two thrust sheets (insert 3).

### ***Variable kinematics***

In addition to the mainly dip-slip normal faults described above, faults are also observed throughout the map area with components of both reverse and strike slip separation. Examples occur in locations Q, T, and U. Many of these reverse and strike-slip faults are considered related.

At location T, in the shale dominated section in Little Feeder Brook, the plane of slip is not preserved. Conjugate kink faults are observed and interpreted as related to the fault. The geometry of the conjugate kink folds indicates a shortening direction consistent with reverse dextral displacement on the fault (figure 3.16).

At location Q, in addition to the ductile normal-sense shear planes described above, there is a group of faults with mostly reverse and dextral kinematic indicators. These faults overprint the ductile normal shear planes and have well developed calcite slip-fibres indicating kinematics on each slip plane. Three graphical fault slip analyses were used on the data collected at location Q. The first method was the dynamic P dihedral method (Angelier and Mechler 1977), which indicated a general northwest-southeast axis of compression (figure 3.17). The P & T axes method (Allmendinger et al 1989), which displays a scatter plot of strain axes derived from individual faults (figure 3.17), yields a cluster of shortening axes with a similar orientation. The extension axes are quite variable (figure 3.17).

Linked Bingham statistics provide objective maxima of the shortening and extension axes for a set of faults (Mardia 1972). These maxima are calculated separately by addition of the kinematic strain axes from each fault. The method results in an unweighted moment tensor summation or, equivalently a tensor summation with uniform weighting (Allmendinger et al 1989, Marrett and Allmendinger 1990). This method indicates a shortening direction with a trend of 123° and plunge of 9° (figure 3.17) consistent with the previous methods. Of the two late crenulation lineations, one is subhorizontal (figure 3.14) and lies approximately within a plane perpendicular to the shortening axis consistent with these faults. This perpendicular plane contains both the intermediate and extensional axes of strain. This geometric relationship perhaps indicates a relationship between one generation of crenulation lineations and the late faults present at location Q.

### ***Map scale E-W block faulting***

In addition to the outcrop-scale faults described above, map scale outcrop patterns require a solution involving late faults. At location U, several faults have been invoked to interpret the relationship of Cooks Brook, Blow me Down Brook, and Irishtown formations, in close proximity along strike. One of these is a well-constrained fault with a horizontal separation of at least 4 km. Individual fault planes do not outcrop but contacts between formations in this area (location U) coincide, in several instances, with linear topographic features observed in the field.

The solution adopted for this area (figure 3.18), specifically, a distinct east-west trending horst structure, requires either dextral strike-slip along an east-west fault or normal dip slip on a southward dipping fault plane, or, most likely, a combination of

these two displacements. As shown in figure 3.18, a series of steeply dipping fault planes, with oblique slip, creates a horst structure and the resulting map pattern.

The orientations and inferred displacement of these faults are possibly related to the compression and shortening calculated from outcrop-scale fault analysis. A northwest-southeast shortening direction (trend 123 plunge 9, figure 3.17) was calculated for the faults at location Q. This shortening direction, when applied to an east-west fault structure, such as the fault interpreted at location U, would result in dextral strike-slip (figure 3.18).

### **3.5.4 Overprinting**

Most of the late structures described above clearly overprint D1 and/or D2 structures. Very few occurrences of later structures overprinting one another are observed, so their relative timing is somewhat tentative. Three groups of later structures are present at the scale of this study: normal dip-slip shear zones, both ductile and brittle; crenulation fabrics and ESE-WNW folds; and shallowly plunging crenulation lineations, kink folds, and oblique slip faults. Within the map area there were no observations of overprinting between the normal shear zones and the ESE-WNW folds. However, in the nearby Old Man's Pond area normal-sense shear zones are folded by northwest-trending folds (Waldron et al 2003). Therefore, in the Corner Brook area the normal shear zones are interpreted to be D3 structures while the ESE-WNW folding and associated crenulation fabrics are interpreted as D4 structures. The shallow crenulation lineations are observed overprinting the L4 crenulation lineations and are interpreted as L5. Additionally, the D5 faults, where observed, cross-cut all earlier fabrics, including a S3 normal ductile shear zone at location Q (figure 3.19).

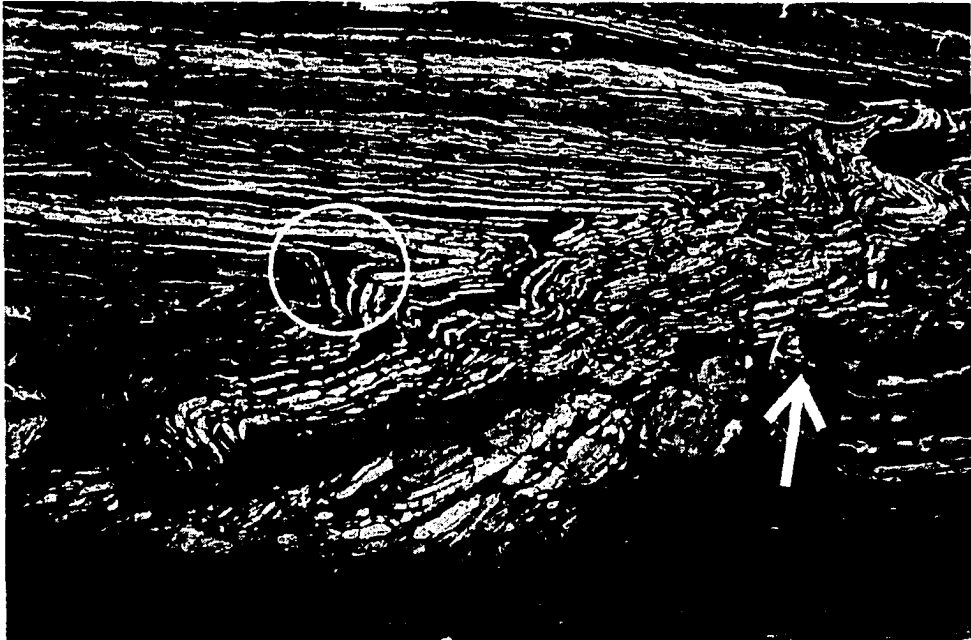
Figure 3.1

Illustrations showing soft sediment deformation.

A) Ribbon limestone of the Cooks Brook formation showing the progression from continuous planar beds (top left) to boudinaged and eventually incoherent bedding (bottom right). Additionally, note the thickening of the black shale in the hinge zone of the circled fold (Class 3 fold). Photo taken in Clarkes Brook, arrow highlights the hammer for scale.

B) Sheet structures creating a ripple-like effect on a sandstone bed surface in the Irishtown formation at location G

A)



B)



Figure 3.2

A) An outcrop-scale F1 isoclinal fold with a line representing the axial trace. B) a hand-sample-scale example of an F1 isoclinal fold. C) demonstrates refolded F1. A and C are taken looking east and show the same west vergent fold.

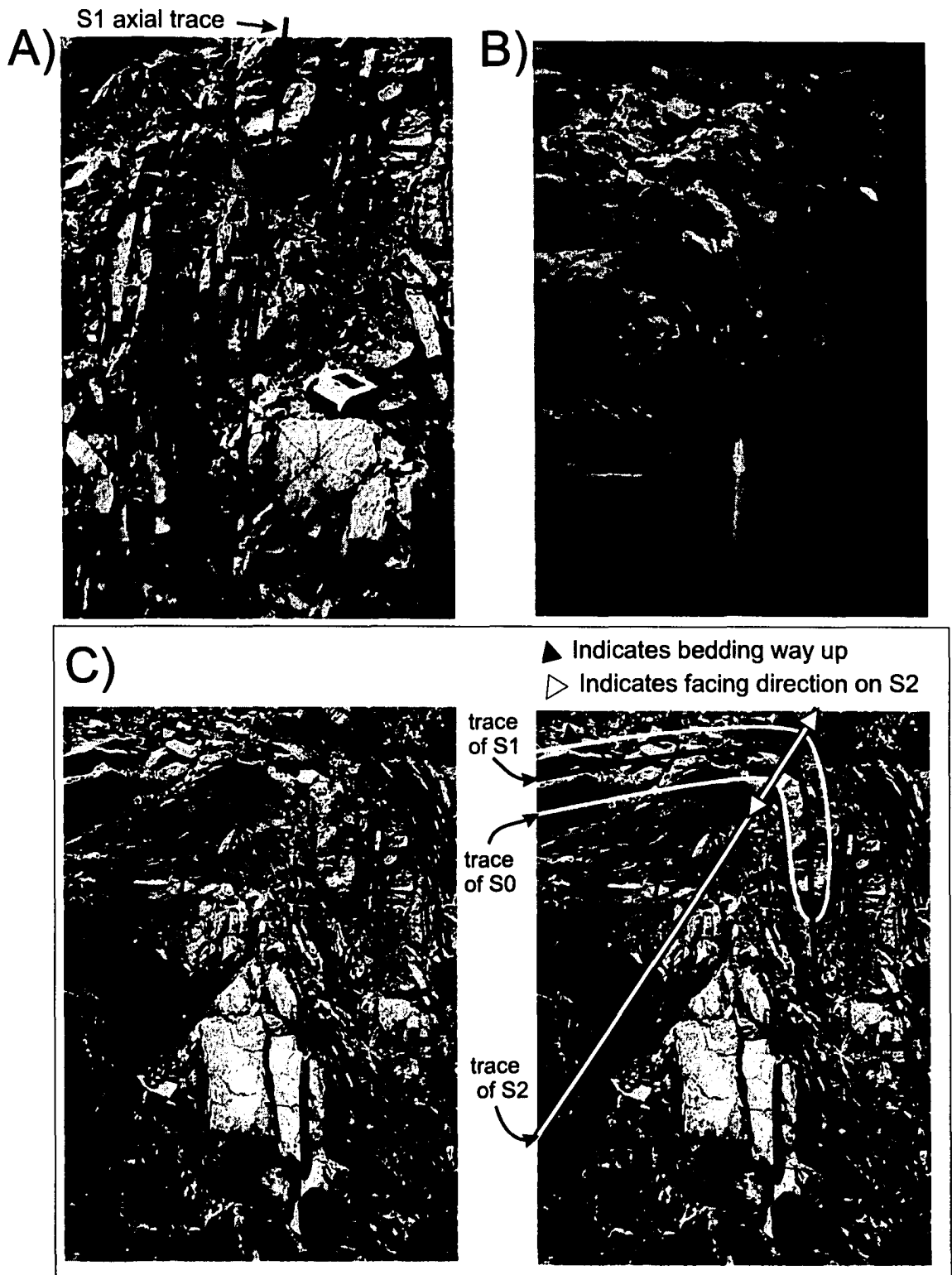


Figure 3.3

Thin section photos showing mica crystals in bed parallel orientations.

A) Bedding folded by F2. Thin section shown under crossed polars.

B) Close up on fine grained portion of the thin section, this photo showing micas oriented in a fabric parallel to bedding. Crossed polars.

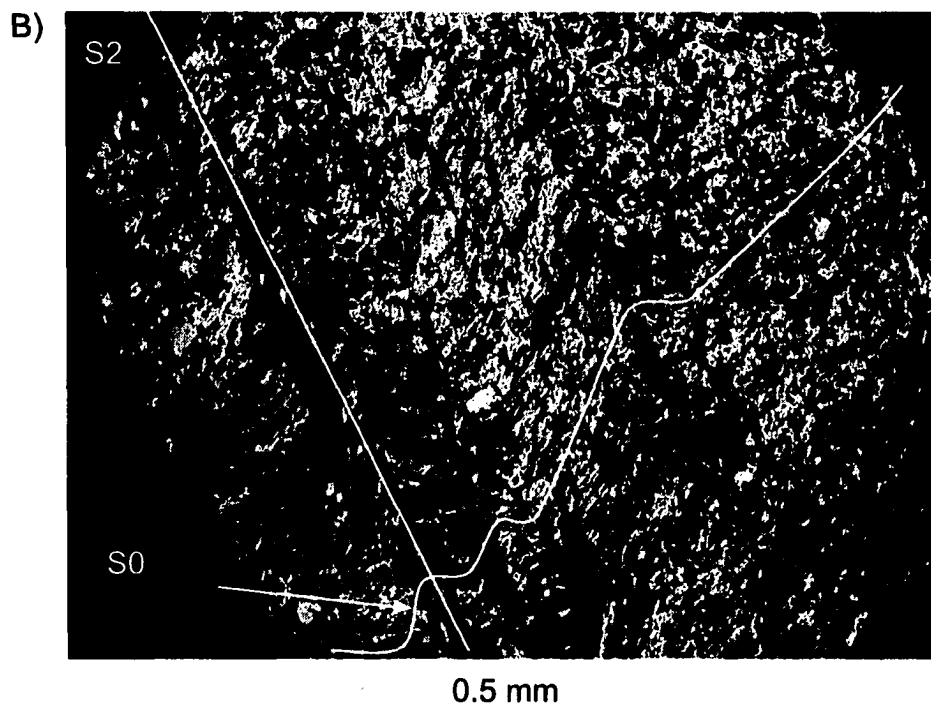
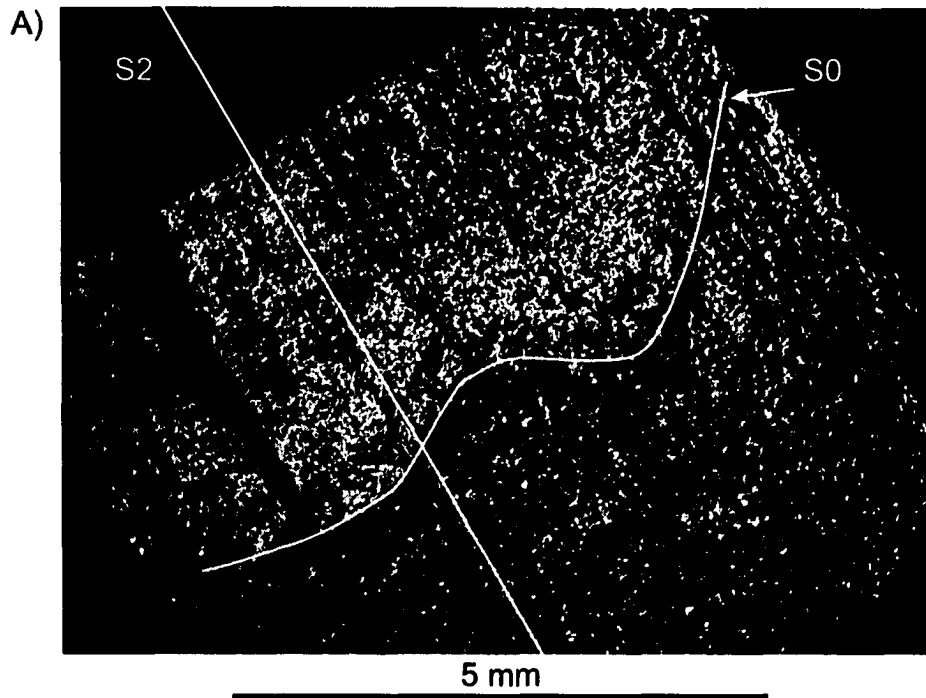


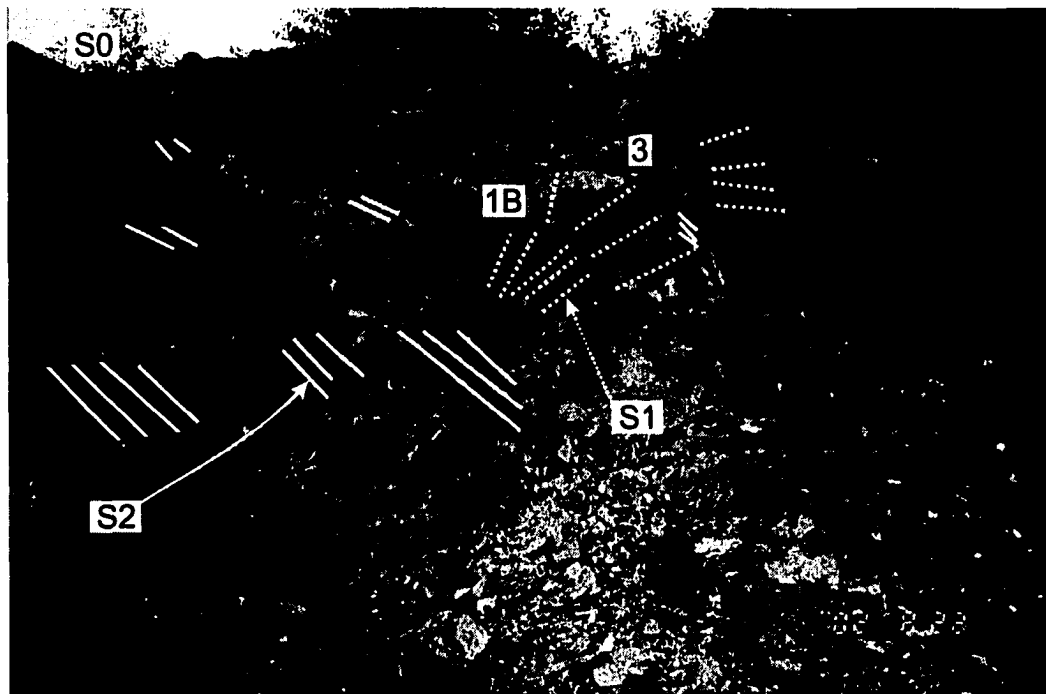
Figure 3.4

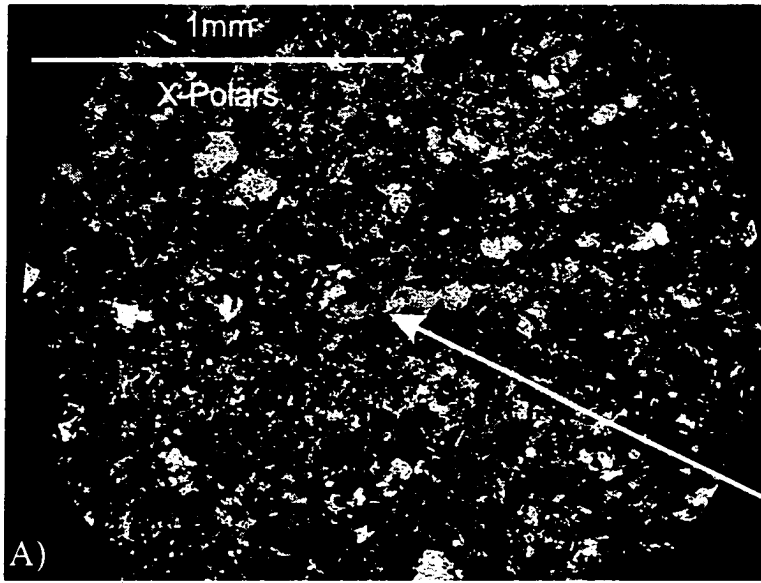
Photo of an F1 west-vergent fold with axial planar S1 dissolution cleavage and cross-cutting S2 slaty cleavage. S1 dissolution cleavage is primarily developed in the hinge zone. Annotations show bedding, S1, and S2 cleavages. Note the refraction of S1 through the competent sandstone beds and the class 1B and class 3 folds in the hinge zone (labelled 1B and 3).



070

250





Partially dissolved quartz grain within pressure solution band

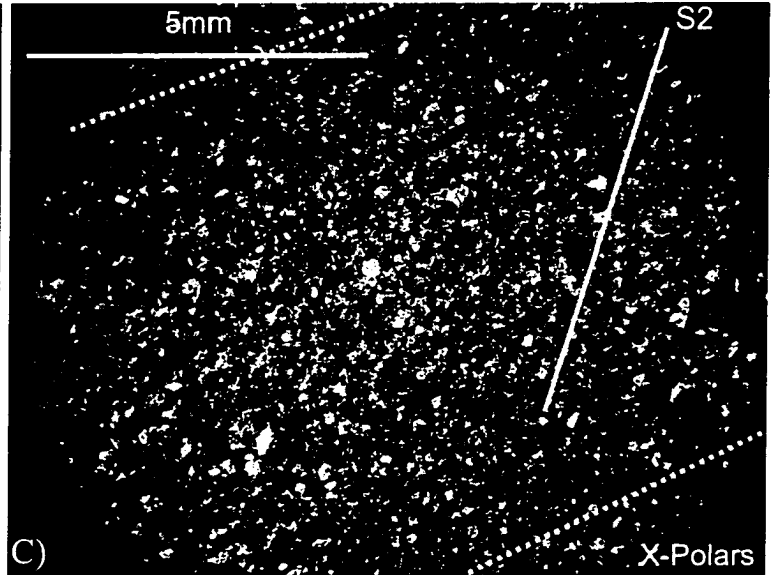
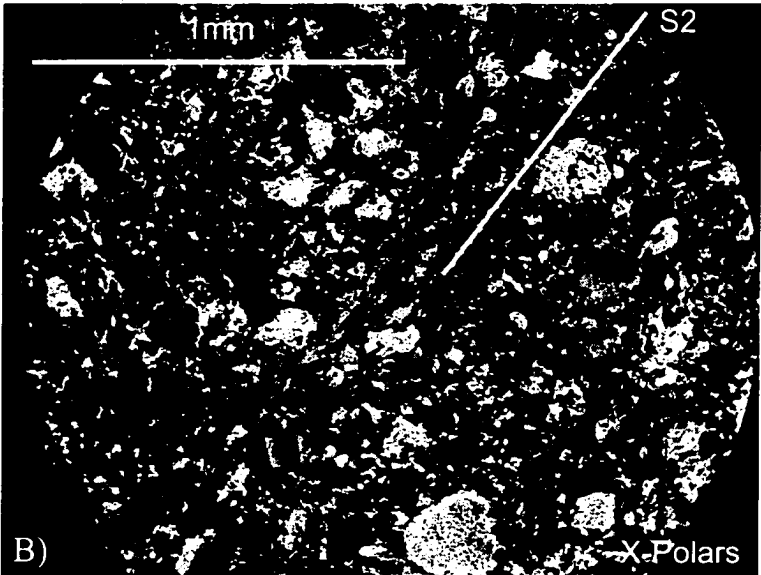


Figure 3.5  
Thin section photos of pressure solution cleavage and the relationship to S2 oriented micas. Sample taken from Watsons Brook (Locality L). A) Quartz- poor microlithon with partially dissolved quartz grain(s) indicating that the spaced foliation is t a dissolution cleavage B) close up of B showing an aggregate cluster of muscovite crystals aligned parallel to S2 C) the relationship between the micaceous S2 cleavage and the S1 dissolution cleavage. Dashed lines highlight dissolution bands that surround an area of preserved initial sediment.

Figure 3.6

Stereonet showing the distribution of F2 fold axes measurements at locations O and N and the curved character of their curved fold hinges. Fold axes range from north plunging to south plunging. Also shown is the distribution of the axial planes of F2 folds at locality O.

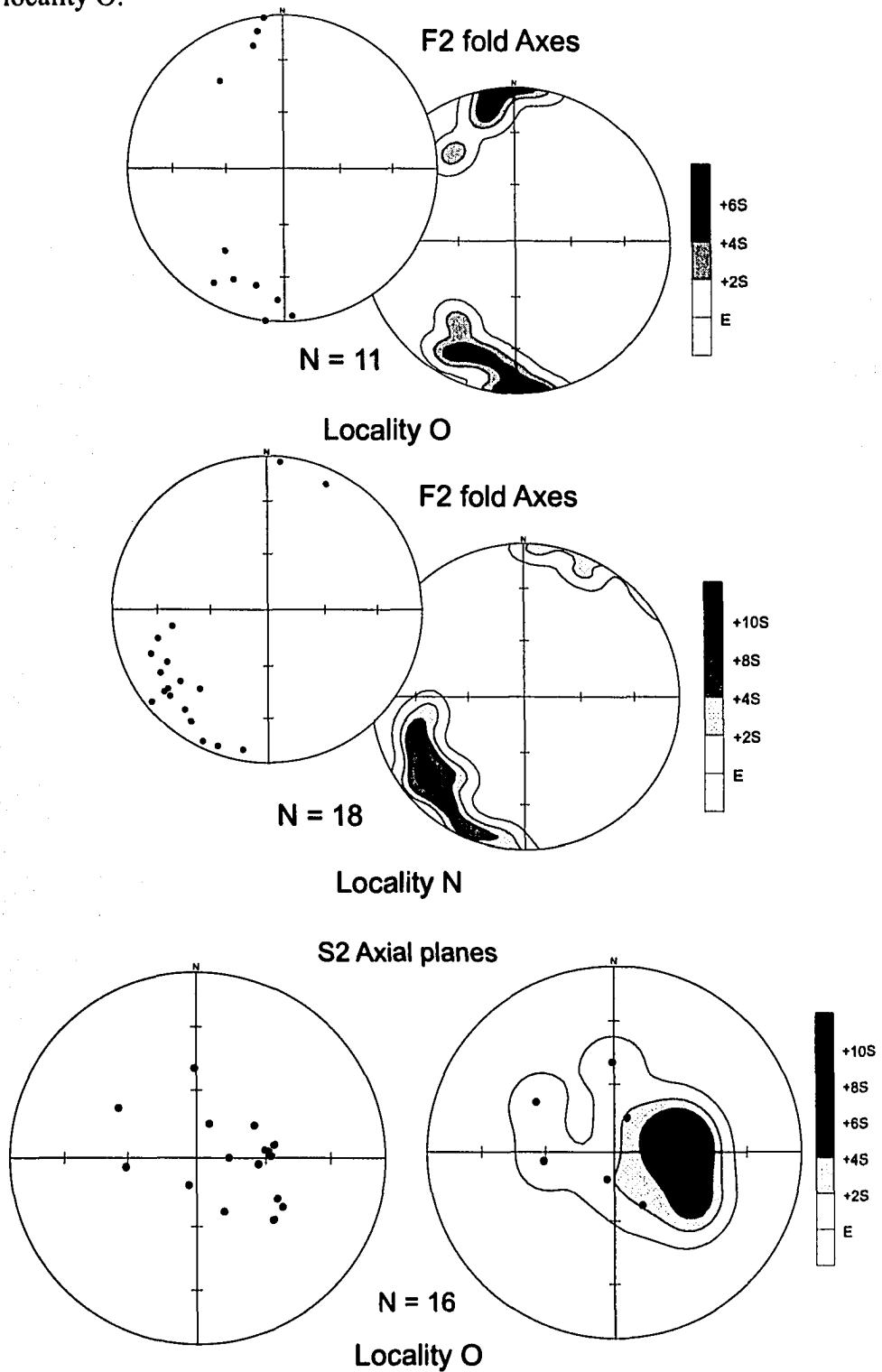


Figure 3.7

Sigma structure showing reverse shear-sense indicators along the S2 foliation. Photo taken looking north, hammer for scale.

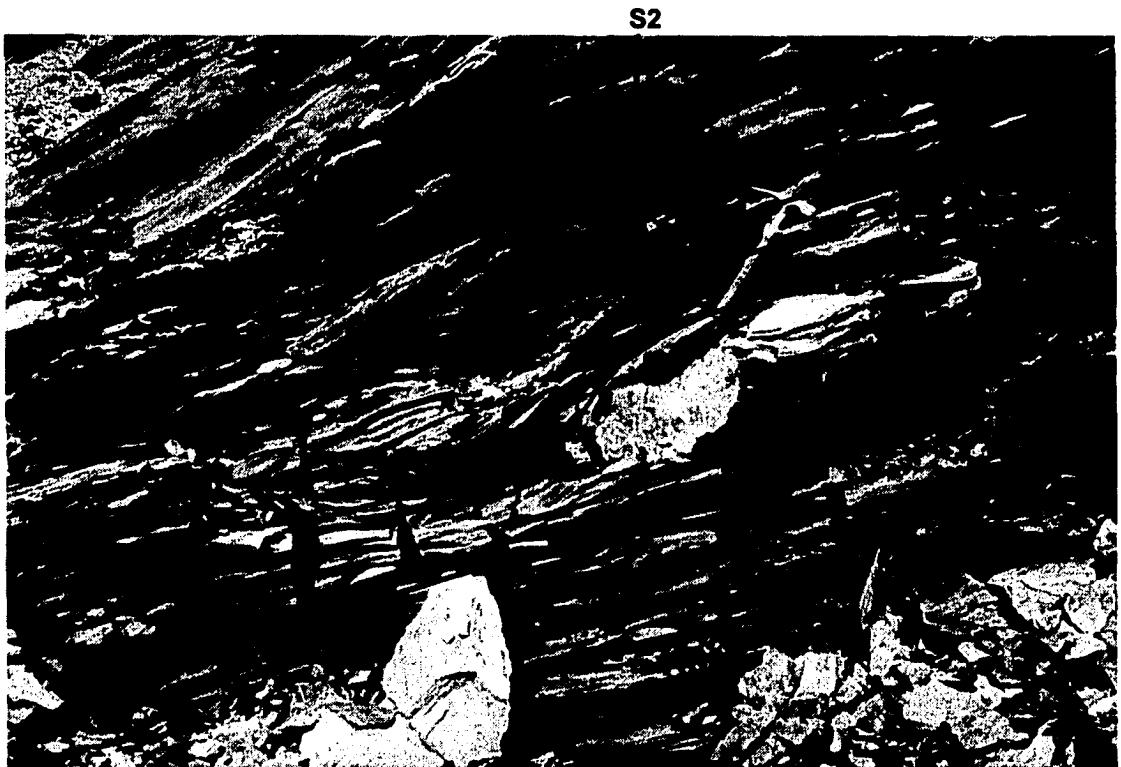


Figure 3.8

Thin section photos showing tectonic mica and chlorite oriented parallel to the S2 foliation. Also shown is deflection of the mica-rich fabric around competent lithic fragments in the rock.

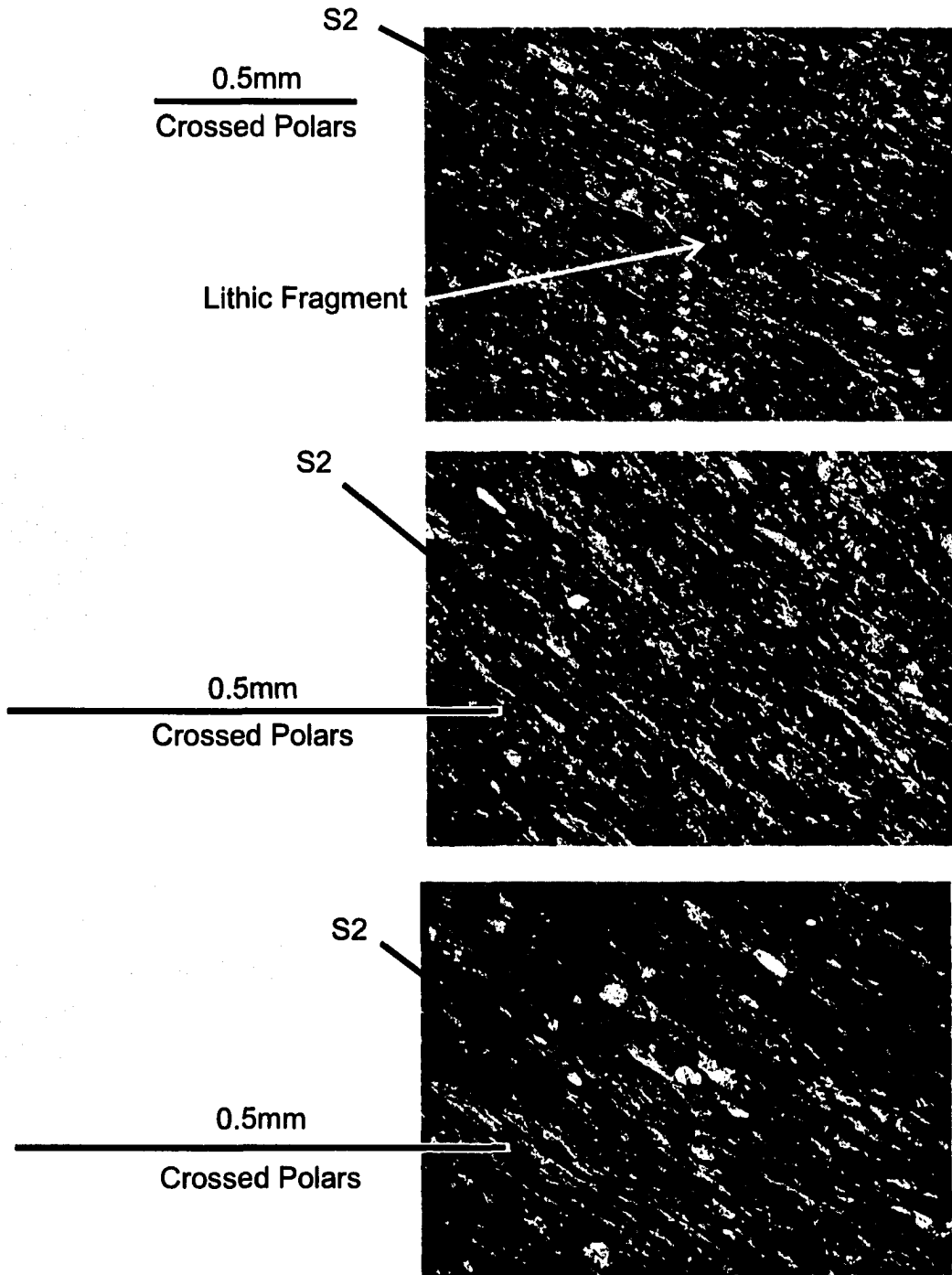
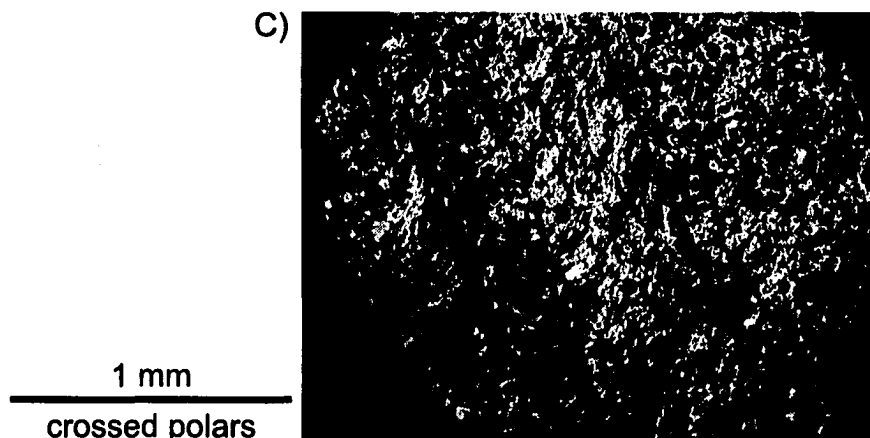
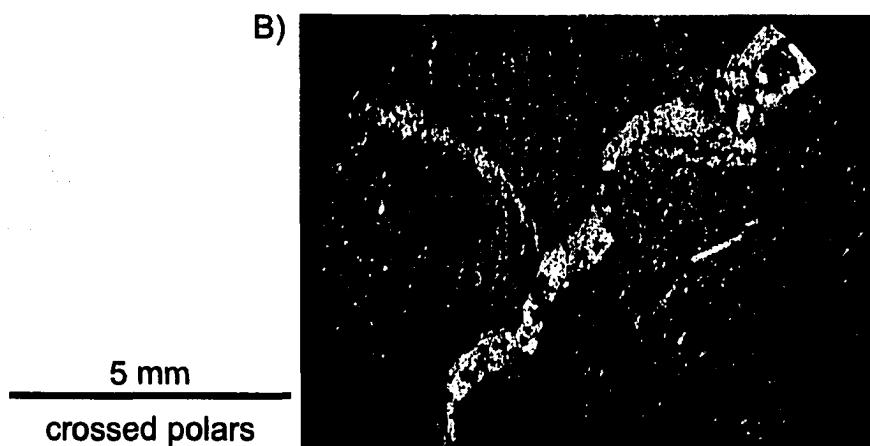
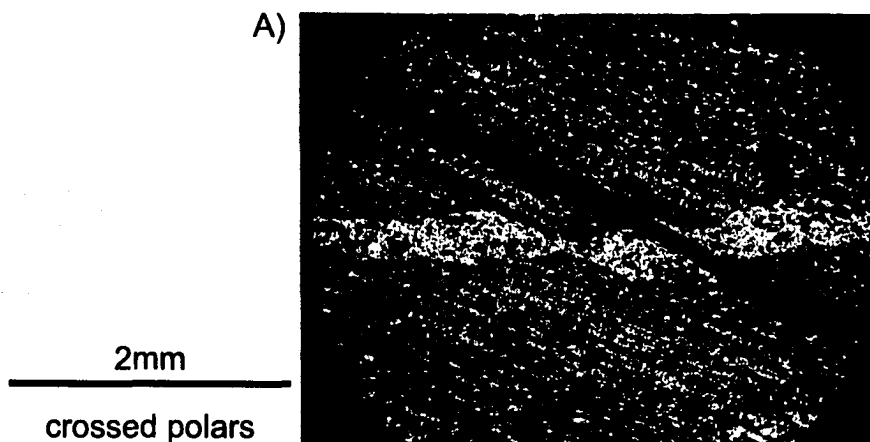
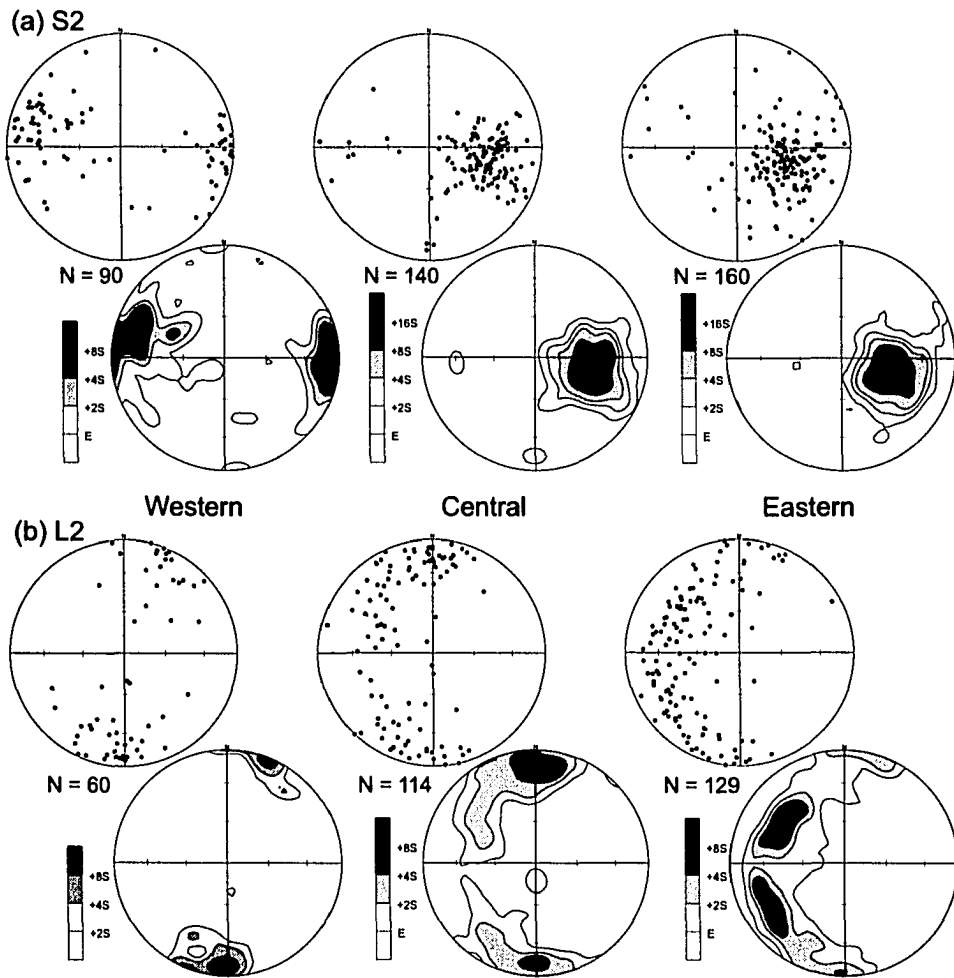


Figure 3.9

Thin section photos showing S2 fabric characterized by a discrete crenulation. The minor displacement observed in A is oblique. Displacement is constrained to dextral and either slightly reverse or slightly normal.



**Figure 3.10**  
 Equal area stereoplots showing the change in orientation of S2 foliation and L2 lineation across the map area. Western, central, and eastern refer to areas shown on map 1.3 (adapted from Waldron et al 2003).



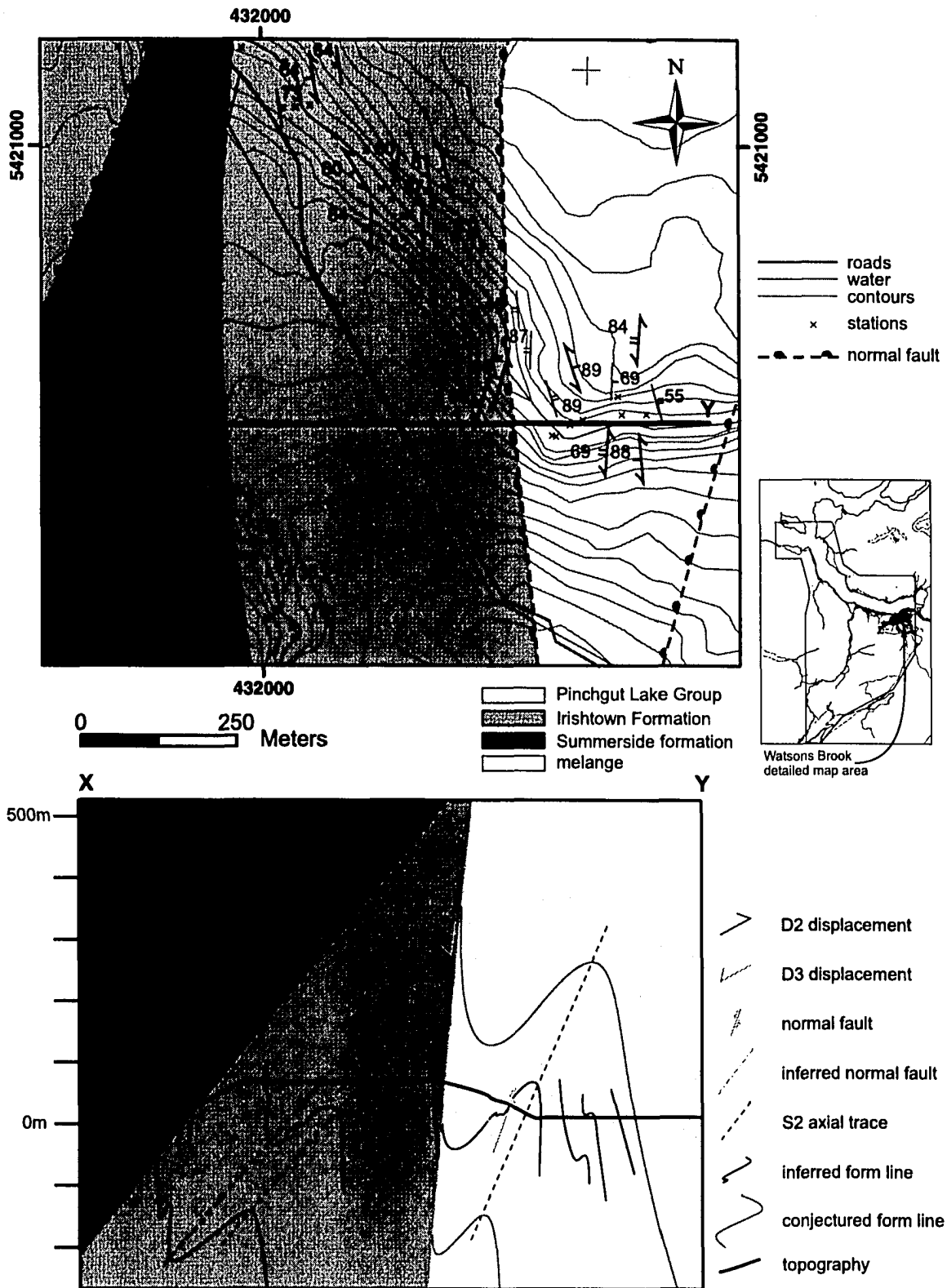


Figure 3.11  
 Map and cross section of the Watsons Brook area. Mapping was executed in this location at 1:5000 scale. The location of this map is shown in the inset and on insert 2.

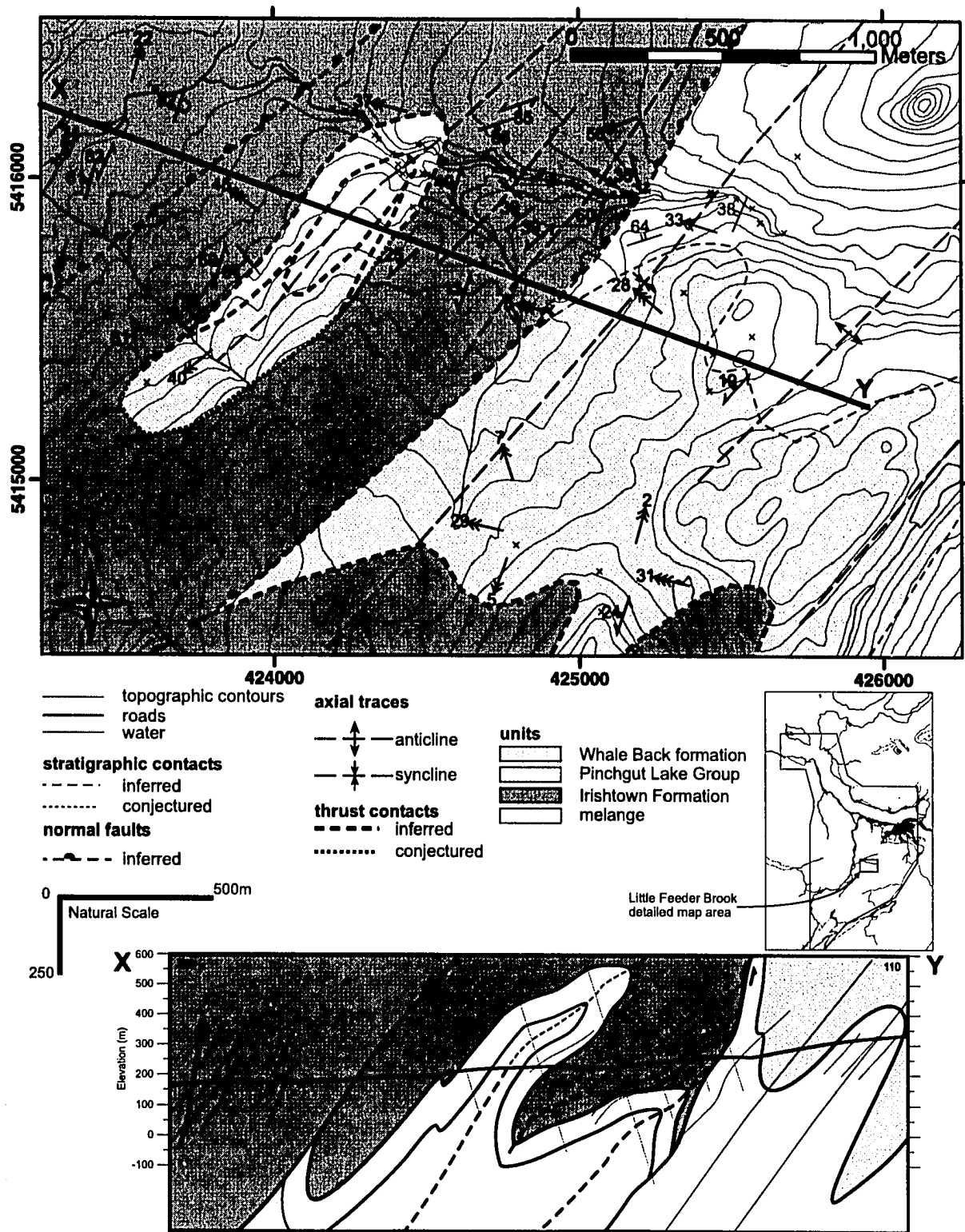


Figure 3.12  
 Map and Cross section of the Feeder Brook area. Mapping was executed at this location at 1:5000 scale. The location of the Feeder Brook area is shown on insert 2.

Figure 3.13

Equal area stereoplots of bedding and S1 fabrics across the map area. The sub-areas from which these measurements are taken are shown in Fig 1.3. S1 and bedding show the strongest parallelism to S2 fabric orientations in the eastern sub-area (Waldron et al 2003).

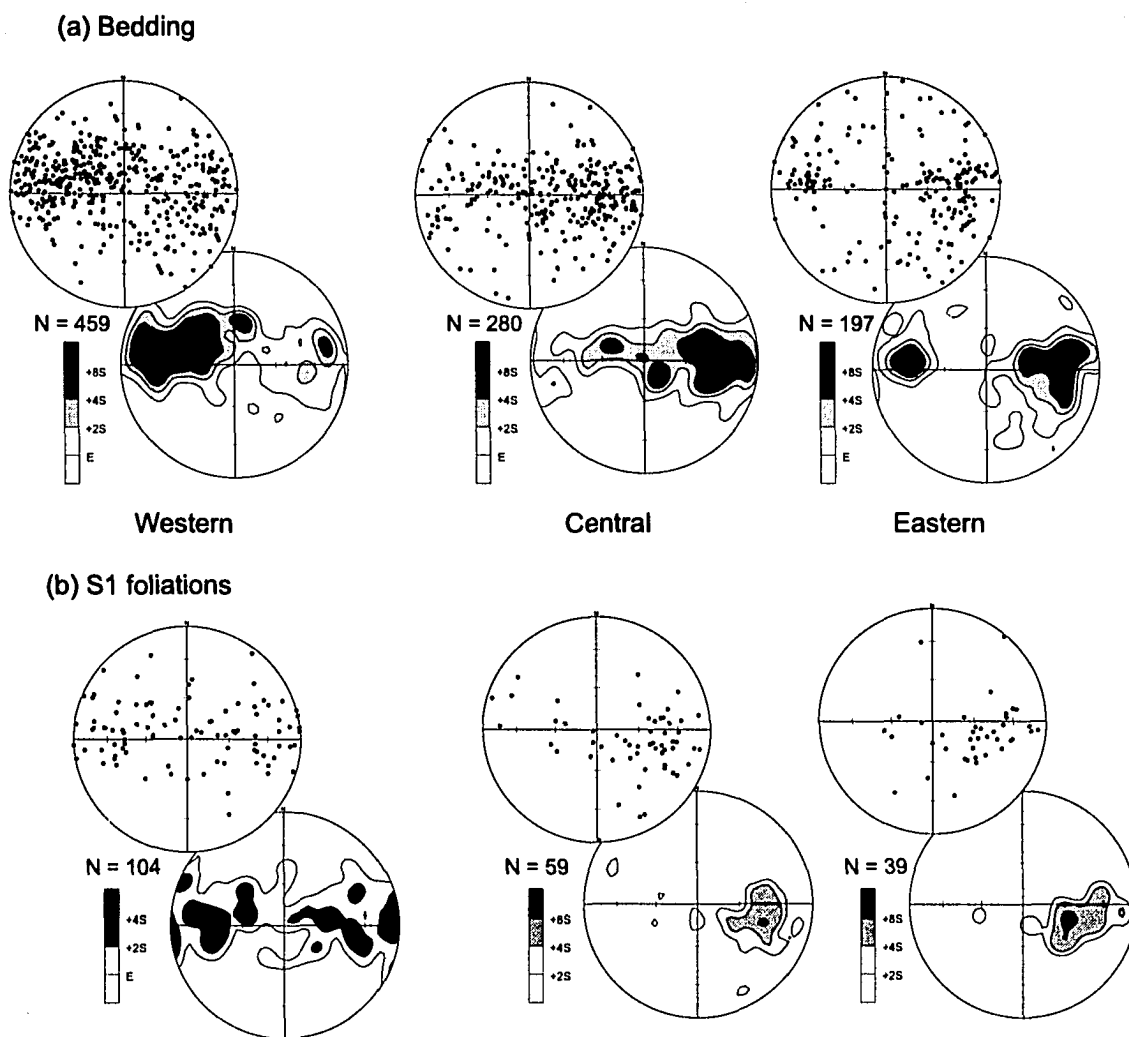


Figure 3.14

Equal area stereoplots of L3 to L5 lineations, and a population of S2 poles gently folded about an F4 fold.

A) Contoured equal area plot of all lineations identified in the field as L3 or higher. Crenulations are most commonly observed on S2 fabrics, indicating that they are later than D2. the dashed line shows the regional S2 fabric from the eastern sub-area of the map (shown in Fig 3.10).

B) Contoured equal area plot of poles to the spaced cleavage and axial planes of late folds, interpreted as S4.

C) Contoured equal area plot of poles to the S2 foliation in the Watsons Brook area (Insert 2). Shows a girdle distribution (strike 052, dip 32 SE) about a westward trending and steeply plunging fold axis (trend 322, plunge 58).

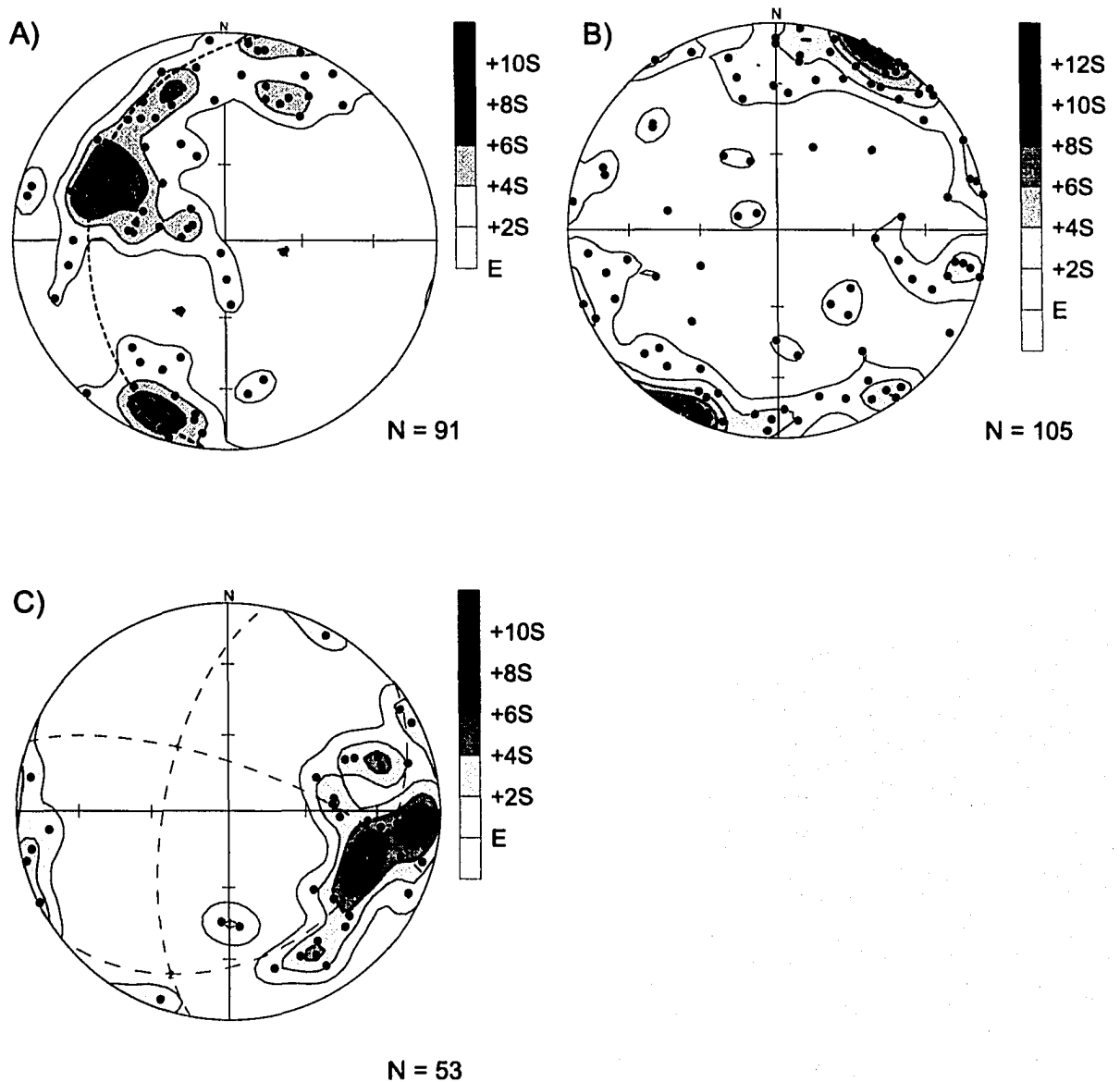


**Figure 3.15**  
**Photo and sketch of S3 shear surfaces deforming L2 lineations showing normal-sense kinematics.**

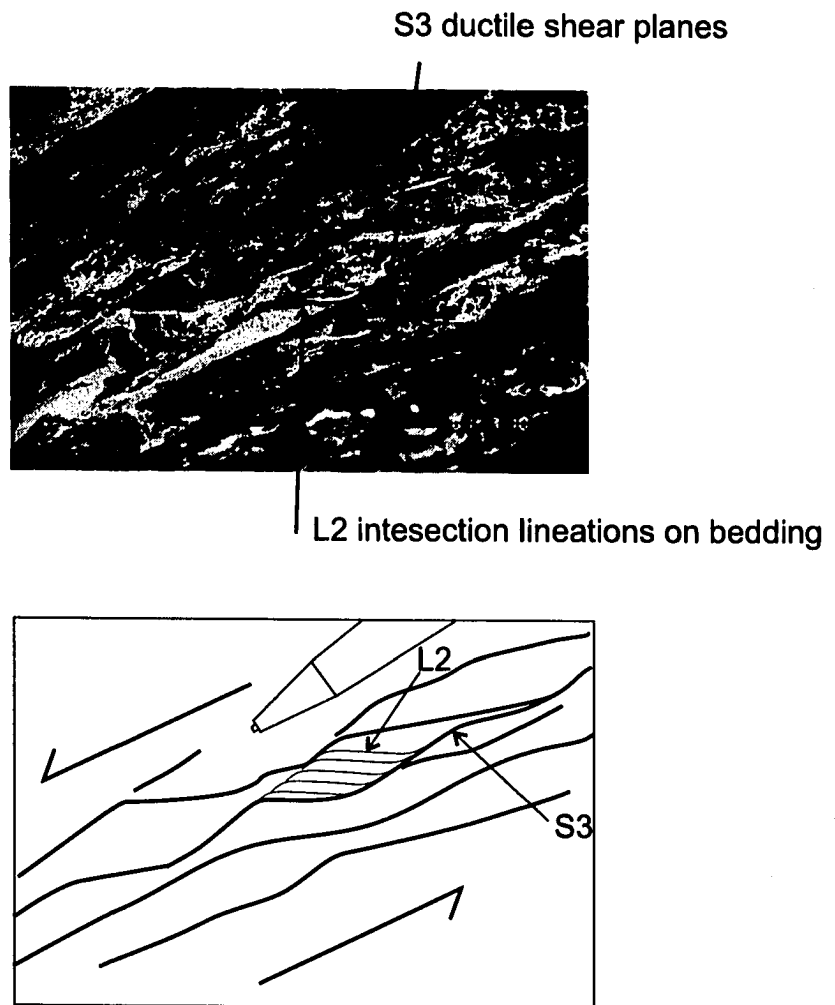


Figure 3.16

Late east-dipping fault zone in Little Feeder Brook and the associated kink fold observed at location T. The lithology is entirely black shale. A conjugate kink fold set is observed in close proximity to the margin of the fault zone. Based on to the orientation of the kink fold, the sense of displacement on the fault is interpreted to be reverse and dextral. Measurements are given in right hand rule notation. Photo was taken looking approximately north.

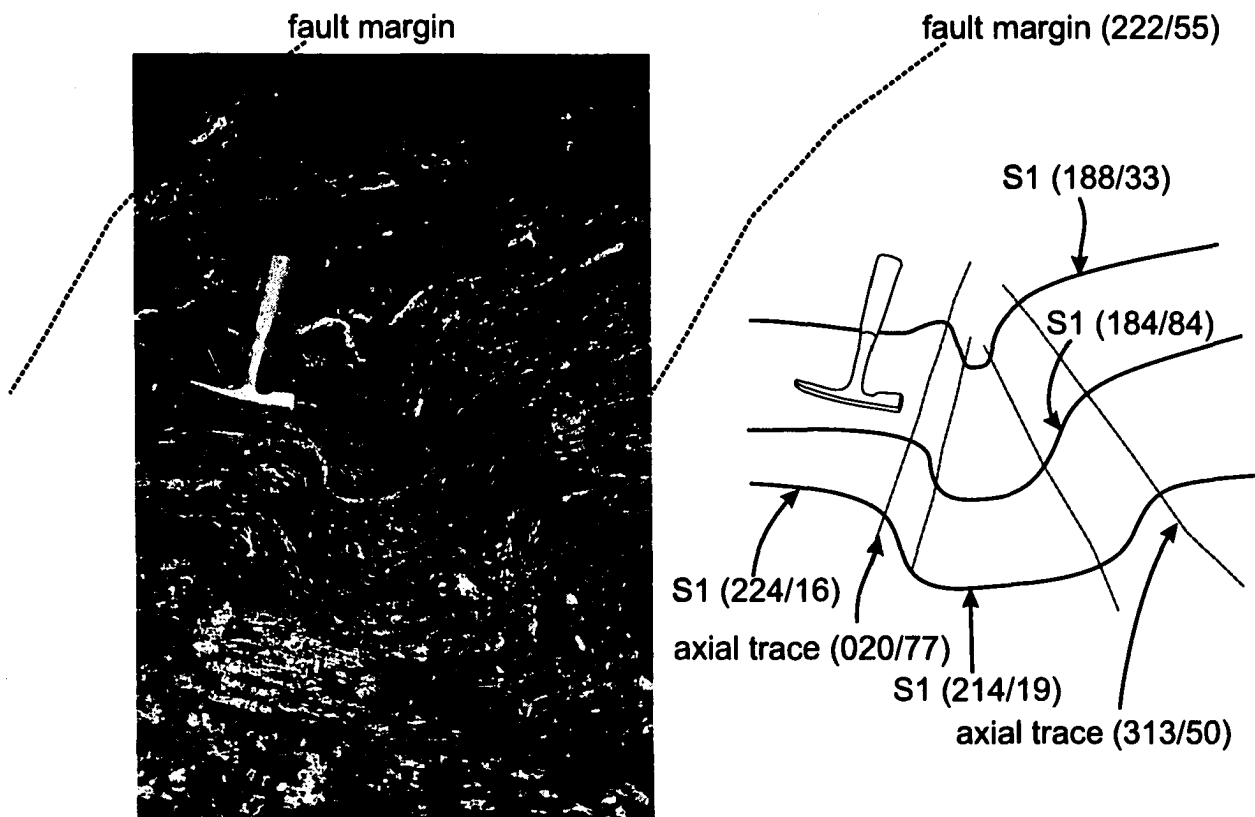


Figure 3.17

Kinematic and dynamic graphical analyses of the faults measured at location O. All plots are on an equal area stereonet. The dataset for all plots is 10 fault planes and lineation measurements.

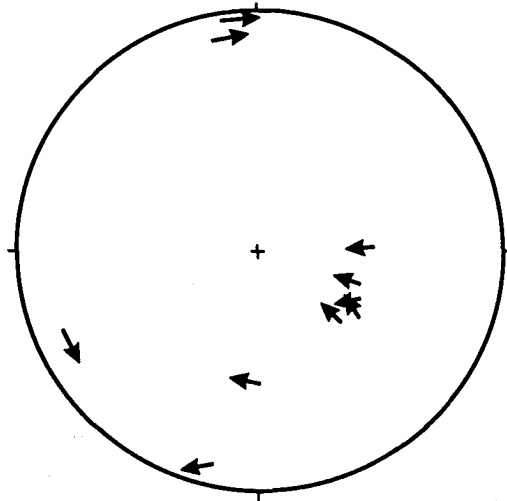
A) Fault planes with arrows indicating the direction of movement of the hanging wall.

B) PT dihedra. Numbers on the plot indicate the number of possible compression quadrant occurrences, out of a total of 10.

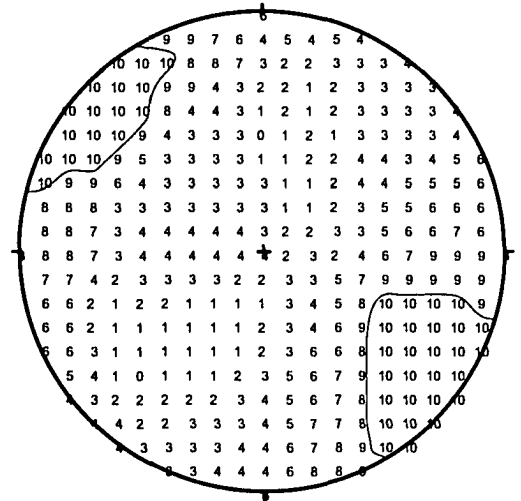
C) Scatter plot of the P and T axes individually plotted for all 10 of the faults measured.

D) Linked Bingham axes showing the axis of shortening at 123/9 (3), the axis of extension at 238/69 (1), and the intermediate axis at 030/18.6 (2). Also on this plot is the fault tensor solution for the Bingham axes. The calculated nodal planes are 234.5°, 39.4° and 017.5°, 56.7° (right hand rule notation).

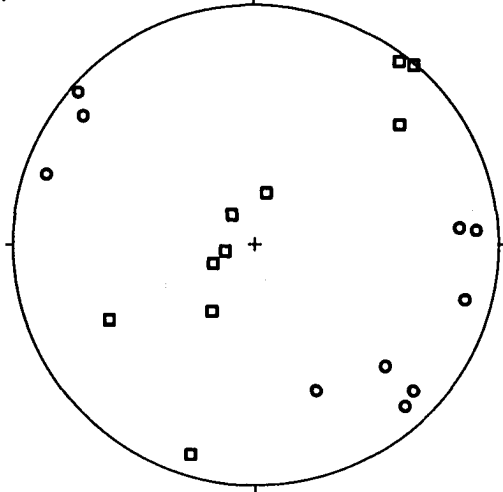
A) Slip Linear Diagram



B) P Dihedra

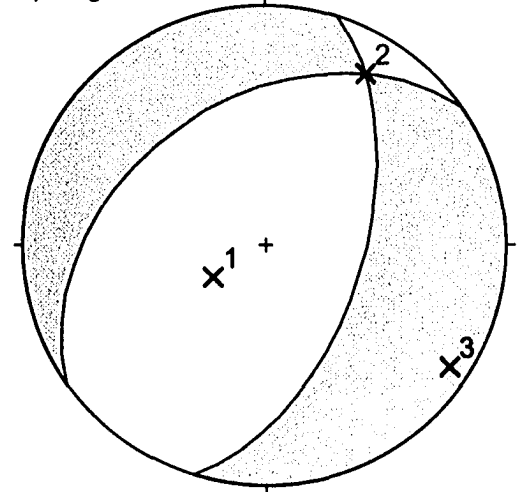


C) P-T Scatter Plot



- Axis of shortening
- Axis of extension

D) Bingham Axes



- Zone of Compression
- × Bingham axes

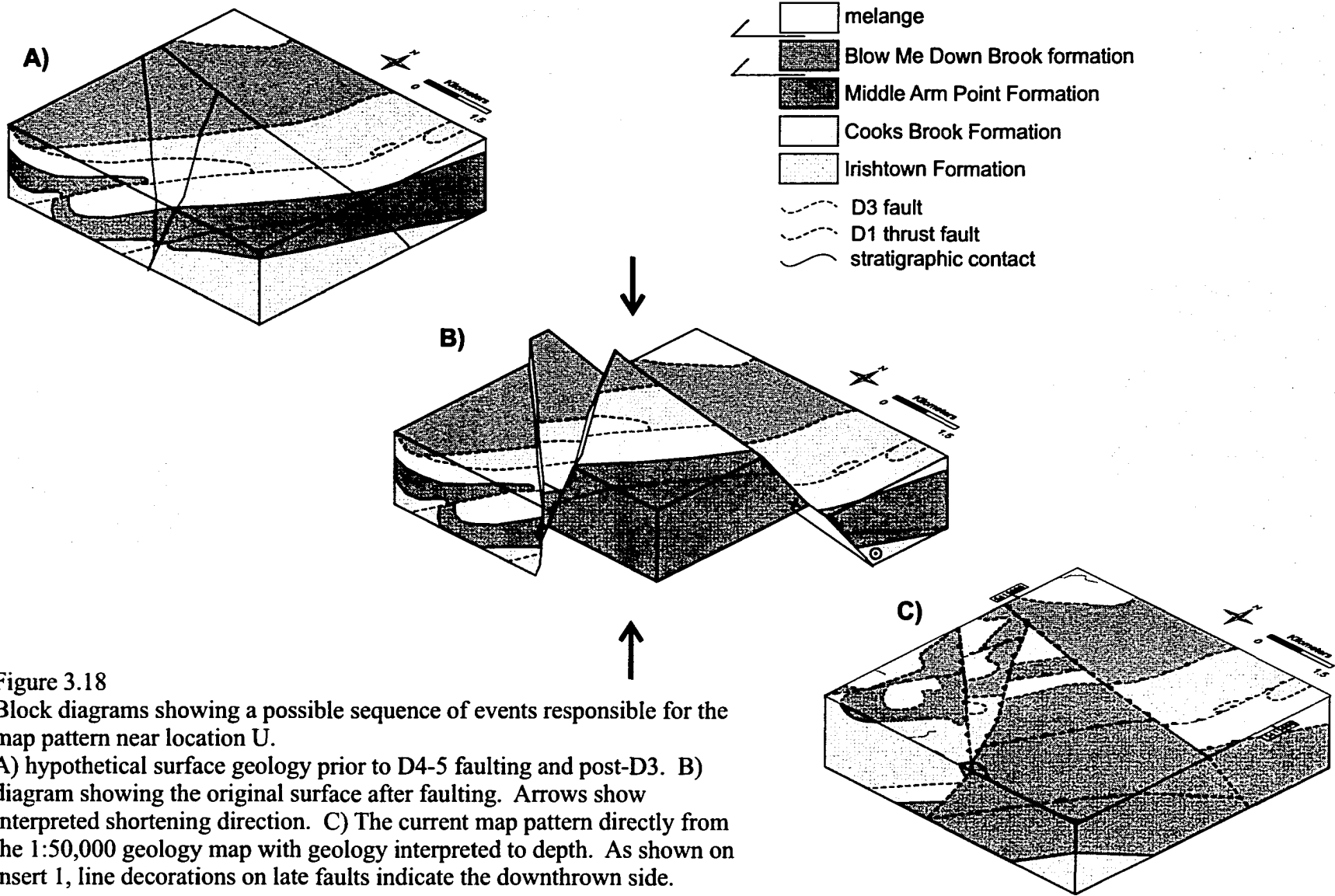
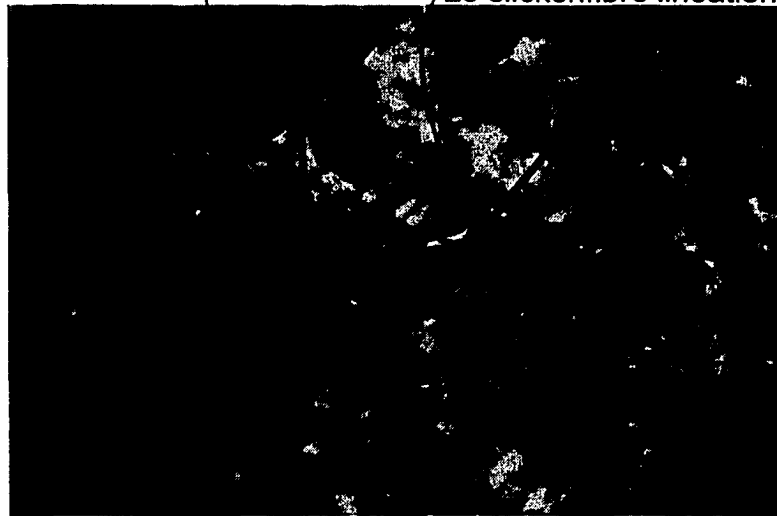


Figure 3.18  
 Block diagrams showing a possible sequence of events responsible for the map pattern near location U.  
 A) hypothetical surface geology prior to D4-5 faulting and post-D3. B) diagram showing the original surface after faulting. Arrows show interpreted shortening direction. C) The current map pattern directly from the 1:50,000 geology map with geology interpreted to depth. As shown on insert 1, line decorations on late faults indicate the downthrown side.

Figure 3.19

D3 normal-sense structures overprinted by a D5 brittle reverse-sense fault. Outcrop photo is taken at location O. The pencil in the photo shows the orientation of the L3 stretching lineation in the surface. Overprinting L3 are calcite slickenfibres that indicate reverse and dextral kinematics.

L3 stretching lineations / L5 slickenfibres lineations



## Chapter 4: Isotopic Dating

### 4.1 Introduction

Many samples from the internal Humber Zone and the Dunnage Zone have been analyzed using various radioactive decay systems to constrain the age of peak metamorphism and plutonism (Dallmeyer 1975, Williams et al 1985, Dunning et al 1987, Whalen et al 1987, van Berkel and Currie 1988, Dunning et al 1990, Cawood and Dunning 1993, Cawood van Gool 1998, Brem et al 2003). However, other than work done on the Bay of Islands ophiolite, in the external Humber Zone there have been relatively few dates collected, most of them on detrital grains. U-Pb isotopic age dates were obtained on detrital zircons to aid in paleogeographic reconstruction of the eastern Laurentian margin (Cawood and Nemchin 2001). Detrital muscovite grains in the Ordovician flysch in the foreland basin were analyzed using  $^{40}\text{Ar}/^{39}\text{Ar}$  isotopic dating, yielding an age range from 460 to 490 Ma (Idleman 1998).

#### 4.1.1 Argon/Argon method

The  $^{40}\text{Ar}/^{39}\text{Ar}$  isotopic age dating method uses the decay of  $\text{K}^{40}$  to  $\text{Ar}^{40}$ , therefore providing a tool to isotopically date potassium-bearing minerals, such as mica. Because argon is commonly gas at crystallization temperatures, it escapes quickly from a mineral if not trapped within a crystal lattice. Closure represents the range of temperature through which a mineral must cool to prevent argon escaping from the crystal lattice. An age recorded by the Ar-Ar system represents a temperature of closure that is different for every mineral; it occurs at  $\sim 350^\circ\text{C}$  for muscovite (McDougall and Harrison 1999). Low

temperature crystallization of muscovite can occur at temperatures less than 350°C.

Therefore, age dates on tectonically grown white micas often record the time of crystal growth and the associated deformation (McDougall and Harrison 1999). The occurrence of mica intergrowth of several generations requires that the fabric relationships need to be well understood if ages based on isotopic dating are to be interpreted.

Samples taken near the eastern contacts of the Watsons Brook succession with the Platform succession, and within shear zones in the platform carbonate units, show tectonically grown mica and chlorite crystals. Twelve mica-bearing samples were analyzed, using whole rock and mineral separate methods, in an effort to determine the age of mica crystallization. Within these samples are several generations of tectonic mica crystals as well as potassium-bearing detrital minerals such as feldspars, micas, and clays.

#### **4.1.2 Rhenium/Osmium**

Rhenium/Osmium (Re-Os) isotopic dating of sulphide minerals is a relatively new geochronological method that uses the decay of  $^{187}\text{Re}$  to  $^{187}\text{Os}$  to calculate the age of sulphide mineralization. Pyrite nodules 3-10 cm in diameter from three samples (JA094C, JD003B, and JD002A) collected within mélange zones near Frenchman's Cove were analyzed for rhenium to determine if they were useful for dating using the Re/Os technique. The concentrations of Re determined from 4 analyses were 2.09ppb, 0.76ppb, 1.22ppb, and 1.00ppb (R. Morelli, personal communication 2004). Given the approximate age of the samples, isotopic decay of  $^{187}\text{Re}$  at these concentrations would not produce sufficient  $^{187}\text{Os}$  to allow for accurate Os isotopic measurement using the current Re-Os methodologies (R. Morelli, personal communication 2004). This method was not pursued further.

## 4.2 Argon dating methodology

The  $^{40}\text{Ar}/^{39}\text{Ar}$  isotopic age method of dating is based on the decay of  $^{40}\text{K}$  to  $^{40}\text{Ar}$ , which is a process that involves electron capture. The original K-Ar method of analysis measures separately the potassium and argon in two aliquots. The resulting ratio of the  $\text{K}^{40}$  and  $\text{Ar}^{40}$  isotopes defines the age of the sample. There are many problems with the K-Ar method and the  $^{40}\text{Ar}/^{39}\text{Ar}$  method is much more commonly used today.

The  $^{40}\text{Ar}/^{39}\text{Ar}$  method is presented in detail by McDougall and Harrison (1999) and is briefly summarized here. The  $^{40}\text{Ar}/^{39}\text{Ar}$  method is based on the indirect measurement of  $^{40}\text{K}$  in the sample using neutron activation analysis and isotope ratios. The sample is irradiated with fast neutrons in a nuclear reactor to convert some  $^{39}\text{K}$  to  $^{39}\text{Ar}$ . Converting the  $^{39}\text{K}$  is desirable because it exists in a constant ratio to  $^{40}\text{K}$ , therefore allowing the  $^{39}\text{Ar}$  to proportionally represent the parent isotope in the decay system. The sample is then incrementally heated, using either a furnace or a laser, in steps (step heated) in a vacuum. The argon isotopes released are measured using a mass spectrometer at successively higher temperature steps. An apparent age is calculated at each step based on the argon isotope ratio. These ages are then plotted on a graph against the fraction of total argon that is released, which is commonly proportional to the temperature increases. This graph is referred to as a spectrum. The argon measured at each step is theoretically produced from increasing depth in the crystal or crystals.

Preparation of samples for use in  $^{40}\text{Ar}/^{39}\text{Ar}$  dating can be done using several methods. Whole rock methods heat and analyze a small chip of the sample. Mineral separate analyses are run on individual size fractions of a specific mineral after various separation techniques; and laser methods use in-situ heating of individual crystals. Laser

techniques are often effective if there are mica crystals larger than the laser spot diameter present. Whole rock step-heating is used in very fine-grained slates/phyllites. However, the whole rock method is unable to differentiate inherited detrital components or multiple generations of growth, which can result in anomalous spectra due to multiple generation input. Sometimes crushing and separation of a specific size fraction can concentrate the crystals and produce a more reliable age.

A significant amount of interpretation is involved in understanding the spectra that result from this dating procedure. The simplest result is a horizontal profile, or plateau spectrum, that results from a population of crystals with homogeneous argon isotope ratios. This indicates that these minerals have experienced no argon loss, or diffusion. If there is a non-planar result, the spectrum is called disturbed. Disturbed spectra can exist in many forms, though they most commonly show an increase in age to the hotter end of the graph, demonstrating a loss of argon that increases towards the outside of the grains. Thermal events in the history of the rock are the most common cause of argon diffusion (McDougall and Harrison 1999).

### ***4.3 Sample descriptions & results***

Twelve mica-bearing samples were analyzed by Ar/Ar step-heating methods using either whole rock samples or mineral separates. The samples that were analyzed came from a variety of locations within and near the map area (figure 4.1). Results from four of the samples were interpreted as plateau ages, although all of the spectra were at least partially disturbed. Eight of the twelve results were discordant and showed some type of disturbed spectrum, making it impossible to interpret a perfect plateau age

although in a few cases weak plateaus were interpreted. Five samples gave total gas ages that were almost identical, allowing tentative interpretation of the time of crystallization.

### **4.3.1 DW170A**

The location of this sample is shown on figure 4.1. It was collected during earlier work outside the current area of mapping within an area covered by Ferguson during (1998), within the Blue Ponds thrust stack. There is abundant indication of ductile deformation through strained conglomerates and stretching lineations in several locations near this area. This sample is a calcite-cemented calc-quartz arenite with significant aggregates of muscovite.

#### ***Description***

This sample appears to have fine grained shear bands, parallel to the muscovite crystals. The finite shortening direction is perpendicular, in 2 dimensions, to the long axis of the muscovite flakes. Folded muscovite is observed in this sample and has been transposed into the same orientation as the shear zones. Additional sample description is in Appendix A.

The muscovite is interpreted as tectonic, formed as a result of shearing. There are no feldspar or clay minerals observed in this sample.

#### ***Spectrum***

Separation of this sample was possible using dissolution of the carbonate material with hydrochloric acid rinsing, producing a muscovite and quartz mineral separate. This separate was analyzed using the step-heating method. The spectrum is shown in figure 4.2 and appendix A and shows a plateau age of  $439 \pm 5$  Ma.

### ***Interpretation***

The isotopic age is interpreted as recording the tectonic crystallization age of the muscovite associated with a shear zone. This sample falls within the same age range as JA083A, JA083B, and DW065A.

#### **4.3.2 DW065A**

The location of this sample is shown on figure 4.1. It is a limestone sample taken from just outside the Corner Brook map area within the Table Point Formation. This sample is a sheared limestone with muscovite crystallization along lineated shear planes. This rock is 99% calcite, with a trace of muscovite. F2 folds and an S1 foliation with a stretching lineation are present here.

### ***Description***

Dark bands are observed in thin section, interpreted as carbonate mylonite. The shear planes are steeply west-dipping. However, the kinematics of shear along these planes are indeterminate. Additional sample description is in Appendix A.

All of the muscovite present in the rock is oriented parallel to, and associated with, the margins of the mylonite bands. Therefore they are interpreted as having crystallized during deformation.

### ***Spectrum***

Separation of the muscovite from this sample was accomplished by a series of hydrochloric acid rinses to remove the calcic material. This sample was analysed using a muscovite mineral-separate step-heating method. The spectrum is shown in figure 4.2 and appendix A. This spectrum was interpreted as showing a plateau age of  $439 \pm 5\text{Ma}$ .

### ***Interpretation***

This age is interpreted to record the age of the muscovite associated with the shear zone. This age is very close to those whole rock ages attained in samples DW170A, DW065A, JA083A, and JA083B.

### **4.3.3 JA083A**

The location of this sample is also within the Summerside formation in the Watsons Brook area (figure 4.1), in the Watsons Brook slice.

### ***Description***

Pressure solution cleavage is observed in this sandstone sample and is interpreted as S1. In outcrop, S1 is folded by S2. In thin section, clean oriented tectonic muscovite crystals are present in the quartz rich bands. The muscovite in the quartz poor bands has a poor to non-existent fabric orientation. Clay minerals within the quartz-poor bands are poorly oriented and the chlorite throughout the sample is not oriented at all. Additional sample description is in Appendix A.

### ***Spectrum***

This sample was analyzed using the whole rock step-heating method. The sample fragment that was analyzed comes from a quartz poor and fine-grained band of the rock. The spectrum is shown in figure 4.2 and appendix A.

### ***Interpretation***

A plateau is interpreted for this sample at  $442 \pm 2\text{Ma}$ . The chip for this analysis was removed from a fine-grained location on the sample. Therefore this plateau is

interpreted as an age of crystallization for the abundant fine-grained mica and clay present in the quartz-poor portion of the rock.

#### **4.3.4 JA083B**

This sample is taken from the same location as JA083A. It is within the Summerside formation in the Watsons Brook (figure 4.1). In this sample however, there are veins filled with fibrous quartz. This sample is a strongly chloritic and micaceous siltstone.

##### ***Description***

There is one dominant fabric in the rock. However, there are subtle hints of another weaker fabric. The weaker fabric is more apparent near quartz and chlorite veins, which it cross-cuts. In these locations, larger groups of muscovite crystals lie parallel to the quartz fibre direction and oblique to the dominant fine-grained fabric. There is also a late kink-like fold present in this sample with an axial plane sub-parallel to the quartz veins.

All the mica present in this sample is oriented. However a component of the fine-grained matrix of this rock is likely reoriented detrital mica. There is tectonic mica present within extremely fine-grained strain shadows near quartz grains and in larger muscovite aggregates within the quartz veins. Additional sample description is in Appendix A.

##### ***Spectrum***

This sample was analyzed using the whole rock step-heating procedure. The fragment of the sample that was analyzed is from the sedimentary portion of the rock,

where the tectonic fabric is well developed. None of the muscovite from within the quartz/chlorite veins was analyzed. The spectrum is shown in figure 4.2 and appendix A. The plateau age of this sample is  $443 \pm 3$  Ma.

### ***Interpretation***

Abundant tectonic mica is developed in a fabric associated with quartz veins in this sample. Additionally, mica defines a slaty cleavage around small detrital quartz grains. The age of  $443 \pm 3$  Ma agrees closely with the other sample from this area, JA083A, and is interpreted as the age of deformation causing crystallization of muscovite.

### **4.3.5 JA023B**

The location of this sample is shown on figure 4.1. It was obtained from the Summerside formation in Watsons Brook. This area is highly deformed and the slate here contains pyrite with quartz-fibre-filled strain shadows. S1 and S2 fabrics as well as F2 and late kink folds are all present in this location.

### ***Description***

This sample is a laminated green slate. Grains within this sample range from 0.05 to 0.15 mm in diameter.

The fabric is present within the entire thin section, although it is very strong in discrete bands. The dominant muscovite crystallization is along the foliation, with a higher concentration in the bands of more intense foliation. Additional sample description is in Appendix A.

### ***Spectrum***

This sample was analyzed using the whole rock step-heating method. The resulting spectrum is shown in figure 4.2 and appendix A. No plateau was picked for this sample. The total gas age for this sample is  $418 \pm 4$  Ma (Late Silurian).

### ***Interpretation***

This sample has abundant tectonic mica. However, it has the youngest total gas age of all of the samples that were analyzed. This leads to the speculation that deformation or hydrothermal activity in the Latest Silurian or Devonian influenced this result.

#### **4.3.6 JA082A**

This sample is laminated green shale obtained from within the Summerside formation along Watsons Brook, within the Watsons Brook Slice (figure 4.1).

### ***Description***

Very small (<0.01 mm) muscovite crystals are penetrative in mica-rich bands along the crenulation fabric. Larger muscovite crystals, up to 0.15 mm, commonly coincide with locations where S2 planes intersect thin quartz veins or thin beds. These larger crystals are somewhat non-penetrative and would require a pinpoint dating method for analysis. Additional sample description is in Appendix A.

### ***Spectrum***

This sample was analysed using the whole rock step-heating method. The location of the fragment analyzed was from a strongly crenulated fine-grained portion of

the sample that has muscovite crystallization apparent along the S2 crenulation fabric. The spectrum from analysis of sample GQ112A is shown in figure 4.2 and appendix A. The spectrum for this sample shows no interpretable plateaus. The total gas age calculated for this sample is  $451 \pm 4$  Ma.

### ***Interpretation***

Two main phases are interpreted as contributors to the total gas age. These are the detrital clay minerals, which are very likely potassium bearing, and the tectonically crystallized muscovite associated with the crenulation fabric.

### **4.3.7 GQ112A**

The location of this sample is also in Watsons Brook and is shown on figure 4.1. This is a red and green slate of Summerside formation slate from the Corner Brook Slice.

### ***Description***

The fabric of this rock is defined by the orientation of minerals. Platy mineral grains are oriented in the same direction.

The muscovite crystals are of various sizes, with a minor recognizable detrital component and mica within the matrix, and are commonly aligned with the fabric. In thinner portions of the thin section, the very fine-grained matrix shows a strongly oriented muscovite fabric. The fabric defined by the orientation of all of these minerals is interpreted as the S2 fabric. Additional sample description is in Appendix A.

### ***Analysis & Spectrum***

This sample was analysed using the whole rock step-heating method. The spectrum from analysis of sample GQ112A is shown in figure 4.2 and appendix A. No plateau age was interpreted for this sample. The total gas age calculated for this sample  $453.4 \pm 4.1$  Ma.

### ***Interpretation***

There is a strong slaty fabric, interpreted as S2, in this sample that is associated with abundant mica crystallization. The total gas age is interpreted as an indicator of the age of mica crystallization during deformation.

#### **4.3.8 HV002A**

This sample is a laminated grey-green strongly cleaved slate collected from the location shown on figure 4.1 in the Irishtown formation within 30 cm of the Crow Hill thrust. Found nearby were large nodules and individual cubes of pyrite with several centimetres of quartz fibres within surrounding strain shadows.

### ***Description***

In this sample is a bed-parallel fabric defined by alignment of muscovite, clay, and platy chlorite. The thin section shows strong S2 crenulation fabric, axial planar to folded bedding and bed-parallel S1. The crenulation fabric varies from a simple crenulation showing microscopic folding of the S1 micaceous material, to a strong dissolution fabric where individual S1 fabric planes are untraceable across S2 crenulation surfaces.

The detrital mica in this sample was definitely anticipated to have an influence on the Argon age date. However, the strong S2 fabric and associated muscovite crystallization were also expected to affect the result. Additional sample description is in Appendix A.

### ***Spectrum***

This sample was analyzed using the whole rock step-heating method. The resulting spectrum is shown in figure 4.2 and appendix A. No plateau was picked for this sample. The total gas age for this sample is  $457.6 \pm 4.2$  Ma.

### ***Interpretation***

Two generations of mica fabric are present in this sample. They are interpreted as the bed parallel S1 fabric the S2 crenulation fabric, they both are interpreted as contributors to the age date. The total gas age is interpreted to be mainly the age recorded by mica crystallization during tectonic deformation.

## **4.3.9 HV123A**

The location of this sample is shown on figure 4.1. This is very close to sample HV002A near the Crow Hill fault. It is green slate from the Summerside formation.

### ***Description***

Within this sample are fine-grained beds and coarser grained beds. Except for a few small muscovite and chlorite crystals aligned parallel to bedding the bed-parallel fabric is virtually non-existent in this sample.

The fine-grained part of the thin section has a stronger and more penetrative crenulation fabric than the coarser portion. There is some dissolution along the cleavage planes that produces a minor normal-sense separation of bedding. This dissolution crenulation fabric is interpreted as S2. The clay matrix has a uniform extinction oblique to the bedding orientation and parallel to the crenulation fabric, perhaps due to transposition of the original clay. Additional sample description is in Appendix A.

### ***Spectrum***

This sample was analysed using the whole rock step-heating method. The spectrum from analysis of sample GQ112A is shown in figure 4.2 and appendix A. The total gas age calculated for this sample is  $454 \pm 4$  Ma. P. Reynolds (personal communication) initially picked a weak plateau on this spectrum with a date of  $455 \pm 3$  Ma. However, this estimate only takes into account the apparent ages from the seven steps from 700°C to 1000°C. Therefore this interpretation was discounted and no final plateau age was picked for this sample.

### ***Interpretation***

The interpretation for this sample is very difficult as a result of the extreme fine-grained nature of any potassium bearing minerals. Using the bulk extinction orientation of the clays in the matrix of this sample as an indication of their orientation leads to the interpretation that they have been transposed into S2. The total gas age is interpreted as a result of ages measured on tectonically grown mica crystals.

#### **4.3.10 HV134A**

The location of this sample is less than 1km west of the Crow Hill thrust (figure 4.1). This is structurally above the thrust and is within the Crow Hill slice. This sample is Summerside formation slate from a location that also contains sandstone interbeds.

##### ***Description***

There is a single major fabric orientation in this sample. Penetrative coarse bands of chlorite and clay occasionally cut detrital grains. This same fabric is also defined by the orientation of the highly birefringent clay-like matrix and is interpreted as S2.

Muscovite crystals are similar sizes to the other grains, elongate, subrounded, and oriented parallel to dominant fabric. Platy chlorite crystals are similarly oriented.

Additional sample description is in Appendix A.

##### ***Spectrum***

This sample was analysed using the whole rock step-heating method. The spectrum from analysis of sample GQ112A is shown in figure 4.2 and appendix A. Dr. P. Reynolds discarded an initially interpreted tentative plateau of  $455 \pm 3$  Ma (personal communication 2004). The total gas age calculated for this sample is  $454 \pm 4$  Ma.

##### ***Interpretation***

The strong fabric in this rock is interpreted as S2 due to the large quantities of very fine-grained micas and clays, both along the dominant fabric and within strain shadows near quartz or feldspar grains. The total gas Ar/ Ar age very similar to that measured in sample HV123A, HV002A, GQ112A, and JA082A is considered to record the timing of tectonic crystal growth.

#### **4.3.11 HY056A**

The location of this sample is shown on figure 4.1. This rock is a green slate of the Summerside formation from near the contact between the Summerside and Irishtown formations in the Crow Hill slice structurally above the Crow Hill thrust. This area is dominated by fine-grained lithologies and is deformed considerably less than the area near Crow Hill thrust where samples HV123A and HV134A were obtained.

##### ***Description***

There is a strong and penetrative fabric in this slate. The bulk extinction angle indicates that reoriented micas and clays are parallel to the fabric. Additional sample description is in Appendix A.

##### ***Spectrum***

This sample was analyzed using the whole rock step-heating method. The resulting spectrum is shown in figure 4.2 and appendix A. No plateau was picked for this sample. The total gas age for this sample is  $503.5 \pm 4.6$  Ma.

##### ***Interpretation***

The fabric that is developed in the fine-grained material in this sample is interpreted as S2. However, the Middle Cambrian total gas age is interpreted as primarily an effect of age results on detrital and/or diagenetic clays and micas, consistent with the lack of evidence for muscovite crystallization associated with the fabric.

#### **4.3.12 HQ092A**

The location of this sample is shown on figure 4.1. This sample came from the furthest distance west in the map area within the Blow Me Down Brook formation in the Woods Island Sheet. This sample is a medium grained, poorly sorted, micaceous sandstone with subangular to rounded clasts.

##### ***Description***

The fabric in this rock is defined by the orientation of detrital mica, chlorite, and irregularly shaped quartz clasts. Strain shadows associated with large quartz clasts contain very fine-grained clay-like material. The boundaries of many of the detrital grains are parallel to the fabric suggesting partial dissolution of clast material.

The muscovite grains are oriented parallel to the fabric direction. However, this parallelism is interpreted as reorientation rather than crystallization due to their detrital appearance and large grain size. Additional sample description is in Appendix A.

##### ***Analysis & Spectrum***

This sample was analyzed using the whole rock step-heating method. The resulting spectrum is shown in figure 4.2 and appendix A. No plateau was picked for this sample. The total gas age for this sample is  $564.2 \pm 5$  Ma.

##### ***Interpretation***

The total gas age of this sample is in the late Precambrian. This age is near the timing of deposition of the Summerside formation. Therefore, this result is interpreted as recording the isotopic signature of detrital and or diagenetic potassium-bearing minerals.

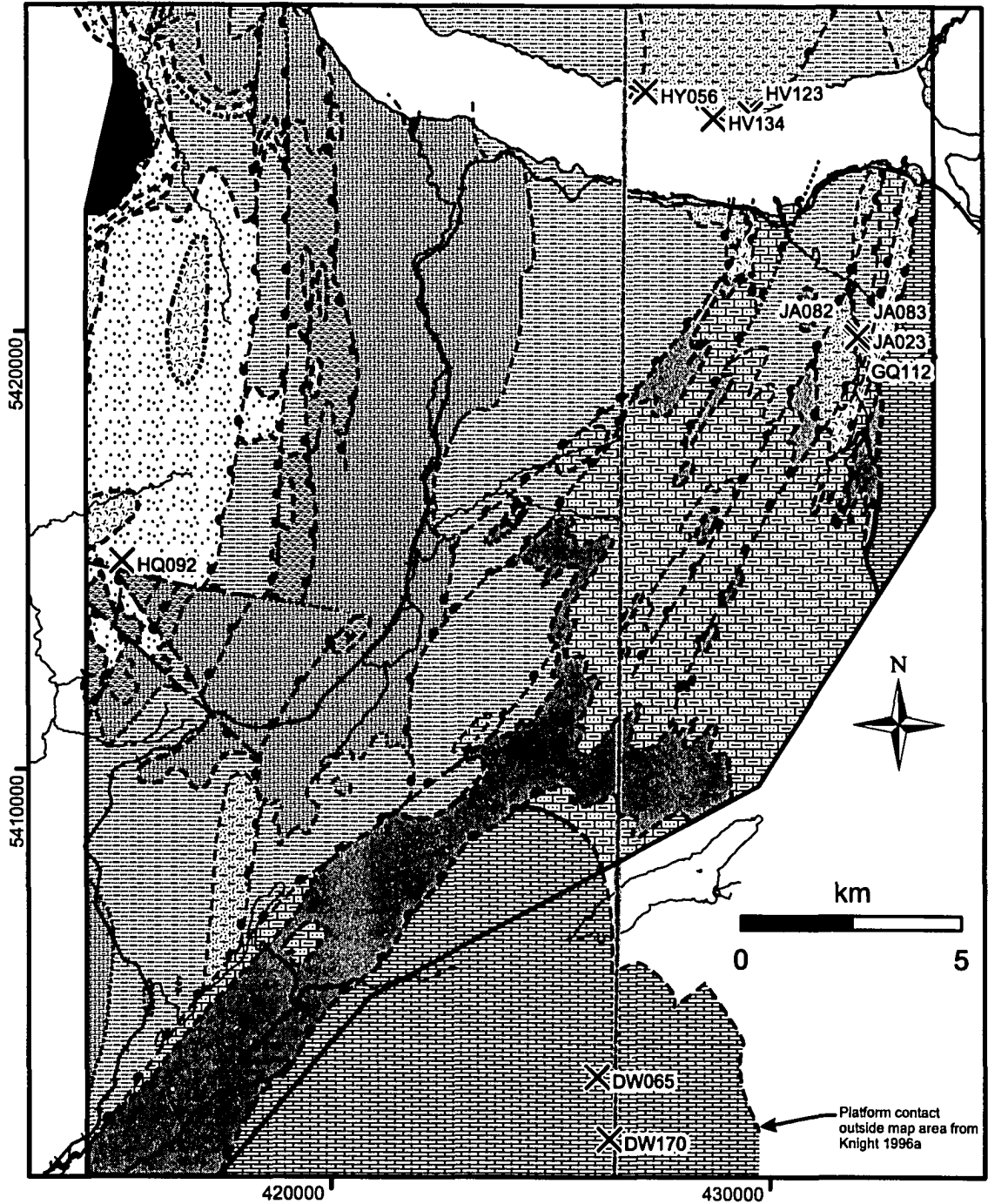
#### **4.4 Conclusion**

These Ar-Ar analyses show 4 different and separate age groups (figure 4.3). Two dominant age groups are composed of nine of the  $Ar^{40}/Ar^{39}$  ages. A confident cluster is at 440 Ma based on plateau ages on two whole rock and two mineral separate ages. The second cluster is based on the total gas ages of five samples, as well as two tentative plateaus from samples HV123A and HV134A, all of which fall between 450 and 460Ma. This range of ages is not represented by isotopic age dating elsewhere in the orogen. This suggests that there is a different generation of deformation recorded and preserved in the rocks of the Humber Arm Allochthon. The correlation of these dates with stratigraphic ages from the foreland basins and isotopic ages within the Internal Humber and Dunnage Zones will be discussed in Chapter 5.

Three of the analyses record ages of less concern to this specific study. There is one sample with an anomalously low total gas age and no identifiable plateaus (418 Ma). This sample is likely recording the effects of a later deformation; this age is not observed in any of the other samples. There were also two ages interpreted as detrital. These are shown on figure 4.3 as well and seem to be approximately dated around the time of deposition of these units.

It is recognized that, especially in an area with multiple generations of tectonic fabrics, whole rock ages may not specifically determine the age of a single generation of potassium-bearing mineral crystals and likely involve components that record several different ages. Further analyses using different methods would be necessary to produce a more robust set of ages.

Figure 4.1  
Argon samples location map.



- |   |  |  |
|---|--|--|
| <ul style="list-style-type: none"> <li>— Map Area Boundary</li> <li>--- NTS Boundaries</li> <li>— Coast</li> <li>— Lakes and Brooks</li> <li>+ Railway</li> </ul> | <p><b>Stratigraphic Contacts</b></p> <ul style="list-style-type: none"> <li>— constrained</li> <li>- - - inferred</li> <li>..... conjectured</li> </ul> <p><b>Tectonic Contacts</b></p> <ul style="list-style-type: none"> <li>..... conjectured, unknown</li> <li>— constrained, normal</li> <li>- - - inferred, normal</li> <li>..... conjectured, normal</li> <li>— constrained, thrust</li> <li>- - - inferred, thrust</li> <li>..... conjectured, thrust</li> </ul> | <p><b>Map Units</b></p> <ul style="list-style-type: none"> <li>Blow Me Down Brook formation</li> <li>Bay of Islands Complex</li> <li>Cooks Brook Formation</li> <li>Goose Tickle Group</li> <li>Irishtown Formation</li> <li>Middle Arm Point Formation</li> <li>Pinchgut Lake Group</li> <li>Platform succession</li> <li>Summerside formation</li> <li>volcanics</li> <li>melange</li> </ul> |
|---|--|--|

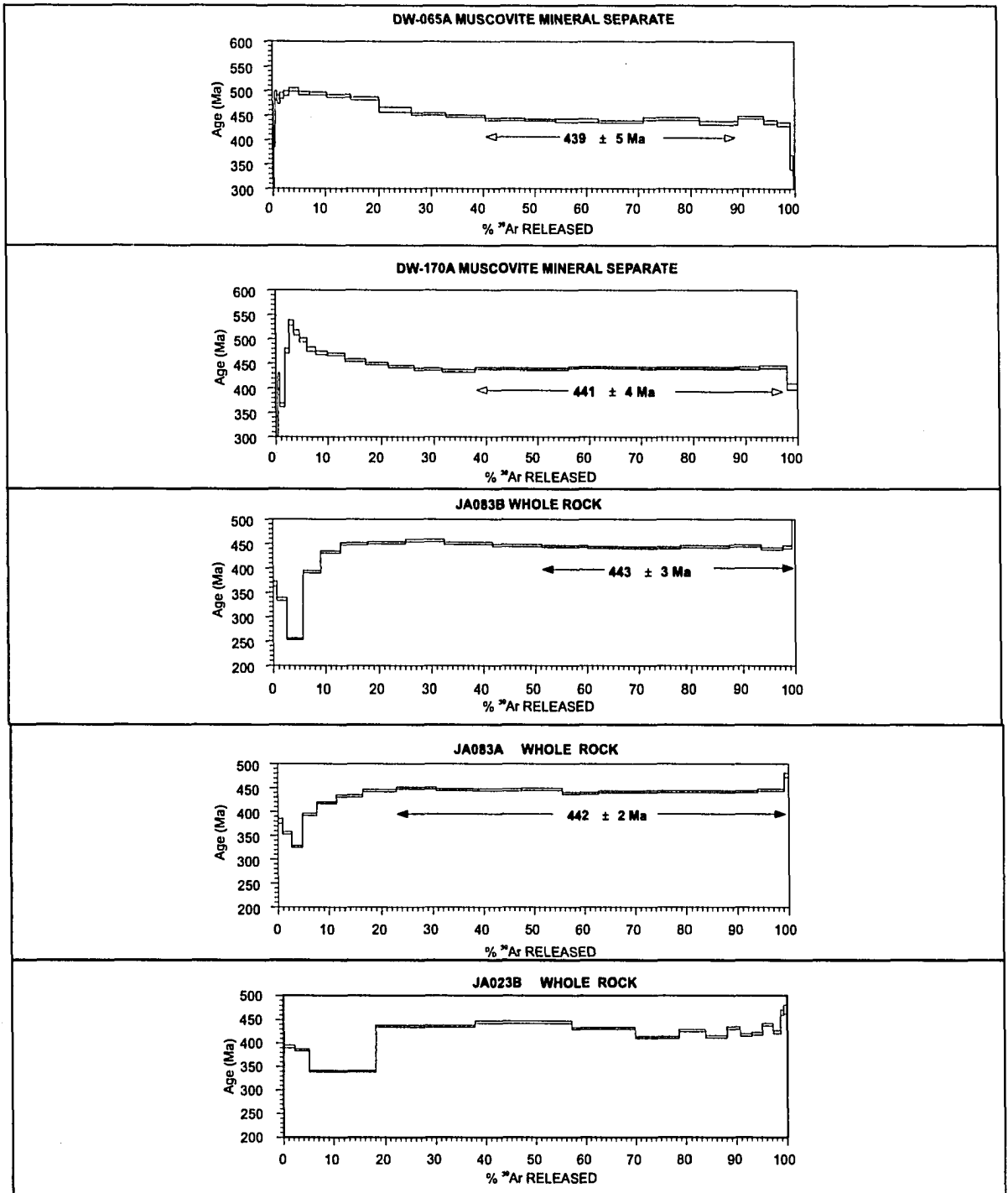


Figure 4.2  
Spectra acquired from argon analyses. The charts showing experimental data are in appendix A.

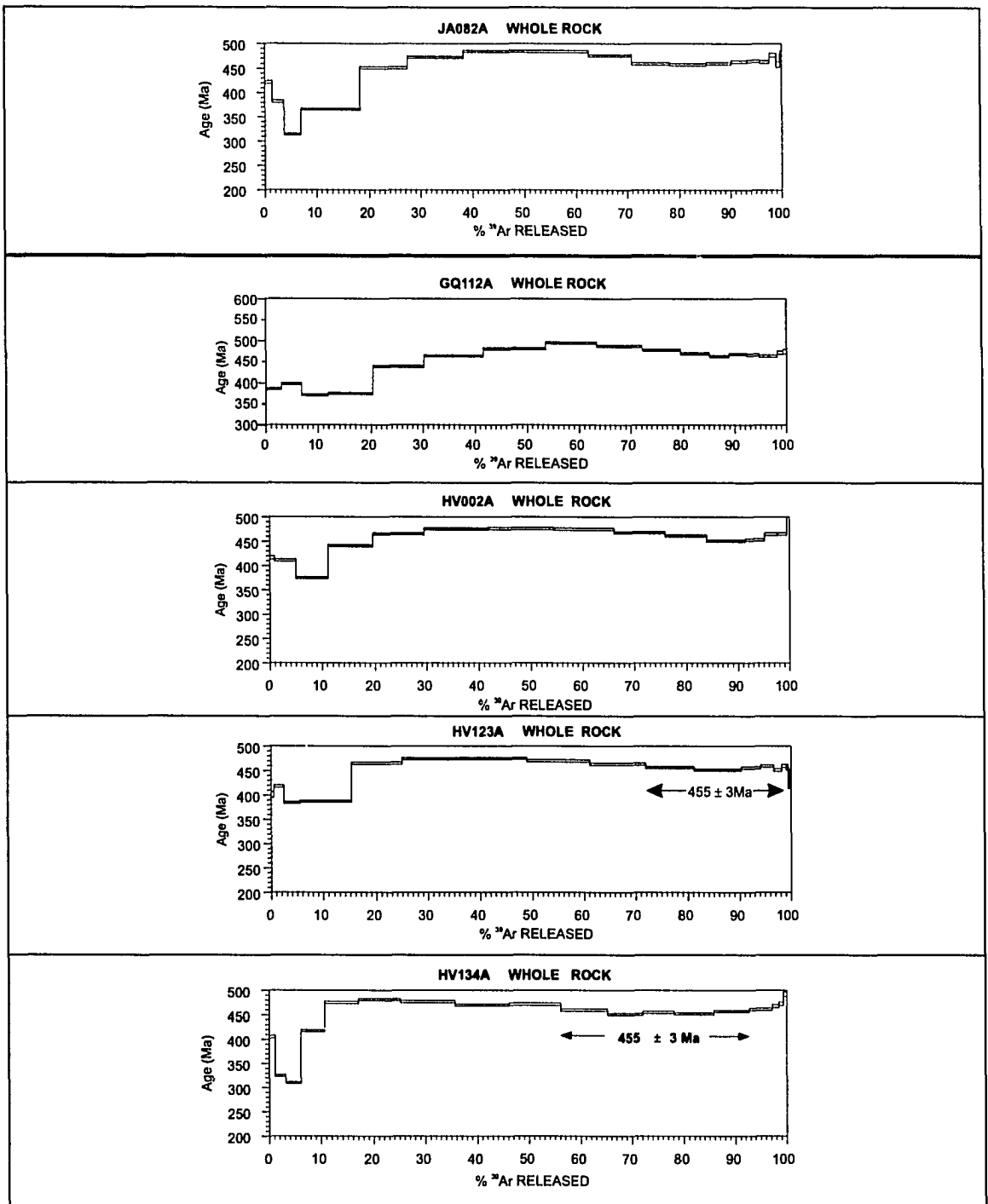


Figure 4.2 continued

The interpretation shown for HV134A is preliminary.

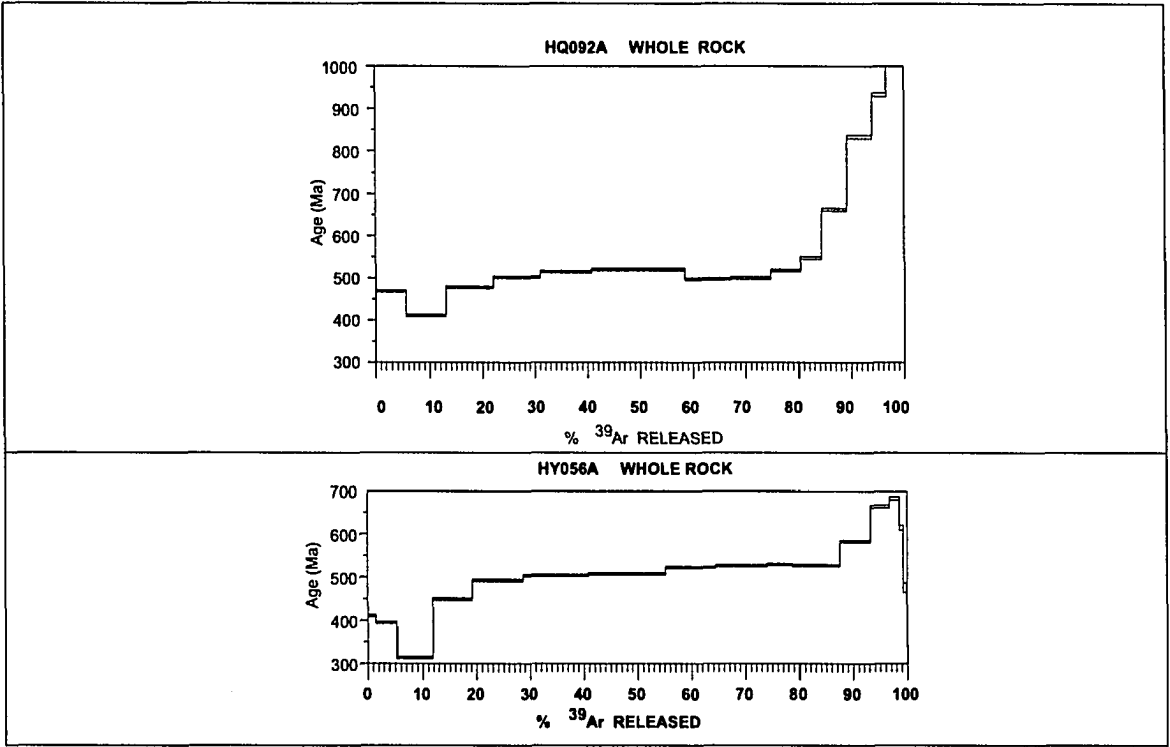
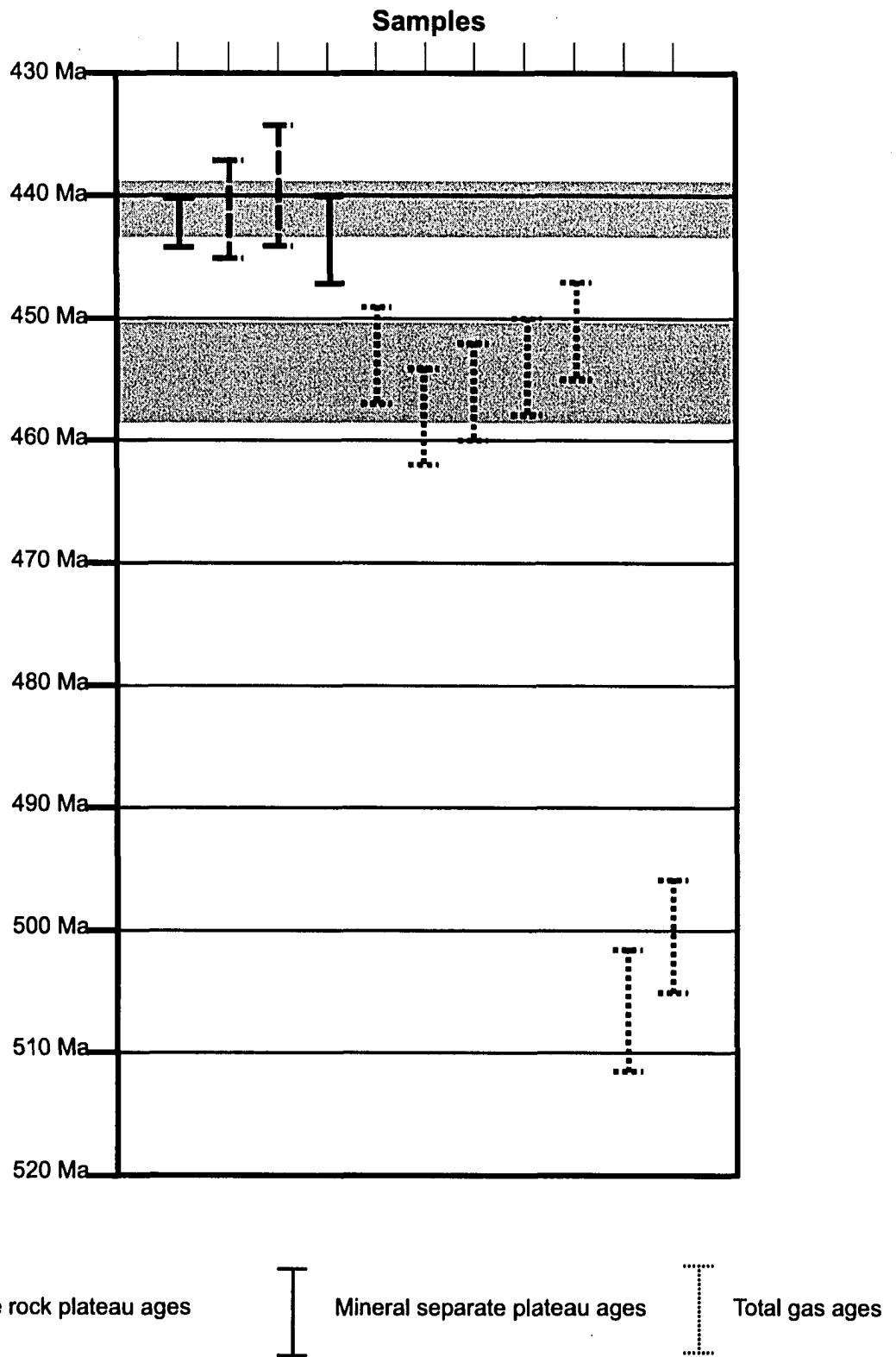


Figure 4.2 concluded

Figure 4.3  
 Summary of the results obtained from argon age dating.



## **Chapter 5: Discussion**

### **5.1 Introduction**

The Humber Arm Allochthon preserves a record of the development of the Laurentian margin and Appalachian Orogen during the Late Proterozoic and Paleozoic. Portions of this record are preserved in the stratigraphy and the structural record of deformation.

The geological history preserved in the stratigraphic units of the Humber Arm Allochthon within the Corner Brook map area includes:

- Late Proterozoic rifting, a record of which is preserved in the lower Curling Group.
- Cambrian-Ordovician passive margin development preserved in the upper Curling and Northern Head Groups.
- Early Ordovician, Taconian, margin destruction, preserved in the Goose Tickle Group and Eagle Island formation flysch sandstones.

The structural history includes:

- D1 deformation, broadly identified here with the Taconian Orogeny.
- D2 - D5 deformation, interpreted as Post-Taconian.

The stratigraphic and tectonic history of the Humber Arm Allochthon can be related to the rock record preserved elsewhere in western Newfoundland. This chapter will relate these two histories in a synthesis of margin development and deformation.

This will involve reconstructing the morphology of the margin and relating the Post-Taconian deformation in the Humber Arm Allochthon to isotopic and structural data to the east, and to foreland basin sedimentation to the west.

## **5.2 *Basement, Rift, and clastic passive margin units***

### **5.2.1 Clastic units in the Humber Arm Allochthon**

The Curling Group, composed of the Summerside, Irishtown, and Blow Me Down Brook formations, has ages within the Late Paleozoic and Cambrian and is interpreted to have been deposited during rifting and early passive margin development. The complex relations between thrust sheets result in major difficulties in determining a definitive stratigraphy for the units of the Humber Arm Allochthon. Facies differences are used here to determine the stacking order and as an indication of relative unit positions in the thrust stack.

#### **5.2.1.1 *Summerside formation***

The Summerside formation is one of the lowest stratigraphic units of the Humber Arm Supergroup and is interpreted as having been deposited in a rift-basin setting. It is interpreted as a rift deposited unit based primarily on its low stratigraphic position in the Allochthon and its similarities to other Early Cambrian deep-water sediments in the orogen (Palmer et al 2001). No volcanics have been observed in stratigraphic contact with the Summerside formation.

### **5.2.1.2 *Irishtown formation***

The Irishtown formation within Corner Brook is interpreted as the stratigraphic unit underlying the Pinchgut Lake Group (insert 3 section Z, Cawood and van Gool 1998), and therefore lies within the Watsons Brook Sheet. The remainder of the Irishtown formation is within the Corner Brook Sheet. The Crow Hill fault is interpreted as a major partition between the lower energy Northern Head Group and the Curling Group to the west and the higher energy Pinchgut Lake Group and Curling Group to the east. This juxtaposition of units leads to the interpretation that the Crow Hill fault is a contact between two D1 thrust sheets (insert 2, 3).

The Irishtown formation has variable characteristics across the area. Conglomeratic material is present in limited areas, and has been interpreted as lenticular coarse-grained channel deposits (Palmer et al 2001). For example, besides the sections by Palmer et al (2001), two sections showing extreme grain size differences are presented in figure 2.1. The section measured near the eastern boundary at location A (figure 2.1a) is very coarse and high-energy. A section was also measured on the west edge of the map area (figure 2.1b) that is very fine-grained and generally lower energy. Palmer et al (2001) measured a section located halfway between location A and B that has an energy level transitional between the sections shown in figure 2.1. Therefore, we observe a map-wide facies change of the Irishtown formation from fine and low-energy in the west to coarse and high-energy in the east.

The variability of the Irishtown formation is not necessarily a lateral variation in its sedimentary character; it may also be explained tectonically. Units currently in the west are interpreted to occupy higher D1 thrust slices, and likely travelled furthest. The

westerly-fining character of the Irishtown formation can be interpreted as a result of increasingly distal, and structurally high, thrust sheets presently exposed to the west (figure 5.1), either as a result of a foreland dipping duplex, a folded thrust stack, or later deformation.

The tectonic interpretation, above, is preferred for explaining differences in the Irishtown formation facies across the map area. Facies changes occur systematically from west to east across the area, and major tectonic boundaries, such as the Crow Hill fault, lie between different facies of the Irishtown formation. Therefore, it is unlikely that these differences can be the result of purely sedimentary processes. The geometry shown in figure 5.2 tectonically separates the proximal, and presumably coarser grained, facies from the distal fine-grained facies.

### **5.2.1.3 *Blow Me Down Brook formation***

The Blow Me Down Brook formation also shows a wide variation in facies. For example, the inland expression of the Blow Me Down Brook formation shows a much higher percentage of fine-grained rocks (figure 2.2) than the coastal exposures of the Blow Me Down Brook formation as described by Palmer et al (2001) and Buchanan (2004), which are dominantly sandstone, with *Oldhamia* occurrences in occasional thin shale/slate beds.

Several explanations are possible to explain the coarse-to-fine grain-size variation in the Blow Me Down Brook formation. The contrast between inland and coastal exposures can be explained stratigraphically, by a lateral facies change, or tectonically, with the presence of an additional finer-grained slice under the coarse Blow Me Down Brook formation. A third explanation was presented by Palmer et al (2001), which

hypothesizes that coastal Blow Me Down Brook formation is atypically coarse grained and that the high shale content in nearby tectonized zones indicates that the sand-rich section is a tectonic remnant after preferential disruption of the finer grained lithologies.

The differences observed in the bulk composition of the Blow Me Down Brook between the coastal and inland exposures is interpreted here to be dominantly the result of a lateral facies change with tectonic complications. Contrary to the multiple thrust slice interpretation for the Irishtown formation, the Blow Me Down Brook formation is not observed to have a systematic grain size difference across its exposure. In fact, it is quite likely that the inland and coastal sections are both components of the same sheet. A lateral facies change such as that shown in figure 5.1 is interpreted as a large reason for the difference. However, there is likely a tectonic component to the variation, as Palmer et al (2001) suggest.

#### **5.2.1.4 Relationships between the Curling Group units**

The Blow Me Down Brook formation and the Summerside formation are of similar age, lithology, and can be interpreted as being deposited in similar environments (Cawood and van Gool 1998, Waldron et al 1998). However, populations of detrital zircon (Cawood and Nemchin 2001) and structural position show a poor match between units, and can be explained by differences in paleogeomorphology of the margin and the early tectonic history of the Humber Arm Allochthon.

The Blow Me Down Brook formation occupies the highest structural position of the sedimentary units in the Bay of Islands, and volcanics are observed at its base. These features suggest the restored position of the Blow Me Down Brook formation to be

farther outboard from the Summerside formation, as illustrated by Waldron et al (1998) and Cawood and Nemchin (2001).

Lithologically the sandstones of the Blow Me Down Brook are very similar to those of the Summerside formation, making field identification difficult.

Petrographically, there are slight differences between the formations, as shown using point counting techniques (Tanton 2003). After a broad study of detrital zircon populations from western Newfoundland, Cawood and Nemchin (2001) determined that there are distinct, and different characteristics to the zircon populations of the Blow Me Down Brook formation and Summerside formation, and therefore their source areas. Cawood and Nemchin (2001) suggest a geomorphological influence on sediment flow as a source control on the sediment supplied to each of the units.

Cawood and Nemchin (2001) interpreted their zircon data as evidence that the provenance of the Summerside formation was very local and sheltered within a graben on the side of the developing rift basin, but still placed the two formations side by side in their reconstruction. The compartmentalization of sediment sources requires several significant grabens to have formed during rifting, each basin with separate sediment sources. Waldron and van Staal (2001) interpret significant margin complexity, including the separation of a micro-continent, the Dashwoods block, during rifting. Early rifting of a microcontinent from Laurentia would have provided an additional sediment source to the southeast. Perhaps the existence of steep-walled deep grabens and longitudinal sediment flow along the deep, narrow rift basin would have assisted in sediment partitioning (figure 5.3).

### **5.3 *Carbonate passive margin***

The two major carbonate units in the area are the Middle Cambrian to Early Ordovician Northern Head Group (Botsford 1988) and the Pinchgut Lake Group (Williams and Cawood 1986). Lithological comparisons indicate that they occupy distal slope and proximal slope positions, respectively (Knight 1996b). These units are also interpreted as roughly correlative to the Cow Head Group, which lies to the north (Botsford 1988).

#### **5.3.1 Northern Head Group**

The Northern Head Group is an upward fining sequence interpreted as off-slope sediments derived from shedding off of the carbonate platform. It represents passive margin deposition and the stratigraphic contact with the Eagle Island formation corresponds to the onset of foreland basin deposition. The Northern Head Group is observed to have a westerly fining trend similar to the Irishtown formation (figure 2.3).

The Northern Head Group present in Rainy Brook is very different than that presented by Botsford (1988) (figure 2.4). In Rainy Brook (location C, figure 1.3, insert 1), there is a 400 m section of thin-bedded and strongly calcite-cemented Irishtown formation with a 100 m section of Cooks Brook formation overlain by almost 400 m of characteristic Middle Arm Point formation with a tectonic top. Additionally, the siliceous mudrocks of the Middle Arm Point formation contain structures consistent with bed parallel extension and stratigraphic thinning, indicating that the Rainy Brook section (figure 2.4) probably represents a minimum thickness. This section is interpreted as a more distal facies of the Northern Head Group than that measured by Botsford (1988). Similar to the tectonic interpretation suggested for the Irishtown formation, the Rainy

Brook section (figure 2.4, 5.2) of the Northern Head Group is interpreted as occupying a higher thrust slice than the occurrences further east.

The difference between the Northern Head and Pinchgut Lake Groups is defined by depositional energy and sediment supply. This is observed across the Crow Hill fault. The Pinchgut Lake Group is interpreted as having occupied a higher position on the depositional margin and a lower position in the Taconian thrust stack than the Northern Head Group (figure 5.2).

### **5.3.2 Pinchgut Lake Group**

The Pinchgut Lake Group is interpreted as a higher energy equivalent of the Northern Head Group, and is thought to lie closer to the margin (Botsford 1998, Knight 1996b). The overall coarser nature of the Pinchgut Lake Group is apparent in good exposures.

Similar to the Eagle Island formation clastic flysch that overlies the Northern Head Group, the Pinchgut Lake Group is overlain by the Whale Back formation clastic flysch. However, the top of the Pinchgut Lake Group does not contain a distal slope section comparable to the Middle Arm Point formation of the Northern Head Group. Where the stratigraphic contact between the Pinchgut Lake Group and the Whale Back formation is observed, there is always a fine-grained component under the contact, although its thickness is rarely more than several metres. The relative absence of the distal slope section in the upper Pinchgut Lake Group suggests a ready supply of sediment. Therefore, in agreement with Knight (1996b), the Pinchgut Lake Group is interpreted to occupy an original position proximal to the slope edge and further inland from the Northern Head Group (figure 2.4).

## **5.4 Taconian Orogeny**

Results of the Taconian Orogeny included destruction of the passive margin, major thrusting and emplacement of the Taconian allochthons, and development of a foreland basin (Chapter 1). Accommodation space was created due to loading on the Laurentian margin during emplacement of allochthons in the Early Ordovician resulting in the deposition of the earliest foreland basin units (figure 5.4). The Table Head and Goose Tickle Groups were deposited during the Taconian Orogeny and are both preserved in allochthonous and autochthonous locations.

### **5.4.1 Taconian Stratigraphy**

The Table Head Group includes a rapidly deposited carbonate platform succession (the Table Point formation) that eventually drowned due to the rapid foreland subsidence during Taconian loading (Whittington and Kindle 1963, Williams et al 1987). Several hundred metres of foreland basin sediment (the Table Cove Formation and the Goose Tickle Group) were deposited in the accommodation space created during this process. The Table Head Group is present both in an assumed allochthonous position within the map area and in an autochthonous position to the west that extends beneath the Gulf of St. Lawrence. The autochthonous Table Head Group is a direct result of accommodation space created by orogenic loading. Therefore, it is an indication of the magnitude of loading that occurred during the Early Ordovician Taconian Orogeny. The allochthonous Table Head Group bordering the east of the map area is highly deformed and occupies a position between the most deformed slope unit, the Pinchgut Lake Group and the highly metamorphosed units of the internal Humber Zone. It is interpreted to have occupied a lower thrust sheet than the slope units of the Humber Arm Allochthon.

The Goose Tickle Group is composed of autochthonous and allochthonous Early to Middle Ordovician clastic flysch sediments of the foreland basin. It contains ophiolite-derived detritus and the sediment source is interpreted to have been advancing allochthons; thus its base represents an indicator of the onset of the Taconian deformation. The top of the Goose Tickle Group is tectonic and faulted in all cases (Quinn 1988, Quinn et al 1995). The Goose Tickle Group within the Corner Brook Area includes the Eagle Island formation and the Whale Back formation.

The Eagle Island formation is coarse-grained clastic flysch that records the earliest effects of Taconian deformation. It overlies the Northern Head Group and has abundant indications of rapid sedimentation and deformation prior to lithification. The Eagle Island formation is derived from sediment shed from advancing thrust sheets (Botsford 1988, Quinn 1988). Its deposition is thought to be middle Arenig and earlier than the rest of the Goose Tickle Group (Botsford 1988). The Eagle Island formation is interpreted to occupy the position furthest from the Laurentian margin, relative to the other units in the Goose Tickle Group, and sedimentation is interpreted to have ceased upon being overtaken by the allochthons.

Flysch sandstones in the Watsons Brook Sheet are classified as the Whale Back formation and although there is a higher proportion of mudrocks, the sandstone beds resemble those of the Middle Ordovician Goose Tickle Group (Quinn 1988) to which they are here assigned. The Whale Back formation is highly deformed, similar to the Pinchgut Lake Group. The Whale Back formation is finer grained than the Eagle Island formation and was interpreted to have been deposited up-slope from the Eagle Island formation, above the Pinchgut Lake Group.

## 5.4.2 Taconian Deformation

### 5.4.2.1 *Fluids and fabric development*

Structures associated with Taconian deformation include scaly fabric, pressure solution cleavage, and quartz veins, inferred to record evidence of fluid conditions at the time of deformation.

Scaly fabrics typically develop in major brittle shear zones under low effective confining pressures (Moore et al 1986). The scaly fabrics in the Humber Arm Allochthon, developed during D1, are interpreted to have been a result of deformation of under-consolidated sediment supported by considerable pore fluid pressure (Waldron et al 1988).

Vein quartz is present in large quantities in outcrops of scaly black shale. It often is present in lozenge shaped domains bounded by films of polished, slickensided, scaly shale characteristic of D1 deformation. This leads to the interpretation that the veins have been boudinaged during D1, and are therefore formed pre- or syn- D1. However, Waldron et al (1988) indicate that the early vein quartz domains show no sign of internal deformation and are therefore a result of syn to post tectonic quartz crystallization. Either option requires that silica rich fluid was present in these zones and precipitated large amounts of quartz.

Pressure-solution cleavage is well developed in structurally low units, most significantly, the Summerside formation. Pressure-solution cleavage requires a significant quantity of fluid to facilitate mobilization of dissolving silica (Kerrich 1978). The contrast between fabrics observed in the Summerside formation and higher units implies that there must be a fundamental difference in fluid transport mechanisms

between formations during deformation. The fluid present in the Summerside formation must have been mobile, allowing transport of silica without creating under-consolidated conditions. The Summerside formation must therefore have been highly permeable. In contrast, scaly fabrics in the Irishtown formation indicate an under-consolidated situation, implying that fluid must have been prevented from expulsion. This contrast may be explained by a formational difference in sediment lithification or consolidation. The older Summerside formation may have experienced a higher degree of lithification and/or dewatering prior to deformation than the Irishtown formation. Additionally, the volume of contiguous sand in the Summerside formation may have allowed better fluid transport once the relatively minor shales had dewatered. The thick packages of black shale in the Irishtown formation would have had very low permeability and likely allowed little fluid flow, causing a build-up of fluid pressure.

#### **5.4.2.2 *Volcanic blocks within mélange***

As indicated in chapter 2, a major field indication used for the identification of mélange was the presence of volcanic blocks within the scaly shale matrix. These blocks could often be identified as pillow basalt, with clearly definable pillows, chilled margins, and rare associated sediment. Buchanan (2004) suggested that these blocks were plucked from higher structural levels through processes involved in the D3 normal-sense deformation. D3 normal-displacement structures are abundant in the Corner Brook Map area. They may explain “exotic” volcanic block emplacement, particularly in close structural proximity to a supply of volcanic material of the Bay of Islands complex. However, on the eastern side of the map area, units containing volcanics are not

preserved in positions to allow for plucking during normal displacement. Therefore this mechanism is not feasible.

However, if volcanic material were originally present in a stratigraphic position below the Humber Arm Supergroup, perhaps associated with the base of the rift-related Summerside formation, then reverse displacement during D2 deformation could potentially have transported volcanic material well above the current position in the thrust stack before D3 normal faults re-transported the source volcanics back to or below their initial structural position.

A comprehensive geochemical study is probably necessary to determine whether these extrusive volcanics can be related to rift volcanism or arc-volcanism, and if they are equivalents of an identifiable nearby source.

## **5.5 *Post Taconian History***

### **5.5.1 D2 deformation**

The most widespread and penetrative fabrics in the map area are S2 and L2. Based on the isotopic data presented in chapter 4, these structures are interpreted as post-Taconian, probably Late Ordovician in age. D2 deformation caused widespread eastward-vergent folding and thrusting. D2 reverse-sense shear planes have subsequently been reactivated, and the original magnitude of D2 displacement is unknown. However, sheared overturned limbs of F2 folds are common and the transposition of earlier structures indicates a significant amount of D2 deformation. This east-west shortening is interpreted to have resulted in considerable thickening within the allochthonous units, and probably throughout the orogen. The eastward vergence of the D2 structures is similar to

the Middle Ordovician to Early Silurian east-directed thrusting in the Buchans region (Dunning et al 1987, Thurlow et al. 1992). There is some speculation as to the reason for the switch in vergence between D1 and D2. Waldron and Van Staal (2001) suggest it is the result of a polarity switch of the subduction zone from east to west-dipping. Cawood and Williams (1988) suggested that it is the result of tectonic wedging, involving a basement duplex that formed during D1 with an overall west dipping roof thrust. Thus, out-of-sequence thrusting and continued tectonic activity would produce surface structures mimicking the basement.

#### **5.5.1.1 *Variability of D2 structures***

The map area can be generally split into two broad areas based on the characteristics of the S2 foliation and the amount of transposition that has occurred. These areas are delimited in figure 5.5 and are referred to as the eastern and western allochthon. The eastern allochthon is characterized by a pervasive transposition of earlier structures into parallelism with a shallow to moderately west-dipping S2 fabric. Folds have curved fold hinges and are tight to rarely isoclinal and commonly overturned. Steeply west- to east-dipping S2 fabrics characterize the western allochthon. Folds are upright and open, and reverse shear along S2 surfaces is less common. Transposition of earlier structures into S2 is much weaker in the western allochthon.

Because of the weaker transposition due to D2 in the western allochthon; D1 structures are more commonly preserved. For example, a large F1 fold is shown in the Blow Me Down Brook formation on cross section Z (insert 3). Additionally, untransposed panels of Northern Head and Curling Group stratigraphy are observed in the western allochthon at locations C and D.

In contrast, preserved F1 folds are relatively rare in the eastern allochthon. Other than centimetre-scale isoclinal F1 folds, significant occurrences are limited to those on Crow Hill (location J) and near Summerside (location K). In both areas (location J and K), F1 folds at outcrop and/or map scale are preserved in the sand-rich Summerside formation, at positions near D1 thrust boundaries.

Preservation of D1, and the change in character of the D2 structures, can be explained by a combination of two effects: 1) the structural position of the Bay of Islands Complex during D2 deformation and 2) the relative rigidity contrast between different units.

In locations J and K, the sand-rich Summerside formation likely formed a rigid framework and reduced the local strain responsible for transposition of earlier fabrics into the S2 shear planes (figure 5.6). Similarly, the less significant shortening observed in the western allochthon may be due to the rigid framework provided by the nearby Bay of Islands Ophiolite Complex; the units immediately below the ophiolite after D1 construction of the thrust stack were effectively sheltered from the strong shearing during D2, in a map-scale strain shadow.

The western allochthon may also have been higher in the thrust stack, and therefore cooler, at the time of D2 deformation. The cooler rock was likely less prone to folding and penetrative shearing. Shortening at this level could have been accommodated by larger, more discrete, brittle structures.

### **5.5.1.2 *Isotopic Dates***

The preliminary argon dates presented in Chapter 4 show an isotopic age cluster between 450 and 458 Ma. This age is tentatively interpreted as representing the age of the D2 deformation within the map area (figure 5.4).

### **5.5.1.3 *Margin/ foreland basin significance***

The absolute timings of structures within the Corner Brook Map Area, and the Humber Arm Allochthon, are critical to determine their relationship to deposition in the foreland basins. The isotopic ages of the D2 fabrics record a very similar age to that of the Long Point Group, a 1 km thick Late Ordovician unit exposed on Port au Port Peninsula (figure 1.2) and present beneath the Gulf of St. Lawrence. This group is interpreted as a foreland basin package deposited as a result of an episode of tectonic loading and subsidence (Quinn et al 1999, Waldron et al 2002b).

The shortening experienced by the allochthon in the Corner Brook map area during D2 deformation is interpreted to have led to a significant amount of thickening within the orogen, resulting in margin loading and the creation of accommodation space to the west. This accommodation space allowed deposition of the Long Point Group.

The Late Ordovician foreland basin sediments are approximately 1000 m thick and relatively significant when compared to 500-1000 m of Taconian foreland basin sediments in the Table Head Group and Goose Tickle Group (Stockmal et al 1995, Quinn 1999). Therefore, loading during D2 must have been of equal or higher magnitude than during the Taconian, D1 deformation. It can be further speculated that the loading event must have been relatively quick, due to the abrupt drowning of the carbonate platform (Lourdes Limestone) and subsequent deposition of the large thickness of clastic material,

within a relatively short period of time during the Caradocian (Stockmal et al 1995, Quinn 1999).

### **5.5.2 D3**

D3 structures are dominated by normal sense shear, both ductile and brittle. These normal faults and shear zones have been observed previously (Waldron et al 2003), but are interpreted here as the dominant structures responsible for most major tectonic contacts between sheets. Contacts interpreted here as D3 normal faults have been previously interpreted as D1 thrusts (e.g. Stevens 1965, Williams 1989, Waldron and Palmer 2000, Waldron et al. 2002, 2003), as well as D2 reverse structures (Cawood and van Gool 1998), based in part on the inferred depositional relationships and the geometry of the D1 thrust stack. In this study, D1 folds, such as the example preserved at Crow Hill (insert 3, cross section W), are observed to have a shallower dip than the D3 normal faults. Additionally, D3 orientations appear to be controlled by S2. This suggests D3 reactivation of F2 overturned fold limbs or S2 shear planes. D3 faults result in the general geometry illustrated in figure 5.7, with successively higher thrust sheets exposed further west.

Within the map area, moderately west-dipping normal faults and shear planes expose units buried progressively deeper in locations increasingly eastward. Regionally, this may be related to the presence of the deeply buried Corner Brook Lake block to the east (figure 5.7). D3 deformation in the Corner Brook area may be related to other nearby faults interpreted to show normal displacement, and to compose major domain boundaries, such as the Hughes Brook and Humber River Faults (Cawood and van Gool 1998).

Argon dating yielded Early Silurian isotopic ages grouped around 440 Ma. These dates are tentatively interpreted as the isotopic age of muscovite crystallization that occurred during D3 (figure 5.4).

D3 deformation in the Humber Arm Allochthon is associated with normal-sense, east-west extension. The isotopic age of 440 Ma for D3 deformation is roughly coincident with an Early to Middle Silurian unconformity in the foreland basin to the west. This unconformity corresponds to a long period of erosion, or non-deposition, within the foreland basin (Quinn et al 1999). D3 normal structures would have unloaded the margin, created uplift, and led to the creation of this unconformity (figure 5.4).

In the internal Humber and Dunnage Zones, deformation is recorded from 435-425 Ma, through isotopic dating of plutonism and metamorphism (e.g. Dunning et al 1990, Cawood and van Gool 1998). These ages are interpreted to record peak Silurian metamorphism in the hinterland, an event termed the Salinian Orogeny. This isotopic record shows that deformation in the internal Humber and Dunnage Zone occurred at least 5 million years later than D3 deformation in the Corner Brook area (figure 5.4). The difference between these isotopic dates and those recorded in the internal Humber Zone may be a result of a disparity in the uplift history between the internal and external Humber zones. Alternatively, it may represent two distinct events in the history of the orogen.

### **5.5.3 D4 and D5 structures**

D4 and D5 structures present in the Corner Brook map area are relatively poorly preserved. However, in the foreland basin there is a record of orogenic events occurring after the Salinian Orogeny.

D4 structures are east-west trending open folds, and D5 structures are brittle faults, mainly with reverse sense. The relative timing of D4 and D5 structures is tentative.

Based strictly on style of deformation, and intended as a preliminary correlation, brittle, reverse-sense, east-vergent D5 faulting can be associated with the Acadian Orogeny (Cawood 1993). This would be consistent with the style and geometry of the roof of the offshore triangle zone (figure 5.8), known to be Acadian in age (Waldron and Stockmal 1994). However, the southeast-northwest shortening may alternatively be a result of transpression during dominantly strike-slip Carboniferous deformation. The orientation of faults would likely be controlled mainly by reactivation of pre-existing planes of weakness in the map area, which are dominantly parallel to S2. Carboniferous deformation manifests itself in several basins, such as the Deer Lake basin, along the margin of the Humber Zone (figure 1.2, Hyde et al 1988, Wright et al 1996).

The Clam Bank and Red Island Road Formations are Late Silurian and Devonian flysch units present in the foreland basins west of the Humber Arm Allochthon. These are both clastic units that sit unconformably above the Long Point Group (Quinn 1999) and are interpreted as a third preserved foreland basin succession (Waldron et al 1998). Although the post D3 structural record in the Corner Brook area is sparse, these foreland units suggest significant Acadian thickening of the orogen.

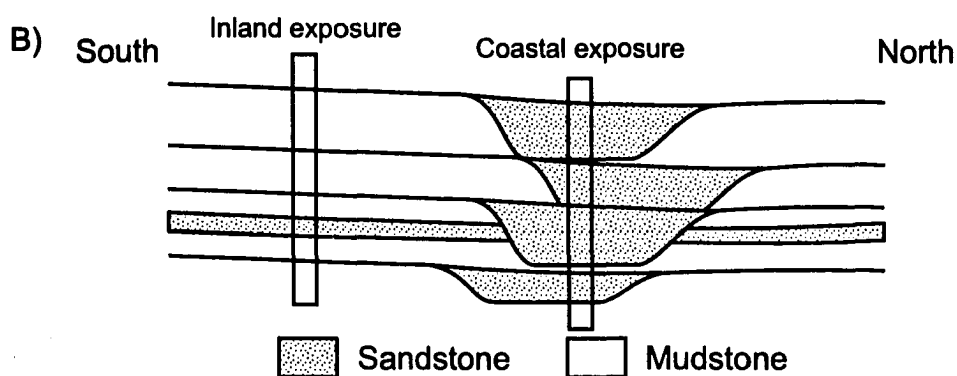
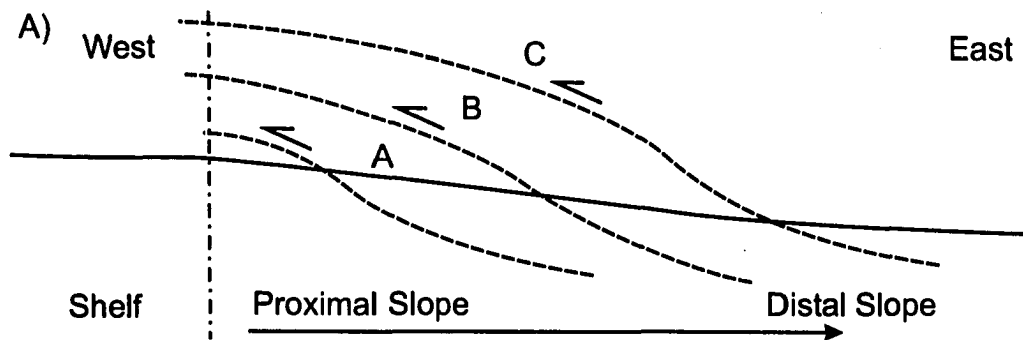


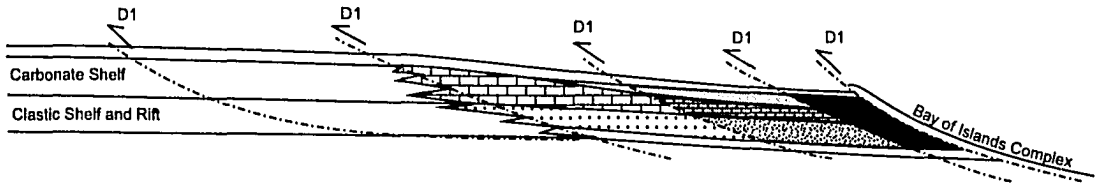
**Figure 5.1**

Models showing the potential for facies differences as a result of sedimentary architecture versus thrust stack transportation.

A) Geometry of a thrust stack showing thrust trajectories on a restored margin, allowing distal, and likely finer grained, sediment to be emplaced in a high structural position in the stack. A, B, and C represent increasingly fine facies of each unit, for example the Irishtown Formation. In the case of the Blow Me Down Brook formation, Sheet C may represent inland exposures, while coastal exposures are structurally higher, and restore to position A.

B) Possible interpretation of lateral facies changes causing a difference in proportion of sand observable in different parts of the map area, such as the difference in the Blow Me Down Brook formation between the coastal exposures and the inland exposures. This explanation involving lenticular coarser grained facies was also employed to

### D0: Margin relationships before thrusting



### D1: possible sedimentary stacking geometry after thrusting

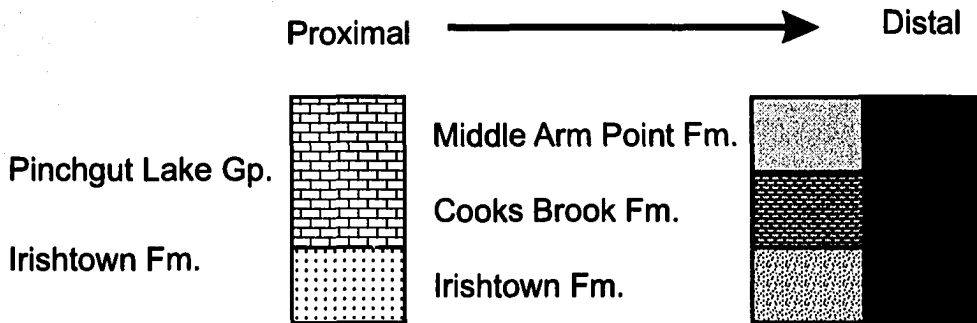
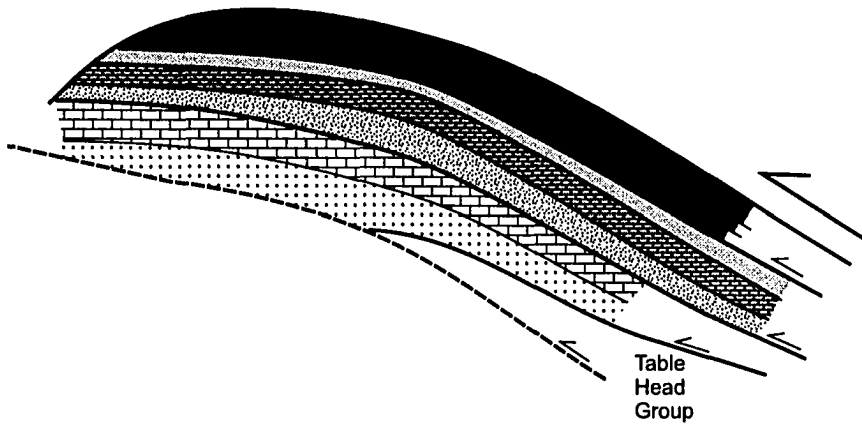


Figure 5.2

Model for structural stacking of units before and after D1 deformation.

Assuming facies changes within formations are relative to the depositional distance from the margin, structural position can be inferred after the construction of the D1 thrust stack. Specifically compared here are facies differences between the Irishtown Formation, the Pinchgut Lake Group, the Northern Head Group. As shown, units interpreted to have been deposited in higher energy environments, such as the Pinchgut Lake Group, occupy the lowest positions in the resulting thrust stack. Note: thrust stack geometry vertically exaggerated.

**Figure 5.3**

**Graben and rift model showing a possible depositional variation between the Summerside and the Blow Me Down Brook formations. A- Summerside formation, input restricted to local sources, B- Blow Me Down Brook formation, located in similar energy regime, except longitudinal flow parallel to the Laurentian margin would supply sediment from further away.**

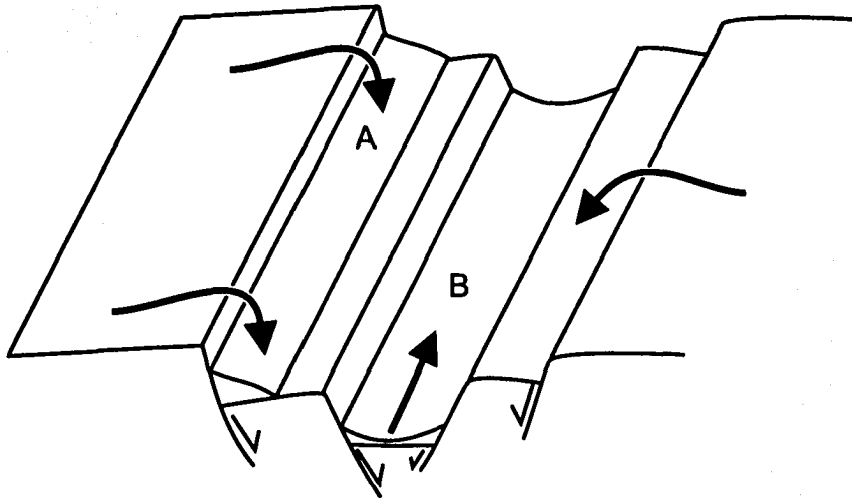
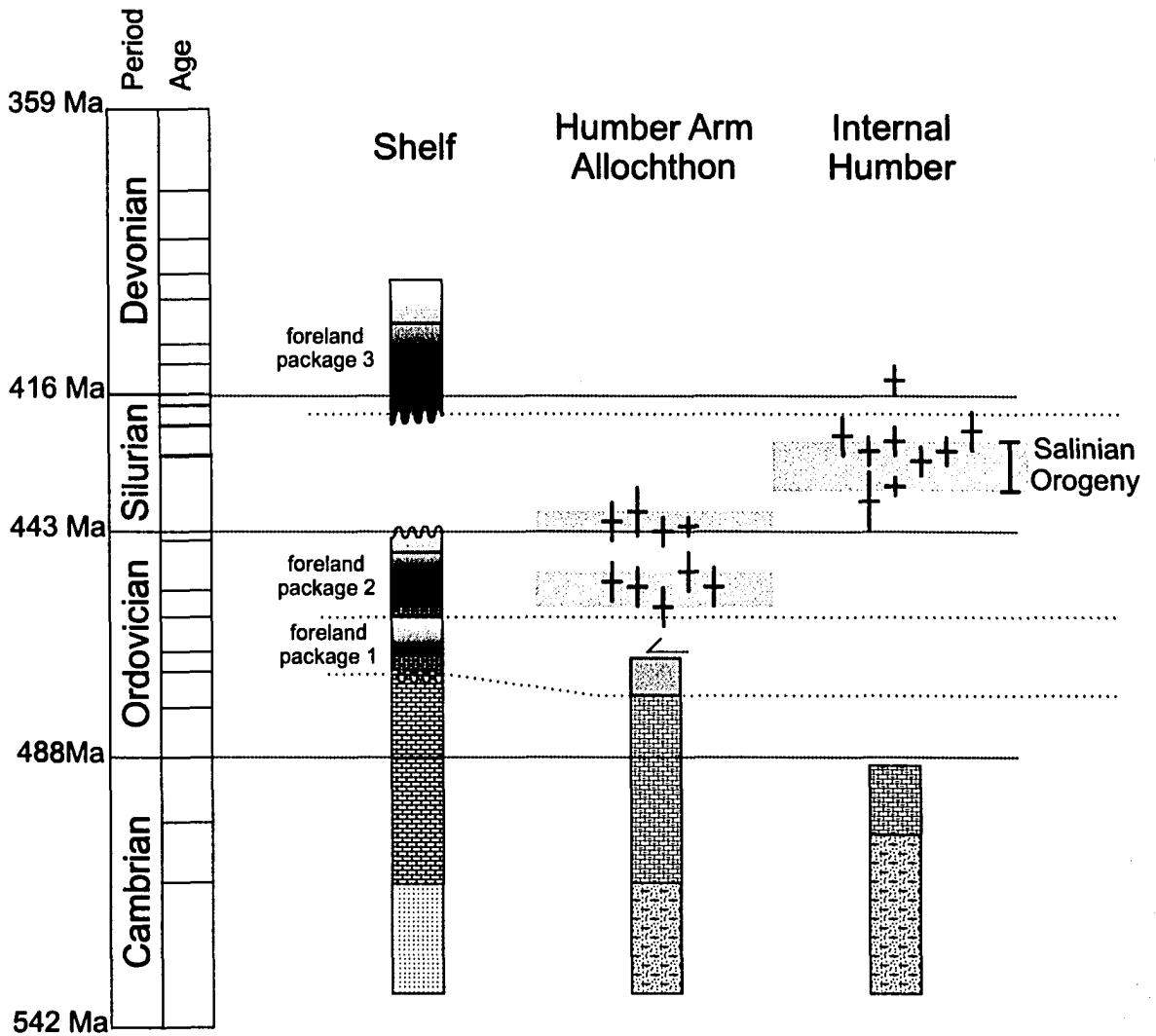
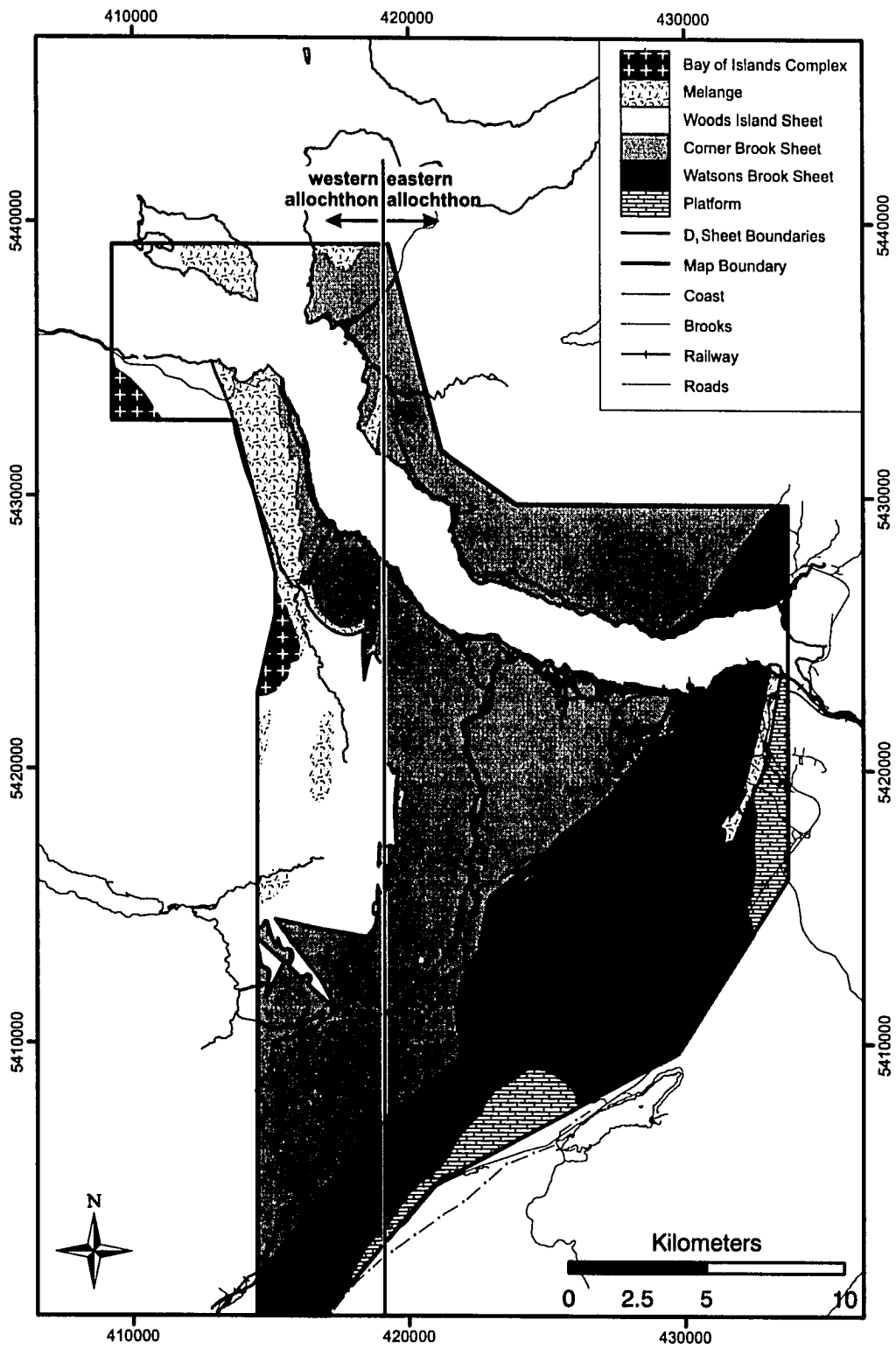


Figure 5.4

Time-Stratigraphic chart of the Early to middle Paleozoic Laurentian margin, focusing on three areas: the continental shelf, the Humber Arm Allochthon, and the internal Humber Zone. Chart includes isotopic age dates from both the allochthon and the internal zone. Geologic time scale used is GTS 2004 (Gradstein et al 2004). The Salinian Orogeny includes the ages determined by Cawood and Van Gool (1998).

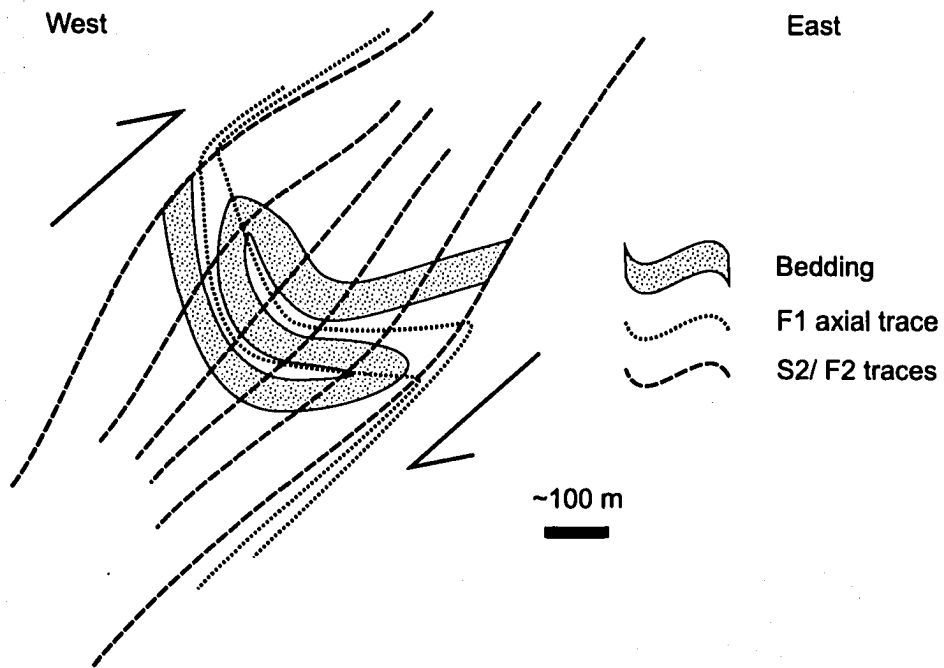


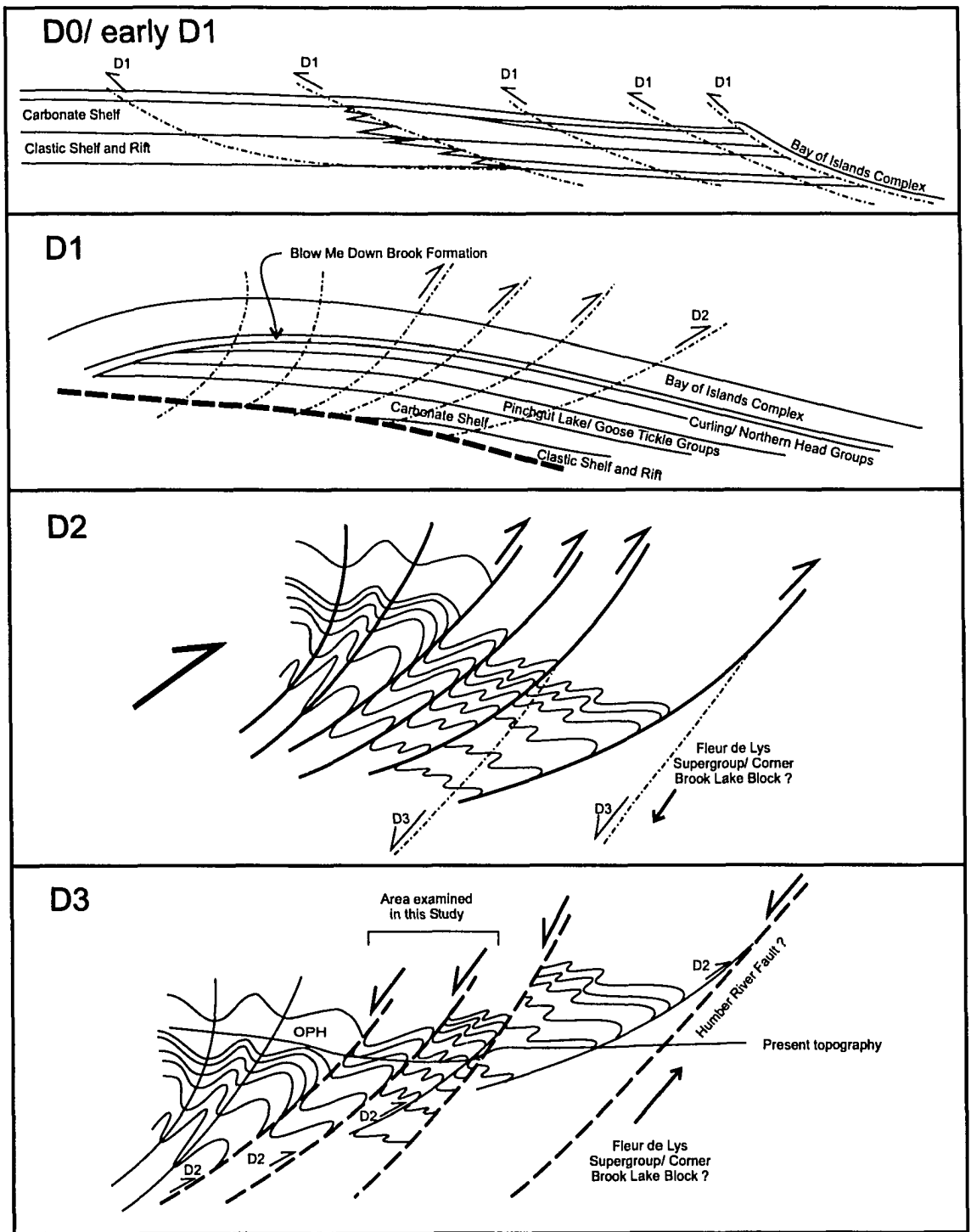


**Figure 5.5**  
**Map of the major thrust sheets and subdivision between the east and west Humber Arm Allochthon.**

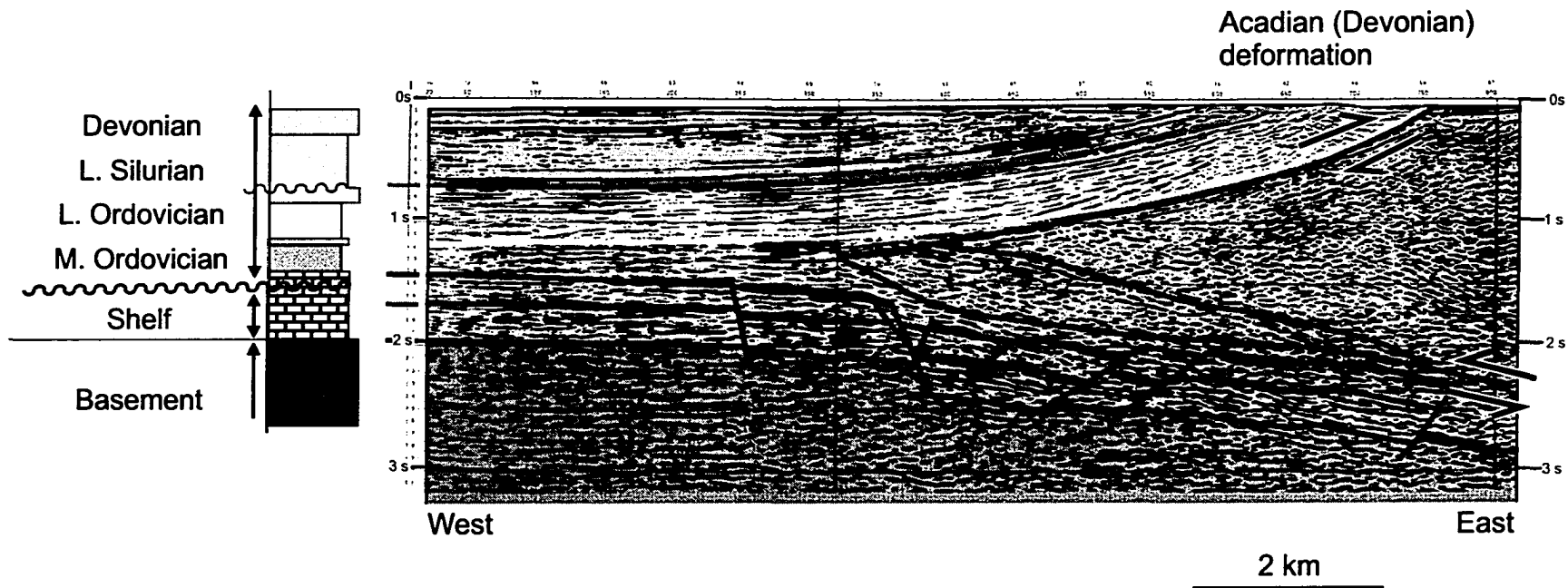
Figure 5.6

Diagram to show F1 folds preserved from transposition into S2, in the HW above the Crow Hill fault (map 1.3, insert 1 and 3). Preservation is interpreted as a result of the presence of a rigid framework of sandstone units. Arrows indicate sense of displacement during D2.





**Figure 5.7**  
 Model of the structural history of the Humber Arm Allochthon from D0 to D3.



**Figure 5.8**

Seismic line showing deformed Late Ordovician to Devonian sediments indicate that later thrusting occurred along the roof thrust of the triangle zone during the Devonian (adapted from Waldron et al 1998). Seismic Line 1606, location shown on map in figure 1.2. Note the vertical thickness of the Late Ordovician foreland basin package.

There is no well data verifying this seismic line. However, outcrop of the yellow unit occurs near this seismic line. Also, correlation to a geomagnetic survey was completed by Waldron et al (2002), which traced the Late Ordovician unit onto Port Au Port Peninsula and allowed an on-land survey of the unit.

## **Chapter 6: Conclusions**

### **6.1 *Geologic History***

Deformation observed in the Corner Brook Area, within the Humber Arm Allochthon, can be correlated to events both in the hinterland and foreland of the orogen. These stratigraphic and structural timing relationships are observed on the area-wide cross section (insert 3), and summarized in figure 5.4.

The Humber Arm Allochthon contains units accumulated during rifting, passive margin development, and foreland basin deposition. Comparisons between different facies of these units allow an interpretation of the morphology of the margin prior to the Taconian Orogeny in the Early Ordovician.

The generations of structures observed within the Humber Arm Allochthon, D1-5, are interpreted to reflect the broader development of the Humber Zone through several Paleozoic orogenic events. Deformation in the Humber Arm Allochthon is the result of several episodes of deformation, D1-D5.

- D1 structures are associated with west-vergent thin-skinned thrusting and are responsible for the duplex-like structure of the thrust stack composed of units transported from successively more distal positions on the continental margin (figure 5.7). D1 deformation within the allochthon is a result of the Taconian Orogeny and is also recorded in the stratigraphy of the on-shelf foreland basin.
- D2 is associated with a Late Ordovician event (~455 Ma). D2 structures are dominantly west dipping and are associated with east-

vergent thrusting (figure 5.7). This event is associated with significant margin loading and was previously identified only in the stratigraphy of the Long Point Group in the foreland basin. It is now tentatively also associated with argon isotopic age dates around 455 Ma from S2 fabrics within the Humber Arm Allochthon.

- D3 deformation occurred during the Early Silurian (~440 Ma) and is associated with unloading of the margin. D3 structures are normal-sense shears and faults that tend to reactivate S2 planes of weakness. The normal-sense displacement partially inverted the shortening that occurred during D2, and is tentatively interpreted as a mechanism whereby the deep and highly metamorphosed units of the internal Humber Zone may have been exhumed (figure 5.7). Based on the Early Silurian argon dates from D3 normal shear planes (~440 Ma), D3 is roughly correlative to a major unconformity in the foreland basin. There may be also be some relationship between D3 in the Humber Arm Allochthon and Silurian events recorded by isotopic ages in the internal Humber Zone (figure 5.4).
- D4, D5 are interpreted as the result of events that occurred during the Devonian, Acadian Orogeny, and/ or strike slip events that ultimately resulted in the formation of several Carboniferous basins.

## **6.2 *Future research***

Several avenues of further research would increase the understanding of the geologic history in the area. Additional mapping and structural studies would be possible

in the Pinchgut Lake Group and Goose Tickle Group to the east of the area, as well as in the Humber Arm Supergroup to the west. Within the Humber Arm Supergroup a change in structural style was noted with a gradient from east to west. Examining this change within the same stratigraphy would contribute to defining the results of D2. Also, a continuation of the facies analysis in areas proposed to be in higher structural slices would benefit the morphological model of the margin and the magnitude of thrust transport necessary in D1.

The accuracy and reliability of argon isotopic dating within the area would benefit from a larger dataset of analyses, as well as other techniques. Separation of muscovite from the rock increases the precision of the analyses and was used for two of the samples in this study. Separation was completed using dissolution of calcic material from the carbonate host rock, leaving the non-carbonate portion behind. This method could be effectively used in samples from the carbonate units. Laser dating of micas in specific fabrics would significantly increase the reliability of the isotopic ages. A major problem with measuring the age of mica crystallization in rocks with several fabrics is the determination of which fabric is the source of radiogenic Argon. Laser spot diameters are too large to analyze individual mica crystals. However in many instances, aggregates of mica, up to one millimetre thick, were observed associated with a single fabric; these aggregates would be possible to analyze using laser dating techniques.

As discussed in Chapter 5, a comprehensive geochemical analysis of the various blocks of basalts in the area to determine whether they are either arc- or rift- source, would be beneficial. Currently there is only speculation as to their origin. Their origin would provide evidence as to whether they lie in stratigraphic contact below the rift

sediments, or were originally part of the arc-volcanics now preserved to the west. If the blocks are arc-related, likely their mechanism of emplacement was strictly tectonic, and associated with mélangé development.

## References

- Allmendinger, R. W., Gephart, J. W. & Marrett, R. A. 1989. Notes on Fault Slip Analysis: Prepared for the Geological Society of America Short Course on "Quantitative Interpretation of Joints and Faults".
- Angelier, J. & Mechler, P. 1977. Sur une methode graphique de recherché des contraintes principales egalment utilisable en tectonique et en seiemologie: La methode des diedres droit. *Bulletin de Societie Geologique de France* **19**, 1309-1318.
- Botsford, J. 1988. Stratigraphy and sedimentology of Cambro-Ordovician deep water sediments, Bay of Islands, western Newfoundland. Unpublished Ph.D. thesis, Memorial University of Newfoundland.
- Bouma, A. H. 1962. *Sedimentology of some Flysch Deposits. A Graphic Approach to Facies Interpretation*. Elsevier, Amsterdam.
- Boyce, W. D., Botsford, J. W. & Ash, J. S. 1992. Preliminary trilobite biostratigraphy of the Cooks Brook formation (Northern Head group), Humber Arm Allochthon, Bay of Islands, Western Newfoundland. *Newfoundland and Labrador, Department of Mines, Mineral Development Division, Report 92-1*, 55-68.
- Brem, A. G., Lin, S. & van Staal, C. R. 2003. Structural Relationships south of Grand Lake, Newfoundland. *Current Research: Newfoundland Department of Mines and Energy Geological Survey, Report 03-1*, 1-13.
- Bruckner, W. D. 1966. Stratigraphy and structure of western Newfoundland. In: *Guidebook - Geology of parts of Atlantic Provinces: Annual Meeting, Geological Association of Canada and Mineralogical Association of Canada* (edited by Poole, W. H.), 137-151.

- Buchanan, C. R. 2004. Structural architecture and evolution of the Humber Arm Allochthon, Frenchman's Cove-York Harbour, Bay of Islands, Newfoundland. Unpublished M.Sc. thesis, Memorial University of Newfoundland.
- Cawood, P. A. & Williams, H. 1988. Acadian basement thrusting, crustal delamination, and structural styles in and around the Humber Arm allochthon, western Newfoundland. *Geology* **16**, 370-373.
- Cawood, P. A. & Suhr, G. 1992. Generation and obduction of ophiolites: constraints from the Bay of Islands Complex, western Newfoundland. *Tectonics* **11**, 884-897.
- Cawood, P. A. 1993. Acadian orogeny in west Newfoundland: Definition, character and significance. In: *The Acadian orogeny: Recent studies in New England, maritime Canada, and the autochthonous foreland* (edited by Roy, D. C. & Skehan, J. W.). *Geological Society of America Special Paper* **275**, 135-153.
- Cawood, P. A. & Dunning, G. R. 1993. Silurian age for movement on the Baie Verte Line: Implications for accretionary tectonics in the Northern Appalachians [abstract]. *Geological Society of America, Abstracts with Programs* **25**, A422.
- Cawood, P. A. & van Gool, J. A. M. 1998. *Geology of the Corner Brook - Grand Lake region, Newfoundland*. Geological Survey of Canada Bulletin 427, Ottawa.
- Cawood, P. A. & Nemchin, A. A. 2001. Paleogeographic development of the east Laurentian margin: constraints from U-Pb dating of detrital zircons in the Newfoundland Appalachians. *Geological Society of America Bulletin* **113**, 1234-1246.
- Dallmeyer, R. D. & Williams, H. 1975.  $^{40}\text{Ar}/^{39}\text{Ar}$  release spectra of hornblende from the Bay of Islands metamorphic aureole, western Newfoundland: their bearing on

- the timing of ophiolite obduction at the Ordovician continental margin of eastern North America. *Canadian Journal of Earth Sciences* **12**, 1685-1690.
- Dunning, G. R., Kean, B. F., Thurlow, J. G. & Swinden, H. S. 1987. Geochronology of the Buchans, Roberts Arm, and Victoria Lake Groups and the Mansfield Cove Complex, Newfoundland. *Canadian Journal of Earth Sciences* **24**, 1175-1184.
- Dunning, G. R., O'Brien, S. J., Colman, S. S. P., Blackwood, R. F., Dickson, W. L., O'Neill, P. P. & Krogh, T. E. 1990. Silurian orogeny in the Newfoundland Appalachians. *Journal of Geology* **98**, 895-913.
- Ferguson, M. 1998. Geology of a folded thrust belt, Pinchgut Lake area, western Newfoundland. Unpublished B.Sc. thesis, Saint Mary's University.
- Gradstein, F. M., Ogg, J.G., Smith, A.G., Agterberg, F.P., Bleeker, W., Cooper, R.A., Davydov, V., Gibbard, P., Hinnov, L.A., House, M.R., Lourens, L., Luterbacher, H.P., McArthur, J., Melchin, M.J., Robb, L.J., Shergold, J., Villeneuve, M., Wardlaw, B.R., Ali, J., Brinkhu. 2004. *A Geologic Time Scale 2004*. Cambridge University Press.
- Gray, D. R. 1977. Morphological classification of crenulation cleavage. *Journal of Geology* **85**, 229-235.
- Henry, A. 2002. Geology and structure of a folded thrust zone, Corner Brook area, Western Newfoundland. Unpublished Honours thesis, University of Alberta.
- Hibbard, J. 1994. Kinematics of Acadian deformation in the northern and Newfoundland Appalachians. *Journal of Geology Chicago* **102**, 215-228.

- Hyde, R. S., Miller, H. G., Hiscott, R. N. & Wright, J. A. 1988. Basin architecture and thermal maturation in the strike-slip Deer Lake Basin, Carboniferous of Newfoundland. *Basin Research* **1**, 85-105.
- Idleman, B. D. 1998. Late Caradocian exhumation of the Taconic Orogen in western Newfoundland; evidence from single-crystal (super 40) Ar/ (super 39) Ar dating of detrital muscovite. *Program with Abstracts - Geological Association of Canada; Mineralogical Association of Canada; Canadian Geophysical Union, Joint Annual Meeting* **23**, 83-84.
- James, N. P. & Stevens, R. K. 1986. *Stratigraphy and correlation of the Cambro-Ordovician Cow Head Group, western Newfoundland*. Geological Survey of Canada Bulletin 366, Ottawa.
- James, N. P., Knight, I., Stevens, R. K. & Barnes, C. R. 1988. *Trip B1. Sedimentology and paleontology of an Early Palaeozoic continental margin, Western Newfoundland*. Field Trip Guidebook, Geological Association of Canada, St John's, Newfoundland.
- Kerrick, R. 1978. A historical review and synthesis of research on pressure solution. *Zentralblatt fur Geologie und Palaeontologie* **5/6**, 512-550.
- Klappa, C. F., Opalinski, P. R. & James, N. P. 1980. Ordovician Table Head Group of western Newfoundland: a revised stratigraphy. *Canadian Journal of Earth Sciences* **17**, 1007-1019.
- Knight, I., James, N. P. & Lane, T. E. 1991. The Ordovician St. George Unconformity, northern Appalachians: The relationship of plate convergence at the St. Lawrence

- Promontory to the Sauk/Tippecanoe sequence boundary. *Geological Society of America Bulletin* **103**, 1200-1225.
- Knight, I. 1996a. *Geological map of parts of the Little Grand Lake (12A/12), Corner Brook (12A/13), Georges Lake (12B/9) and Harrys River (12B/16) map areas.* Geological Survey, Newfoundland and Labrador Department of Mines and Energy, Map 95-20.
- Knight, I. 1996b. *Geology of Cambro-Ordovician carbonate-shelf and co-eval off-shelf rocks, southwest of Corner Brook, western Newfoundland.* Newfoundland and Labrador, Department of Natural Resources, Geological Survey, Open File 2602.
- Laird, M. G. 1970. Vertical sheet structures - a new indicator of sedimentary fabric. *Journal of Sedimentary Petrology* **70**, 428-434.
- Lilly, H. D. 1963. *Geology of Hughes Brook - Goose Arm Area, West Newfoundland.* Memorial University of Newfoundland Department of Geology Report **2**, 123.
- Lindholm, R. M. & Casey, J. F. 1989. Regional significance of the Blow Me Down Brook Formation, Western Newfoundland: new fossil evidence for an Early Cambrian age. *Geological Association of America Bulletin* **101**, 1-13.
- Lindholm, R. M. & Casey, J. F. 1990. The distribution and possible biostratigraphic significance of the ichnogenus *Oldhamia* in the shales of the Blow Me Down Brook Formation, western Newfoundland. *Canadian Journal of Earth Sciences* **27**, 1270-1287.
- Mardia, K. V. 1972. *Statistics of Directional Data.* Academic Press, London, U. K.
- Marrett, R. & Allmendinger, R. W. 1990. Kinematic analysis of fault-slip data. *Journal of Structural Geology* **12**, 973-986.

- Moore, J. C., Roeske, S., Lundberg, N., Schoonmaker, J., Cowan, D. S., Gonzales, E. & Lucas, S. E. 1986. Scaly fabrics from Deep Sea Drilling Project cores from forearcs. *Geological Society of America Memoir* **166**, 55-73.
- McDougall, I. & Harrison, T. M. 1999. *Geochronology and Thermochronology by the  $^{40}\text{Ar}/^{39}\text{Ar}$  Method*. Oxford University Press, New York.
- Palmer, S. E., Burden, E. & Waldron, J. W. F. 2001. Stratigraphy of the Curling Group (Cambrian), Humber Arm Allochthon, Bay of Islands. In: *Current Research (2001)*. Newfoundland Department of Mines and Energy, Geological Survey Report 2001-1, 105-112.
- Quinn, L. 1988. Distribution and significance of Ordovician flysch units in western Newfoundland. In: *Current Research, Part B. Geological Survey of Canada Paper 88-1B*, 119-126.
- Quinn, L. 1996. Middle Ordovician foredeep fill in western Newfoundland. In: *Current Perspectives in the Appalachian-Caledonian Orogen* (edited by Hibbard, J. P., van Staal, J. R. & Cawood, P. A.). *Geological Association of Canada Special Paper 41*, 43-64.
- Quinn, L., Williams, S. H., Harper, D. A. T. & Clarkson, E. N. K. 1999. Late Ordovician foreland basin fill: Long Point Group of onshore western Newfoundland. *Bulletin of Canadian Petroleum Geology* **47**, 63-80.
- Ramsay, J. G. 1967. *Folding and Fracturing of Rocks*. McGraw-Hill Book Company, Toronto.

- Stenzel, S. R., Knight, I. & James, N. P. 1990. Carbonate platform to foreland basin: revised stratigraphy of the Table Head Group (Middle Ordovician), western Newfoundland. *Canadian Journal of Earth Sciences* **27**, 14-26.
- Stevens, R. K. 1965. Geology of the Humber Arm, west Newfoundland. Unpublished M.Sc. thesis, Memorial University.
- Stevens, R. K. 1970. Cambro-Ordovician flysch sedimentation and tectonics in west Newfoundland and their possible bearing on a Proto-Atlantic Ocean. In: *Flysch sedimentology in North America* (edited by Lajoie, J.). *Geological Association of Canada Special Paper* **7**, 165-177.
- Stockmal, G. S., Waldron, J. W. F. & Quinlan, G. S. 1995. Flexural modeling of Paleozoic foreland basin subsidence, offshore western Newfoundland; Evidence for substantial post-Taconian thrust transport. *Journal of Geology Chicago* **103**, 653-671.
- Suhr, G. & Cawood, P. A. 1993. Structural history of Ophiolite obduction, Bay of Islands, Newfoundland. *Geological Society of America Bulletin* **105**(3), 399-410.
- Suhr, G. & Cawood, P. A. 1993. Structural history of Ophiolite obduction, Bay of Islands, Newfoundland. *Geological Society of America Bulletin* **105**(3), 399-410.
- Tanton, J. 2001. Determining formation relationships and classifications with the use of sedimentary petrography Corner Brook Area, Western Newfoundland. Unpublished Honours thesis, University of Alberta.
- Thurlow, J. G., Spencer, C. P., Boerner, D. E., Reed, L. E., & Wright, J. A. 1992. Geological interpretation of a high resolution reflection seismic survey at the

- Buchans mine, Newfoundland. *Canadian Journal of Earth Sciences* **29**, 2022-2037.
- van Berkel, J. T. & Currie, K. L. 1988. Geology of the Puddle Pond (12A/5) and Little Grand Lake (12A/12) map areas, southwestern Newfoundland. *Newfoundland Department of Mines, Mineral Development Division Report 88-1*, 99-107.
- Waldron, J. W. F. 1985. Structural history of continental margin sediments beneath the Bay of Islands Ophiolite, Newfoundland. *Canadian Journal of Earth Sciences* **22**, 1618-1632.
- Waldron, J. W. F., Turner, D. & Stevens, K. M. 1988. Stratal disruption and development of mélangé, Western Newfoundland: effect of high fluid pressure in an accretionary terrain during ophiolite emplacement. *Journal of Structural Geology* **10**, 861-873.
- Waldron, J. W. F. & Stockmal, G. S. 1994. Structural and tectonic evolution of the Humber Zone, western Newfoundland 2. A regional model for Acadian thrust tectonics. *Tectonics* **13**, 1498-1513.
- Waldron, J. W. F., Anderson, S., Cawood, P., Goodwin, L. B., Hall, J., Jamieson, R. A., Palmer, S. E., Stockmal, G. S. & Williams, P. F. 1998. Evolution of the Appalachian Laurentian margin: Lithoprobe results in western Newfoundland. *Canadian Journal of Earth Sciences* **35**, 1271-1287.
- Waldron, J. W. F. & Palmer, S. E. 2000. Lithostratigraphy and structure of the Humber Arm Allochthon in the type area, Bay of Islands, Newfoundland. In: *Current Research, Newfoundland Department of Mines and Energy, Geological Survey Report 2000-1*, 279-290.

- Waldron, J. W. F. & Van Staal, C. R. 2001. Taconian orogeny and the accretion of the Dashwoods block: A peri-Laurentian microcontinent in the Iapetus Ocean. *Geology* **29**, 811-814.
- Waldron, J. W. F., Henry, A. D. & Bradley, J. C. 2002a. Structure and polyphase deformation of the Humber Arm Allochthon and related rocks west of Corner Brook, Newfoundland. In: *Current Research (2002). Newfoundland Department of Mines and Energy, Geological Survey, Report 02-1*, 47-52.
- Waldron, J. W. F., DeWolfe, J., Courtney, R. & Fox, D. 2002b. Origin of the Odd-twins anomaly: magnetic effect of a unique stratigraphic marker in the Appalachian foreland basin, Gulf of St. Lawrence. *Canadian Journal of Earth Science* **39**, 1675-1687.
- Waldron, J. W. F., Henry, A. D., Bradley, J. C. & Palmer, S. E. 2003. Development of a folded thrust stack: Humber Arm Allochthon, Bay of Islands, Newfoundland Appalachians. *Canadian Journal of Earth Science* **40**, 237-253.
- Whalen, J. B., Currie, K. L. & van Breeman, O. 1987. Episodic Ordovician Silurian plutonism in the topsails igneous terrane, western Newfoundland. *Transactions of the Royal Society of Edinburgh: Earth Sciences* **78**, 17-28.
- Whittington, H. B. & Kindle, C. H. 1963. Middle Ordovician Table Head Formation, Western Newfoundland. *Geological Society of America Bulletin* **74**, 745-758.
- Williams, H. 1975. Structural succession, nomenclature, and interpretation of transported rocks in western Newfoundland. *Canadian Journal of Earth Sciences* **12**, 1874-1894.

- Williams, H. 1979. Appalachian Orogen in Canada. *Canadian Journal of Earth Sciences* **16**, 792-807.
- Williams, H., Gillespie, R. T. & van Breeman, O. 1985. A late Precambrian rift-related igneous suite in western Newfoundland. *Canadian Journal of Earth Sciences* **22**, 1727-1735.
- Williams, H. & Cawood, P. 1986. Relationships along the eastern margin of the Humber Arm allochthon between Georges Lake and Corner Brook, Newfoundland. In: *Current Research Part A. Geological Survey of Canada Paper 86-1A*, 759-765.
- Williams, H. & Hiscott, R. N. 1987. Definition of the lapetus rift-drift transition in western Newfoundland. *Geology* **15**, 1044-1047.
- Williams, S. H., Boyce, W. D. & James, N. P. 1987. Graptolites from the Lower - Middle Ordovician St. George and Table Head Groups, western Newfoundland, and their correlation with trilobite, brachiopod, and conodont zones. *Canadian Journal of Earth Sciences* **24**, 456-470.
- Williams, H. & Cawood, P. A. 1989. Geology, Humber Arm Allochthon, Newfoundland. In: *Geological Survey of Canada Map. 1:250 000 1678A*.
- Williams, H. 1995. Temporal and spatial divisions. In: *Geology of the Appalachian-Caledonian Orogen in Canada and Greenland* (edited by Williams, H.). *Geology of Canada* **6**. Geological Survey of Canada, 23-44.
- Wright, J. A., Hoffe, B. H., Langdon, G. S. & Quinlan, G. M. 1996. The Deer Lake Basin, Newfoundland: structural constraints from new seismic data. *Bulletin of Canadian Petroleum Geology* **44**, 674-682.

## Appendix A

This appendix is intended to accompany Chapter 4, and contains the full sample descriptions not included in the text and the summaries of the isotope measurements and apparent age calculations collected during the argon isotope analysis.

### Argon Analyses

The full dataset of the argon isotope work is contained within this Appendix. Each analysis completed has 9 columns of data represented here. Values reported for the  $^{37}\text{Ar}/^{39}\text{Ar}$ ,  $^{36}\text{Ar}/^{40}\text{Ar}$  and  $^{39}\text{Ar}/^{40}\text{Ar}$  isotope ratios are corrected for mass spectrometer discrimination, interfering isotopes, and system blanks.

- 1) **T°C** is the temperature of the furnace at the time when the isotope measurement was made.
- 2)  **$^{39}\text{Ar}(\text{mV})$**  is a direct measurement of the electrical current resulting from the collection of positive ions in the mass spectrometer.
- 3)  **$^{39}\text{Ar}(\%)$**  is the % of  $^{39}\text{Ar}$  that is released at each single temperature steps as a percentage of the total  $^{39}\text{Ar}$  released (100%).
- 4) **AGE (Ma)  $\pm 1$**  apparent age calculation based on the Argon isotopes measured at each temperature step.
- 5) **% ATM** this percentage is calculated from the  $^{36}\text{Ar}$  measured in the analysis. The number is given as atmospheric  $^{40}\text{Ar}$  as a percentage of the total  $^{40}\text{Ar}$ .
- 6)  **$^{37}\text{Ar}/^{39}\text{Ar}$**  represents the measured ratio of these argon isotopes.  $^{37}\text{Ar}$  is used to calculate the amount of interference there is due to Ar produced by decay from Ca.
- 7)  **$^{36}\text{Ar}/^{40}\text{Ar}$**  represents the measured ratio of these argon isotopes.  $^{36}\text{Ar}$  is used to calculate the presence or amount of atmospheric argon during analysis.
- 8)  **$^{39}\text{Ar}/^{40}\text{Ar}$**  represents the measured ratio of these argon isotopes.  $^{39}\text{Ar}$  is the product of radioactive decay from  $^{40}\text{K}$  and is used to calculate the age of the sample.
- 9) **%IIC** is the interfering isotopes correction, which is a correction calculation used to remove the effects of non-radiogenic Argon. This calculation uses the  $^{37}\text{Ar}/^{39}\text{Ar}$  ratio.

### Sample list and locations

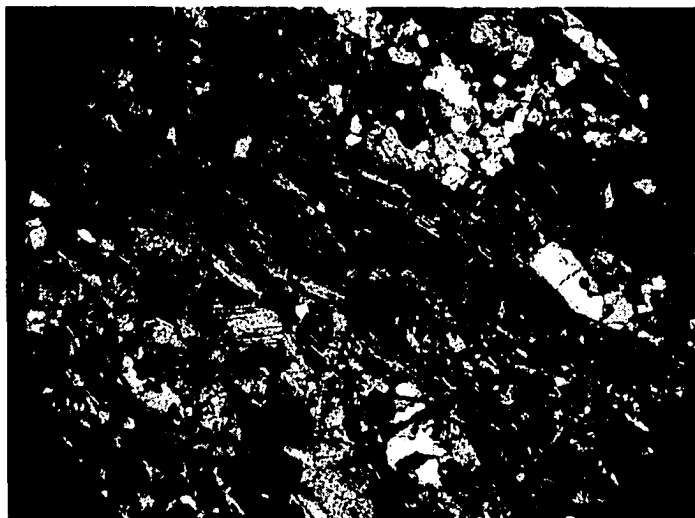
Station	Sample label	UTMX	UTMY	Elevation
DW065	DW065A	426055	5402975	?
DW170	DW170A	426325	5401551	?
GQ112	GQ112A	431974	5419872	146
HQ092	HQ092A	415286	5414761	311
HV002	HV002A	429643	5425049	57
HV123	HV123A	429625	5425037	41
HV134	HV134A	428774	5424924	1
HY056	HY056A	427240	5425532	30
JA023	JA023B	432017	5419934	165
JA082	JA082A	432029	5419946	166
JA083	JA083A	432043	5420034	141
JA083	JA083B	432043	5420034	141

## **A.1 DW170A**

### **A.1.a Description**

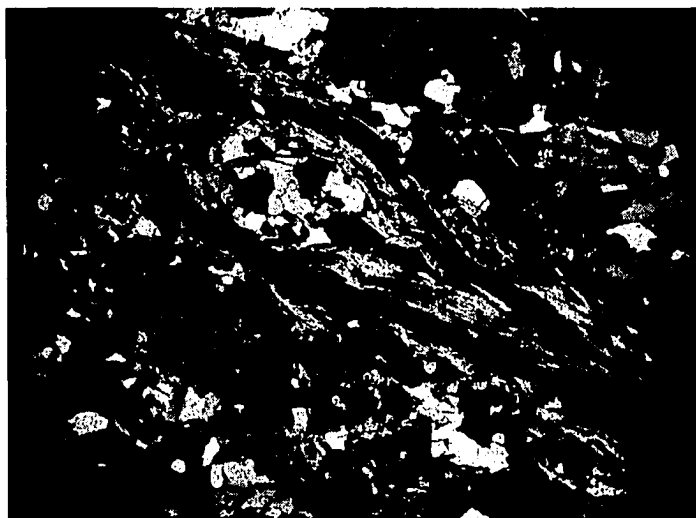
This sample is composed of 45% calcite, both grains and cement; 35% detrital sub-rounded quartz grains and 20% muscovite.

Quartz grains range from 0.2mm to 0.5 mm; calcite crystals are larger than the quartz, 0.3 to 1.2 mm. Initial grain size is comparable but has increased due to calcite overgrowth. Muscovite crystals occur as aggregates of many very thin flakes. Maximum size of individual crystals is 0.05 mm thick and 0.5 mm long. Aggregates occur up to 0.5 mm thick and some are longer than the length of the thin section (> 3 cm).



Thin section photo taken under crossed polars. Aggregates of muscovite flakes in thin section looking down the stretching lineation.

1mm



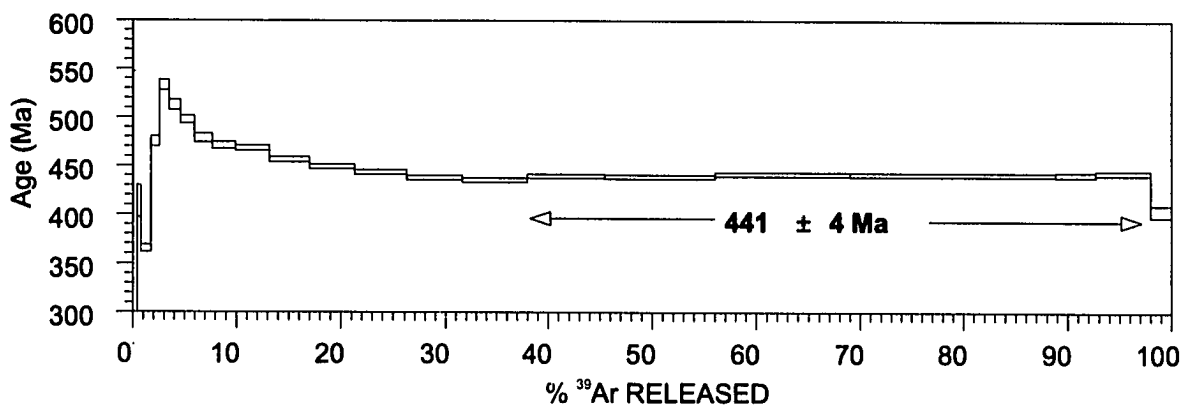
Thin section photo taken under crossed polars. illustrates the sedimentary grain size variation and shows additional aggregates of tectonic muscovite, interpreted as shear related.

1mm

### A.1.b Muscovite Argon Summary

T°C	<sup>39</sup> Ar(mV)	<sup>39</sup> Ar(%)	AGE(Ma)±1σ	% ATM	<sup>37</sup> Ar/ <sup>39</sup> Ar	<sup>36</sup> Ar/ <sup>40</sup> Ar	<sup>39</sup> Ar/ <sup>40</sup> Ar	% IIC
600	0.6	0	0 ± 704	320.1	37.66	0.010812	0.007217	1.52
650	0.9	0	0 ± 267	241.1	26.73	0.008152	0.007385	0.68
700	1.6	0.1	0 ± 81	132	10.8	0.004467	0.008226	1.37
750	2.5	0.1	233 ± 40	60.3	4.18	0.002041	0.006652	0.8
800	4.9	0.3	413 ± 16	26	1.76	0.000883	0.006647	0.23
850	14.2	0.9	365 ± 3	0.8	0	0.000027	0.010249	0
875	11.6	0.8	475 ± 5	0.7	0	0.000023	0.007634	0
900	13.6	0.9	533 ± 5	2.3	0	0.00008	0.006577	0
925	16.1	1.1	512 ± 5	6	0	0.000206	0.006617	0
950	19.7	1.3	497 ± 3	6.9	0	0.000235	0.006787	0
975	24.9	1.7	478 ± 4	17.6	0	0.000597	0.006278	0
1000	31.8	2.2	471 ± 3	12.6	0	0.000427	0.006783	0
1025	46.9	3.2	468 ± 2	2.2	0	0.000077	0.007636	0
1050	54.9	3.8	456 ± 2	1.8	0	0.000062	0.007897	0
1075	62.4	4.3	449 ± 2	1.3	0	0.000046	0.008079	0
1100	70.8	4.9	443 ± 2	1.1	0	0.000039	0.008216	0
1125	77.3	5.3	438 ± 2	1.1	0	0.000038	0.008337	0
1150	91.9	6.3	435 ± 2	1.2	0	0.000041	0.008385	0
1175	107.8	7.4	439 ± 2	0.3	0	0.000011	0.008372	0
1200	152	10.5	438 ± 2	0.5	0	0.000017	0.008373	0
1250	187.2	12.9	441 ± 2	0.5	0	0.000018	0.008311	0
1300	286.1	19.8	441 ± 2	1.3	0	0.000046	0.008252	0
1350	55.4	3.8	441 ± 2	3.4	0	0.000116	0.008076	0
1450	76.4	5.3	443 ± 2	5.6	0	0.00019	0.007855	0
1500	29.1	2	403 ± 6	24.1	0.67	0.000818	0.007001	0.09
J = .002318 ± 2.318E-05								

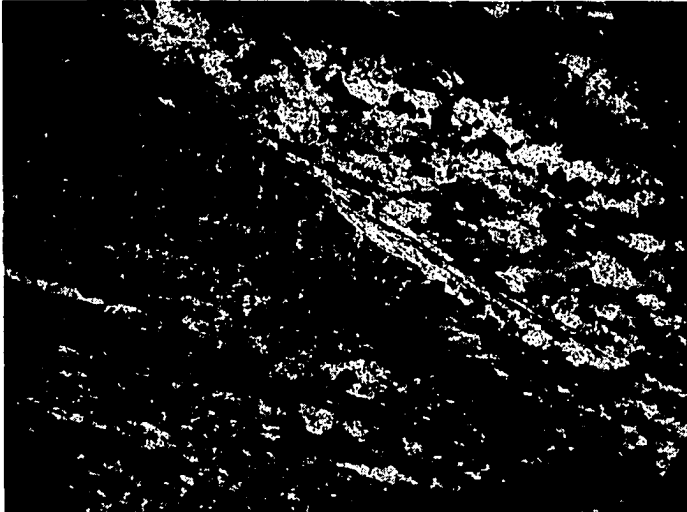
### A.1.c Muscovite mineral separate spectrum



## **A.2 DW065A**

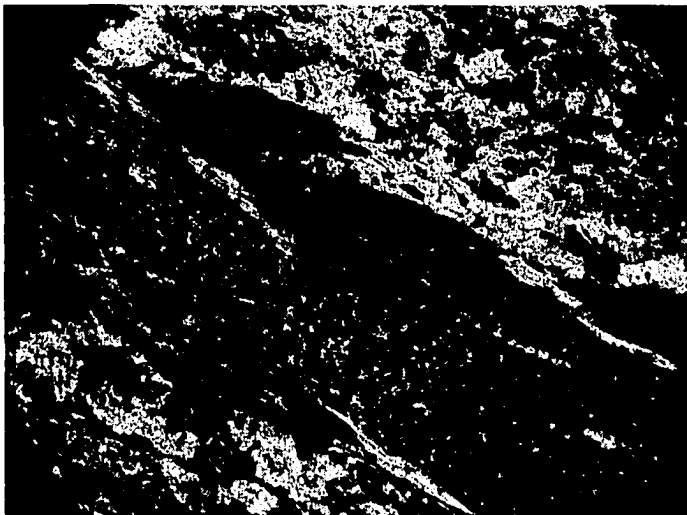
### **A.2.a Description**

This a sample of limestone. The size of the grain components, which are all calcite, ranges from 0.25 mm to 1.5 mm. All of the matrix in this rock is carbonate and has a muddy texture. There are sub-parallel bands of very fine and mostly opaque carbonate throughout he sample. These bands are commonly associated with the fine-grained muscovite that is present. The muscovite is again present in aggregates. Individual grain sizes are too small to determine, but achieve a maximum of 0.2 mm thick and 1.2 mm long.



Thin section photo taken under crossed polars. The northeast corner of this photo shows less deformed calcite grains and the dark band is interpreted as a mylonite zone. The muscovite is only developed along the margins of this mylonite.

1mm



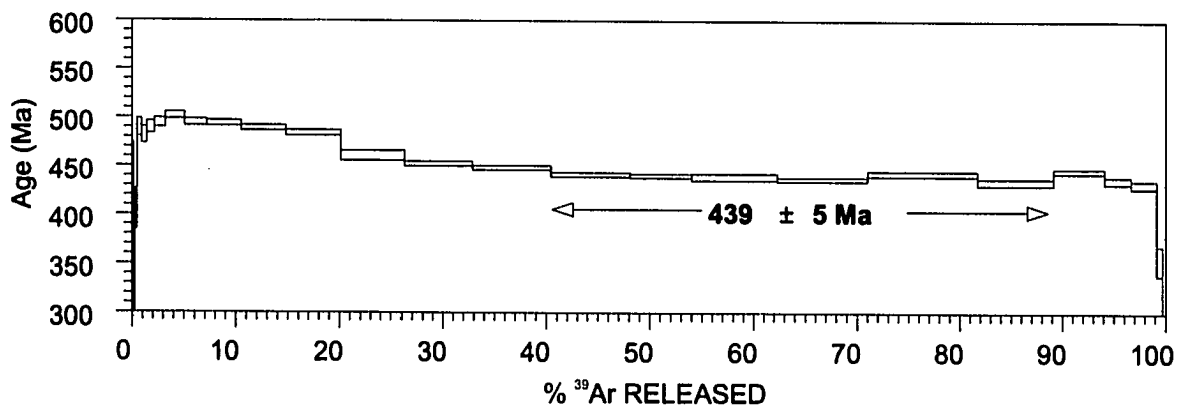
Thin section photo taken under crossed polars. The same features are shown as those in the above photo. Muscovite associated with the mylonite bands.

1mm

## A.2.b Muscovite Argon Summary

T°C	<sup>39</sup> Ar(mV)	<sup>39</sup> Ar(%)	AGE(Ma)±1σ	% ATM	<sup>37</sup> Ar/ <sup>39</sup> Ar	<sup>36</sup> Ar/ <sup>40</sup> Ar	<sup>39</sup> Ar/ <sup>40</sup> Ar	% IIC
600	1.7	0.1	444 ± 29	26.6	0.3	0.000903	0.006069	0.03
650	1.6	0.1	331 ± 36	42.4	0.81	0.001434	0.006615	0.12
700	3.1	0.2	405 ± 20	26	0.5	0.000881	0.006796	0.06
750	6.5	0.4	489 ± 9	10.7	0.25	0.000363	0.006627	0.03
775	8	0.5	481 ± 8	10.5	0.23	0.000355	0.006766	0.02
800	11.1	0.7	489 ± 5	6.9	0.16	0.000235	0.006904	0.02
825	15.4	1	494 ± 4	5	0.14	0.000172	0.006968	0.01
850	27	1.8	502 ± 3	4.5	0.08	0.000153	0.006887	0.01
875	31.4	2.1	494 ± 3	4.4	0.06	0.000151	0.007007	0
900	48.8	3.3	494 ± 2	4.3	0.03	0.000148	0.007025	0
925	64	4.3	489 ± 2	6.3	0.02	0.000215	0.006957	0
950	78.6	5.3	484 ± 2	11.3	0.01	0.000385	0.006665	0
975	90.3	6.1	461 ± 5	2.6	0.4	0.00009	0.007739	0.05
1000	98.8	6.6	452 ± 2	1.4	0	0.000049	0.008005	0
1025	111.6	7.5	448 ± 2	0.8	0	0.000027	0.00814	0
1050	113	7.6	441 ± 2	1	0	0.000034	0.008271	0
1075	87.9	5.9	440 ± 2	0.4	0	0.000013	0.008342	0
1100	122.6	8.2	439 ± 3	4.6	0.08	0.000157	0.008011	0.01
1150	128.4	8.6	436 ± 2	0.3	0	0.000012	0.008423	0
1200	158.6	10.7	442 ± 2	3.2	0.01	0.00011	0.008058	0
1250	109.9	7.4	434 ± 3	9.4	0.09	0.000319	0.007706	0.01
1300	72.7	4.9	445 ± 2	3.8	0.05	0.00013	0.007947	0
1350	38.3	2.5	435 ± 3	18.5	0.1	0.000627	0.006901	0.01
1400	36.7	2.4	431 ± 3	17.5	0.17	0.000592	0.007067	0.02
1450	8	0.5	353 ± 14	41	1.29	0.00139	0.006296	0.18
1500	4.4	0.3	211 ± 32	73.6	3.14	0.002491	0.004911	0.64
J = .002316 ± 2.316E-05								

## A.2.c Muscovite mineral separate spectrum



### A.3 JA083A

#### A.3.a Description

This sample is from a sandstone bed that has been partially dissolved through pressure solution cleavage. There is some variability in the thicknesses of dissolution bands but the rock is generally composed of quartz-rich bands and very fine-grained quartz-poor bands, with a proportion of 80-90% quartz-rich, to 10-20% quartz poor.

Within the quartz-rich bands, quartz and feldspar grains are present with sizes ranging from 0.1 to 0.5 mm in diameter, 10% feldspar and 47% quartz. The remaining 40% of the quartz rich bands is composed of very fine-grained (>0.5mm diameter) quartz matrix and chlorite (approximately 20%). There are also rare tectonic micas and detrital zircons within this portion (<1%), as well as 1-2% opaque minerals.

Within the quartz poor bands there are large grains of quartz (30%), feldspar (10%), and opaques (5%). The grain size of these minerals is very close to those recorded in the quartz-rich portion. The remaining composition of these bands is matrix composed of 10-15% muscovite crystals ranging from clay sized up to 0.1mm and 20-25% clay minerals and 20-25% chlorite.

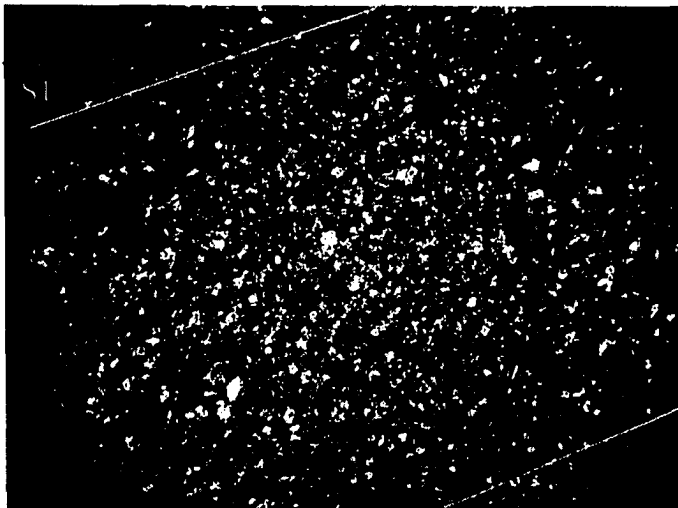


Photo taken under crossed polars. Quartz rich microlithon from the ENE to WSW with dissolution bands along the top and bottom of the field of view. S2 trends slightly counter-clockwise to the S1 dissolution bands.

5mm

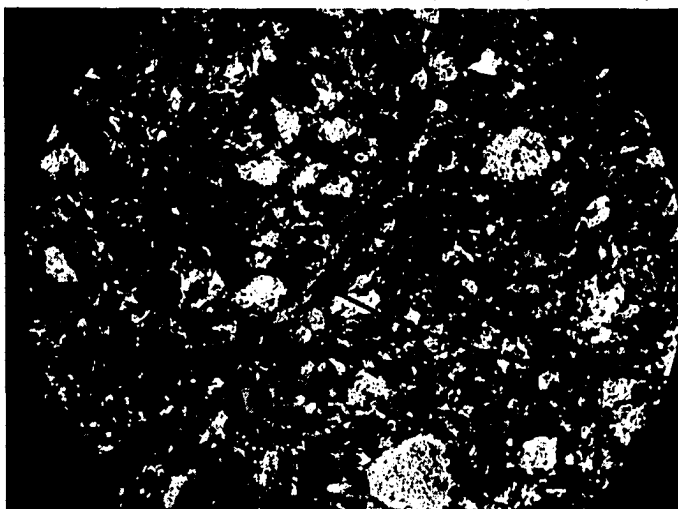


Photo taken under crossed polars. Field of view shows a portion of the quartz-rich portion of the sample with an example of a larger muscovite crystal.

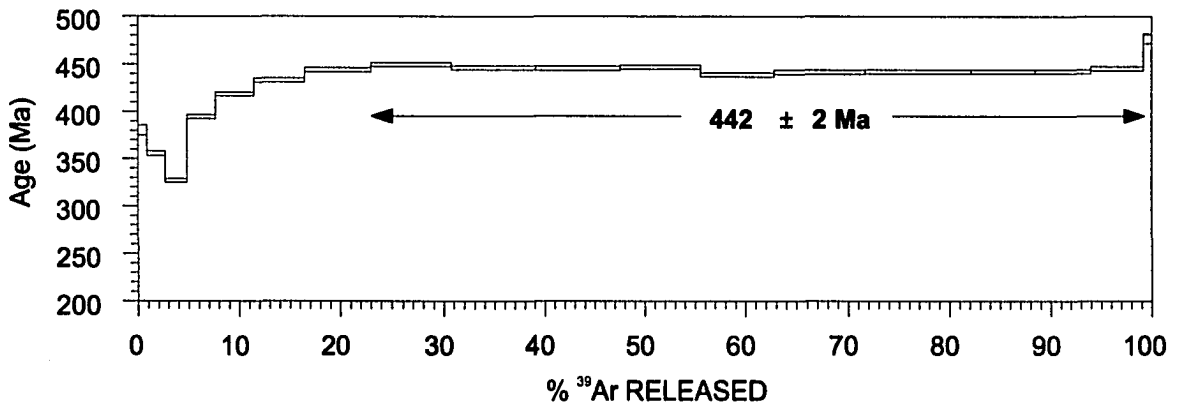
Muscovite crystals

1mm

### A.3.b Whole Rock Argon Summary

T°C	<sup>39</sup> Ar(mV)	<sup>39</sup> Ar(%)	AGE(Ma)±1σ	% ATM	<sup>37</sup> Ar/ <sup>39</sup> Ar	<sup>36</sup> Ar/ <sup>40</sup> Ar	<sup>39</sup> Ar/ <sup>40</sup> Ar	% IIC
450	27.7	0.8	380 ± 5	6.8	0.01	0.000231	0.009543	0
500	58.4	1.8	355 ± 2	2.6	0.02	0.000089	0.01074	0
525	68.4	2.1	326 ± 1	1	0.01	0.000033	0.01198	0
550	89.9	2.8	394 ± 2	0.5	0	0.000017	0.009789	0
575	122.9	3.8	418 ± 1	0.4	0	0.000014	0.009168	0
600	160.7	5	433 ± 2	0.3	0	0.000012	0.008829	0
625	210.4	6.5	444 ± 2	0.3	0	0.00001	0.008586	0
650	247.8	7.7	449 ± 2	3.1	0	0.000105	0.008228	0
675	266.5	8.3	446 ± 2	0.8	0	0.000028	0.008494	0
700	272.8	8.5	445 ± 2	0.2	0	0.00001	0.008552	0
725	256.8	8	447 ± 2	0.1	0	0.000006	0.008532	0
750	231.4	7.2	439 ± 2	0.1	0	0.000006	0.008709	0
800	284.5	8.8	441 ± 2	0.1	0	0.000006	0.008649	0
850	334.3	10.4	442 ± 2	0.6	0	0.00002	0.008602	0
900	203.8	6.3	442 ± 2	0.6	0.01	0.000023	0.008596	0
950	177.3	5.5	442 ± 2	1.4	0.01	0.000048	0.008528	0
1100	165.9	5.1	445 ± 2	3.5	0.08	0.00012	0.008279	0.01
1420	26.4	0.8	477 ± 4	19.9	1.93	0.000676	0.006352	0.24
J = .002405 ± .0000121								

### A.3.c Whole rock argon spectrum



## **A.4 JA083B**

### **A.4.a Description**

This sample is a strongly chloritic and micaceous siltstone. Quartz grains are dominantly  $< 0.1$  mm and make up approximately 20% of the sample. Rare feldspars are present ( $< 5\%$ ) as well as detrital zircons,  $\sim 0.005$  mm in diameter, composing less than 1% of the rock. The rest of the rock is composed of very fine-grained micas and unidentifiable clay minerals, mostly less than 0.01 mm in length. Bedding is indeterminate, partially due to the massive nature of the rock and partially due to obliteration by deformation. There is also discrete quartz veins in this thin section up to 3 mm wide.

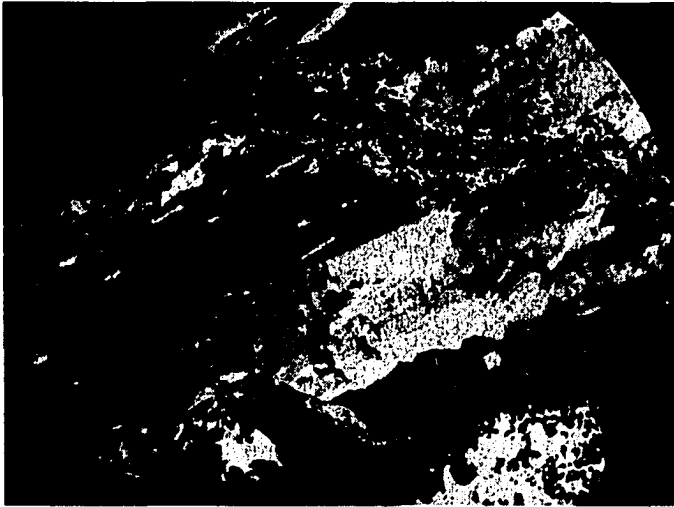


photo taken under crossed polars. This photo shows larger muscovite crystals associated with a thick quartz vein.

1mm

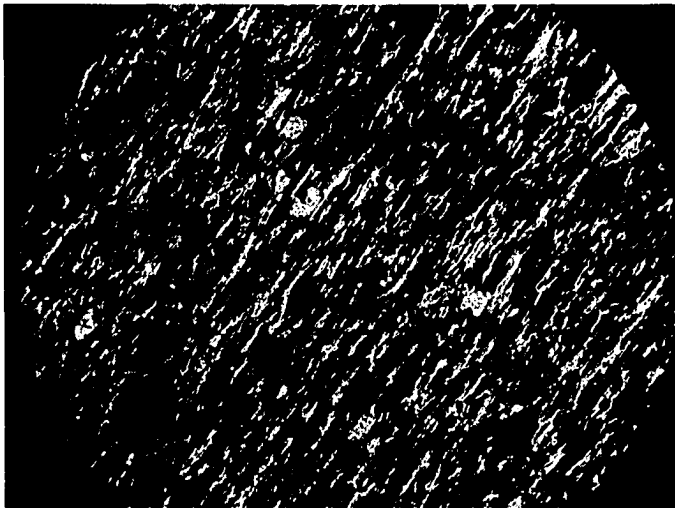


Photo taken under crossed polars. This photo shows a mica-rich fabric wrapping around opaques and sedimentary quartz grains.

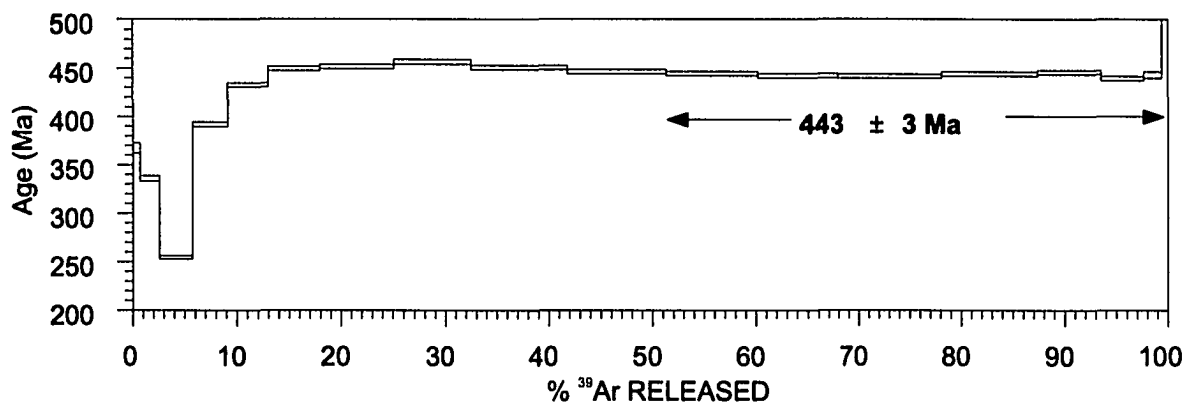
1mm

### A.4.b Whole Rock Argon Summary

T°C	<sup>39</sup> Ar(mV)	<sup>39</sup> Ar(%)	AGE(Ma)±1σ	% ATM	<sup>37</sup> Ar/ <sup>39</sup> Ar	<sup>36</sup> Ar/ <sup>40</sup> Ar	<sup>39</sup> Ar/ <sup>40</sup> Ar	% IIC
450	12.2	0.6	367 ± 5	5.2	0.02	0.000178	0.01009	0
500	34.4	1.9	335 ± 2	2.4	0.02	0.000082	0.011468	0
525	57.2	3.1	254 ± 1	1.2	0.01	0.000041	0.015679	0
550	61	3.3	392 ± 2	0.6	0	0.000022	0.009845	0
575	69.8	3.8	432 ± 2	0.4	0	0.000015	0.008836	0
600	90.1	4.9	449 ± 2	0.6	0	0.000021	0.008442	0
625	130.2	7.1	451 ± 2	0.6	0	0.00002	0.0084	0
650	133.4	7.3	456 ± 2	8.7	0	0.000294	0.007625	0
675	168	9.2	450 ± 2	1.4	0	0.000048	0.008354	0
700	171.9	9.5	446 ± 2	0.6	0	0.000021	0.00851	0
725	160.8	8.8	444 ± 2	0.4	0	0.000015	0.00857	0
750	139.1	7.6	442 ± 2	0.4	0	0.000016	0.008619	0
800	184.5	10.1	441 ± 2	0.6	0	0.000023	0.008611	0
850	168.4	9.3	444 ± 2	1.9	0	0.000065	0.008449	0
900	110.5	6.1	445 ± 2	1.8	0.01	0.000063	0.008422	0
950	74.8	4.1	439 ± 2	1.5	0.03	0.000053	0.00858	0
1100	31.2	1.7	443 ± 3	10	0.34	0.000341	0.007763	0.04
1420	10.8	0.5	536 ± 11	32.7	2.21	0.001107	0.004672	0.25

J = .002406 ± .0000121

### A.4.c Whole rock argon spectrum



## ***A.5 JA023B***

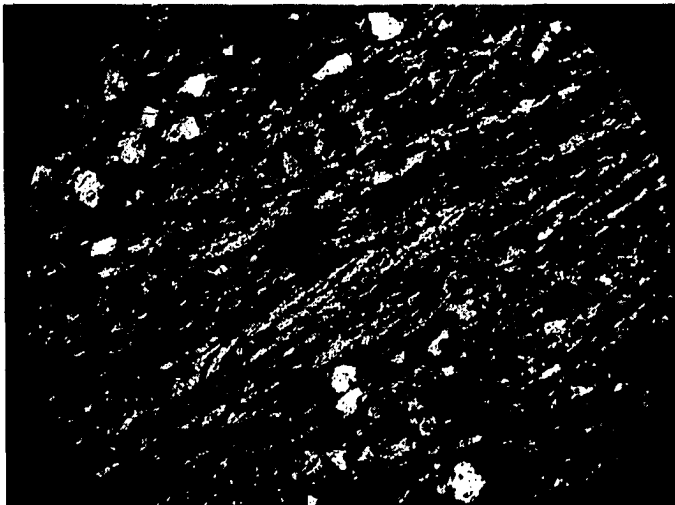
### **A.5.a Description**

This sample is a laminated green slate. 30% of the sample is composed of quartz grains, 5% feldspar grains, and 5% opaques. The remaining 60% is fine-grained matrix composed dominantly of clay minerals and micas.



This photo was taken under crossed polars. This photo shows the distinction between portions of well developed fabric and less well developed.

1mm



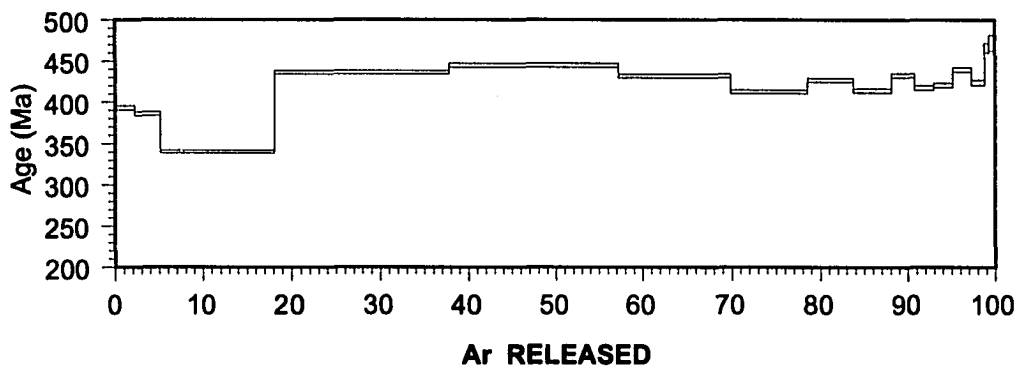
This photo was taken under crossed polars. This illustrates the very fine grained mica fabric developed in the sample.

1mm

### A.5.b Whole Rock Argon Summary

T°C	<sup>39</sup> Ar(mV)	<sup>39</sup> Ar(%)	AGE(Ma)±1σ	% ATM	<sup>37</sup> Ar/ <sup>39</sup> Ar	<sup>36</sup> Ar/ <sup>40</sup> Ar	<sup>39</sup> Ar/ <sup>40</sup> Ar	% IIC
450	55.7	2.2	392 ± 2	7.8	0	0.000266	0.009131	0
500	73.5	2.9	385 ± 2	2.4	0	0.000081	0.009869	0
550	325.6	12.9	340 ± 1	1	0.01	0.000037	0.011486	0
600	494.7	19.7	436 ± 2	0.4	0	0.000014	0.00878	0
650	487.8	19.4	444 ± 2	4.1	0	0.000139	0.008271	0
700	318.1	12.6	431 ± 2	0.7	0	0.000024	0.008854	0
750	217.8	8.6	412 ± 2	0.6	0	0.00002	0.009331	0
800	130.5	5.1	426 ± 2	0.6	0.01	0.000021	0.008978	0
850	108.5	4.3	414 ± 2	0.8	0.01	0.000028	0.009272	0
875	66	2.6	432 ± 2	1.1	0.02	0.000037	0.008805	0
900	55.8	2.2	417 ± 2	1.4	0.03	0.000047	0.00913	0
925	54.1	2.1	420 ± 2	1.8	0.05	0.000061	0.009025	0
950	53.7	2.1	439 ± 2	2.4	0.1	0.000084	0.008527	0.01
1000	37.7	1.5	423 ± 3	5.8	0.28	0.000198	0.008574	0.03
1100	14.5	0.5	465 ± 5	11.3	1.16	0.000385	0.007256	0.14
1450	16.1	0.6	472 ± 9	48.6	2.73	0.001645	0.004141	0.34
TOTAL GAS AGE = 418.7 ± 4 Ma								
J = .002413 ± 2.413E-05								

### A.5.c Whole rock argon spectrum



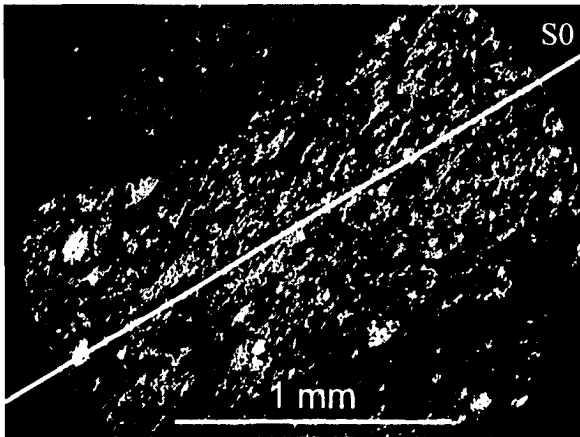
## A.6 JA082A

### A.6.a Description

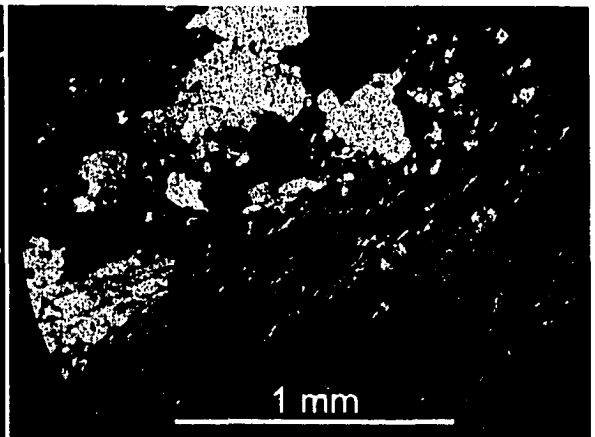
This sample is a laminated green slate. In thin section, the dark laminations are slightly coarser grained and contain more quartz grains (20%) than the slate (1-2%). Quartz grains within beds are 0.05 to 0.3 mm in diameter and always smaller than 0.3 mm in the fine-grained portions. There is some chlorite present, as well as rare detrital zircon.

The fine-grained material in this rock is impossible to identify optically. It has a faint extinction parallel to bedding, interpreted as due to the orientation of detrital clay minerals, with perhaps some extremely small mica.

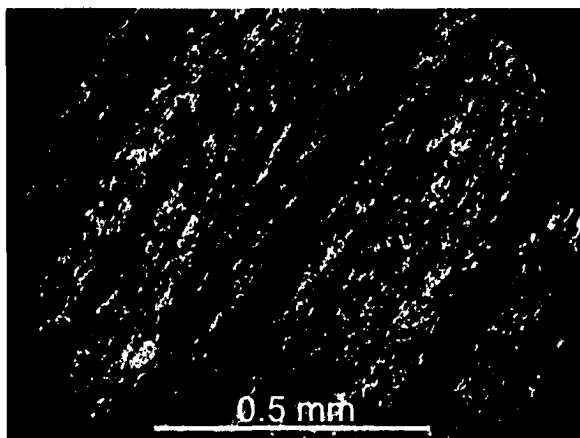
The bed parallel fabric is quite poor, most likely a detrital orientation rather than S1. The S2 crenulation fabric is penetrative in this sample and deflects bedding and bed parallel clay minerals. There also is a certain amount of dissolution along S2 as the coarser laminations are often offset along S2 planes. The finer grained material shows a simple crenulation rather than dissolution. Quartz fibres elongate in the S2 direction are present in the strain shadows associated with pyrite nodules.



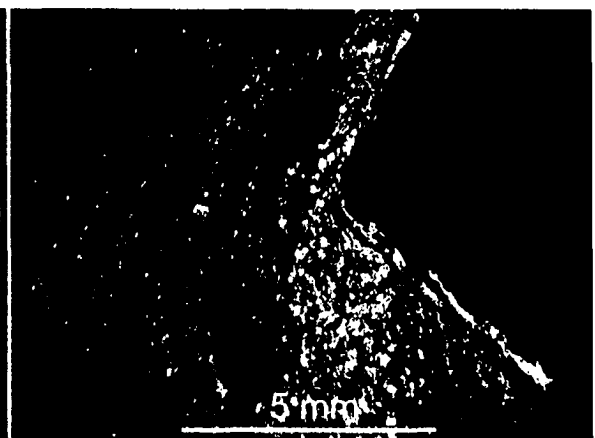
Thin section photo of bedding and S2 under crossed polars.



Thin section photo with crossed polars showing larger muscovite crystals developing associated with a quartz vein.



Thin section photo under crossed polars showing the muscovite developing along microscopic crenulation fabric

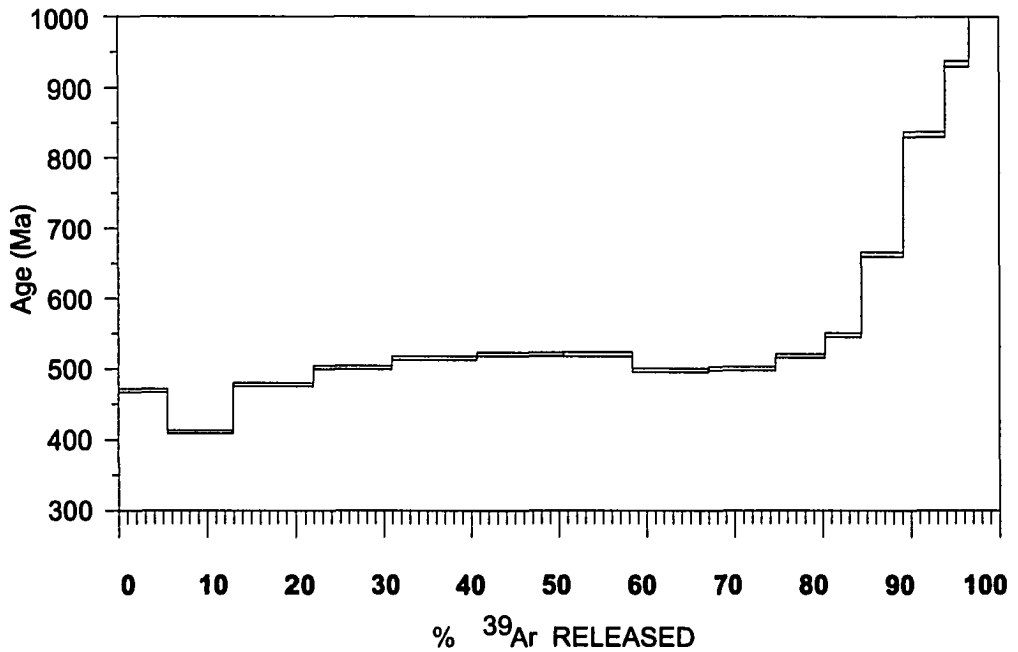


Thin section photo under plane polarized light showing the deflection of the fine crenulations around a pyrite margin

### A.6.b Whole Rock Argon Summary

T°C	<sup>39</sup> Ar(mV)	<sup>39</sup> Ar(%)	AGE (Ma)±1σ	% ATM	<sup>37</sup> Ar/ <sup>39</sup> Ar	<sup>36</sup> Ar/ <sup>40</sup> Ar	<sup>39</sup> Ar/ <sup>40</sup> Ar	% IIC
450	34	1.4	421 ± 2	4.8	0.01	0.000164	0.00867	0
500	53.7	2.2	381 ± 2	1.7	0.01	0.000058	0.009999	0
525	76.8	3.2	313 ± 1	0.7	0.01	0.000023	0.012533	0
550	269.9	11.2	365 ± 1	0.5	0.01	0.000017	0.010606	0
575	221.7	9.2	451 ± 2	0.3	0	0.00001	0.008405	0
600	258	10.7	471 ± 2	0.4	0	0.000014	0.007981	0
625	277.8	11.6	484 ± 2	0.5	0	0.000017	0.007748	0
650	300	12.5	483 ± 2	3	0	0.000104	0.007555	0
675	201.2	8.4	475 ± 2	0.6	0	0.000022	0.007903	0
700	176.5	7.3	459 ± 2	0.5	0	0.00002	0.008206	0
750	169.9	7.1	458 ± 2	0.6	0.01	0.000021	0.008241	0
800	116.8	4.8	460 ± 2	2.8	0.01	0.000095	0.008014	0
850	72.8	3	463 ± 2	2	0.02	0.000067	0.008014	0
900	59.7	2.4	465 ± 2	1.9	0.04	0.000067	0.00799	0
950	44.4	1.8	463 ± 2	5.2	0.09	0.000178	0.007745	0.01
1000	32	1.3	476 ± 4	13.8	0.21	0.000469	0.006831	0.02
1100	17.7	0.7	458 ± 5	14.1	2	0.000478	0.007116	0.25
1450	7.5	0.3	470 ± 13	53	4.71	0.001796	0.003772	0.59
TOTAL GAS AGE = 450.9 ± 4.1 Ma								
J = .002398 ± 2.398E-05								

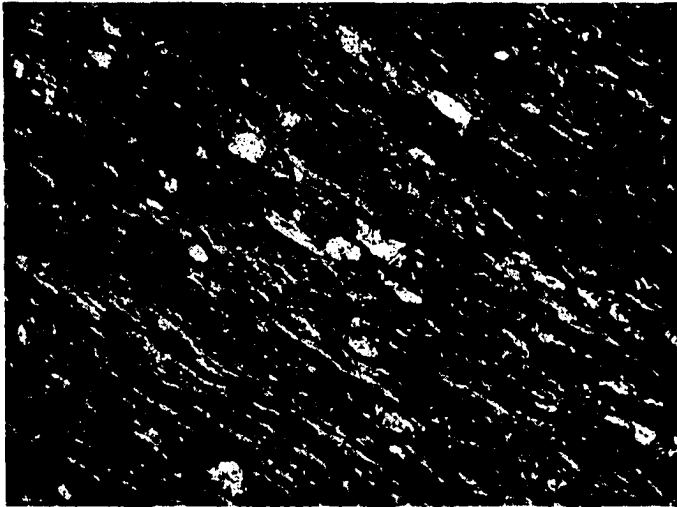
### A.6.c Whole rock argon spectrum



## A.7 GQ112A

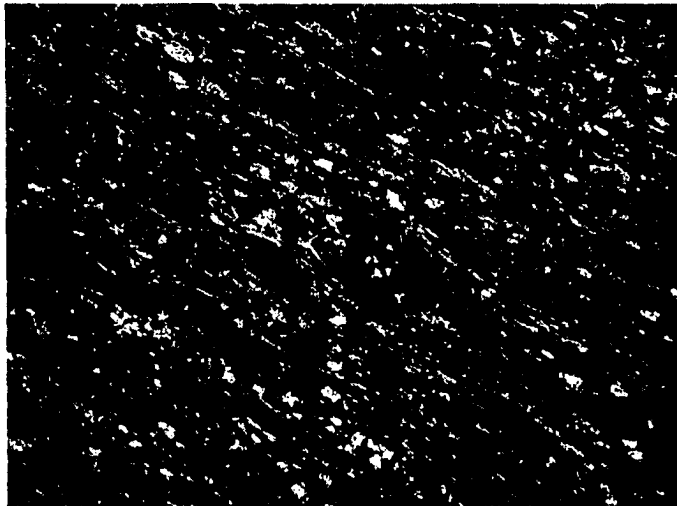
### A.7.a Description

This sample is a red and green slate. It is very poorly sorted and contains angular-subangular grains of many minerals, 0.03-0.05 mm in diameter. The main grain components are: 15% quartz grains, 10% opaques, <1% zircon, <2% detrital muscovite, and 5% chlorite. The remaining ~80% of the sample is very fine-grained matrix.



Thin section photo under crossed polars and high magnification .  
Strong, very fine-grained, oriented muscovite fabric interpreted as S2

0.25mm



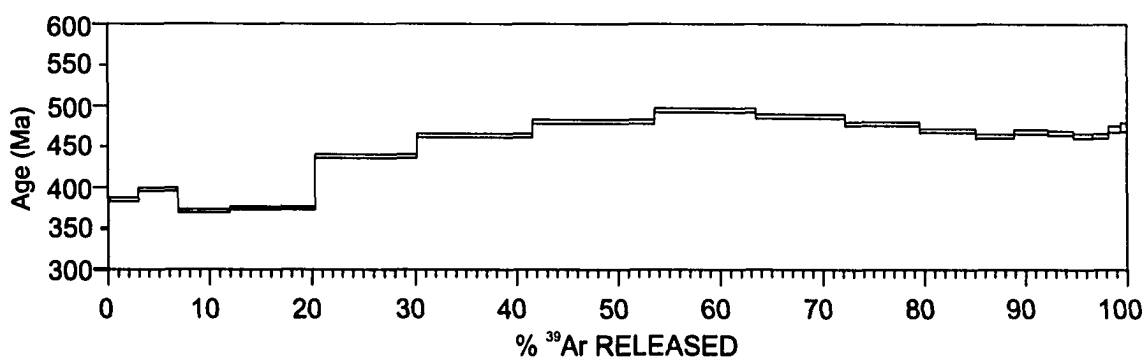
Thin section photo under crossed polars. This thin section shows deflection of the S2 fabric around a more competent portion of the original rock.

0.5mm

### A.7.b Whole Rock Argon Summary

T°C	<sup>39</sup> Ar(mV)	<sup>39</sup> Ar(%)	AGE (Ma)±1σ	% ATM	<sup>37</sup> Ar/ <sup>39</sup> Ar	<sup>36</sup> Ar/ <sup>40</sup> Ar	<sup>39</sup> Ar/ <sup>40</sup> Ar	% IIC
450	73.8	2.9	385 ± 2	4.2	0.01	0.000143	0.009687	0
500	97.1	3.8	397 ± 2	0.8	0.01	0.000027	0.009685	0
525	128.2	5.1	371 ± 1	0.2	0.01	0.000009	0.010503	0
550	210	8.3	374 ± 1	0.1	0.01	0.000006	0.010405	0
575	247.2	9.8	438 ± 2	0.1	0.01	0.000004	0.008747	0
600	285.8	11.4	463 ± 2	0.1	0.01	0.000005	0.008205	0
625	300.3	11.9	480 ± 2	0.2	0.01	0.000009	0.007868	0
650	247.8	9.8	494 ± 2	1.8	0	0.000061	0.007497	0
675	219.2	8.7	487 ± 2	0.9	0	0.000032	0.007689	0
700	183.2	7.3	478 ± 2	0.4	0	0.000015	0.007902	0
725	140.1	5.5	469 ± 2	0.4	0.01	0.000016	0.008058	0
750	96.1	3.8	463 ± 2	0.4	0.01	0.000016	0.008191	0
800	83.1	3.3	468 ± 2	3.6	0.02	0.000123	0.007827	0
850	62.3	2.4	466 ± 2	1.5	0.03	0.000054	0.008028	0
900	47.2	1.8	463 ± 2	4.4	0.08	0.000149	0.007855	0.01
950	40	1.5	463 ± 2	5.2	0.13	0.000176	0.007792	0.01
1100	28.6	1.1	471 ± 3	14.7	0.77	0.0005	0.006865	0.09
1450	16.3	0.6	474 ± 5	18.2	2.43	0.000617	0.006549	0.3
TOTAL GAS AGE = 453.4 ± 4.1 Ma								
J = .002409 ± 2.409E-05								

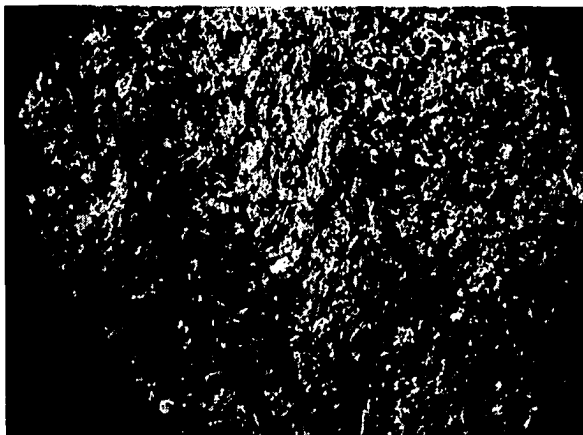
### A.7.c Whole rock argon spectrum



## A.8 HV002A

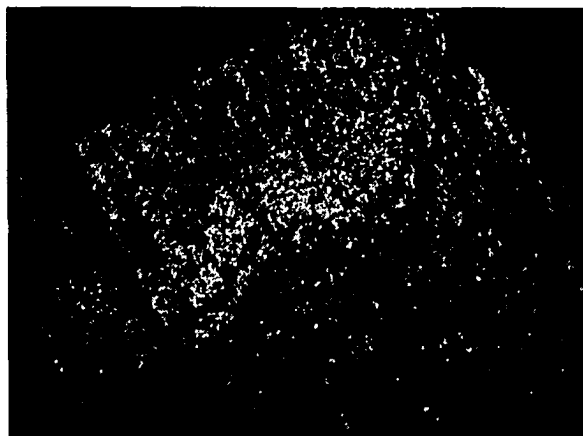
### A.8.a Description

This is a strongly cleaved grey-green slate. Individual beds are composed of up to 75% quartz grains ranging from 0.05-0.1 mm in diameter. Finer laminations commonly show less than 20% detrital quartz grains. Other detrital grains include 5% chlorite and rare zircon. This is a very micaceous sample, consisting of 60-80% clay and mica minerals. There are thin (<1 mm thick) quartz veins present parallel to both the bedding and the foliation.



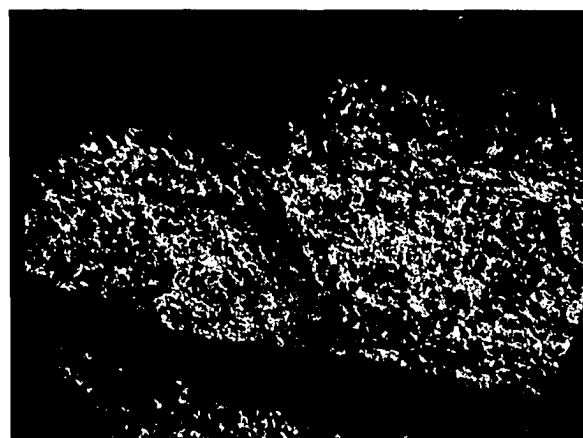
Thin section photo under crossed polars. This thin section shows bed parallel micas interpreted as S1, as well as a strong crenulation interpreted as S2. The crenulation varies from simple to stylolitic in this photo.

1 mm



Thin section photo under crossed polars. This thin section shows the folded bedding in this sample as well as fine axial planar crenulation

1 mm



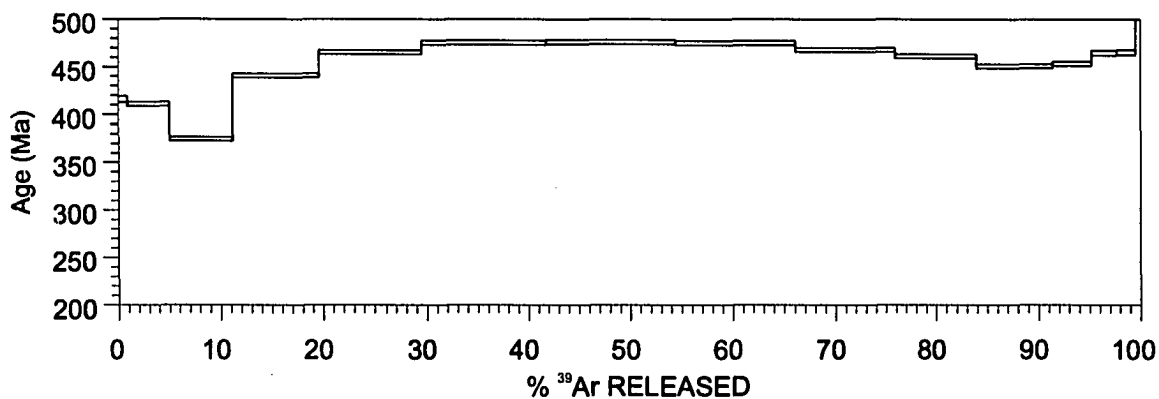
Thin section photo under cross polars. This thin section shows both the muscovite parallel to the folded S1 fabric and the muscovite parallel to the S2 crenulation cleavage.

1 mm

### A.8.b Whole Rock Argon Summary

T°C	<sup>39</sup> Ar(mV)	<sup>39</sup> Ar(%)	AGE(Ma)±1σ	% ATM	<sup>37</sup> Ar/ <sup>39</sup> Ar	<sup>36</sup> Ar/ <sup>40</sup> Ar	<sup>39</sup> Ar/ <sup>40</sup> Ar	% IIC
450	25.2	0.8	415 ± 3	3.7	0.01	0.000128	0.008905	0
500	121.7	4.1	410 ± 2	1.8	0.01	0.000064	0.009206	0
525	182.3	6.1	374 ± 1	0.7	0.01	0.000026	0.010312	0
550	248.7	8.4	440 ± 2	0.3	0	0.000012	0.008643	0
575	292.3	9.9	465 ± 2	0.2	0	0.000008	0.008139	0
600	363	12.2	475 ± 2	0.2	0	0.000008	0.007939	0
625	373.9	12.6	476 ± 2	0.3	0	0.00001	0.007921	0
650	343.2	11.6	475 ± 2	1.6	0	0.000056	0.007832	0
675	291.9	9.8	467 ± 2	0.6	0	0.000022	0.008051	0
700	235.6	7.9	461 ± 2	0.4	0	0.000014	0.008204	0
750	220.8	7.4	450 ± 2	0.5	0	0.000019	0.008407	0
800	112.4	3.8	453 ± 2	1.3	0.01	0.000046	0.008285	0
850	72.7	2.4	464 ± 2	2.6	0.03	0.000091	0.007948	0
900	53.5	1.8	465 ± 2	3.6	0.07	0.000124	0.007858	0
1450	14.8	0.5	526 ± 5	21.8	1.62	0.00074	0.005536	0.19
TOTAL GAS AGE = 457.6 ± 4.2 Ma								
J = .002401 ± 2.401E-05								

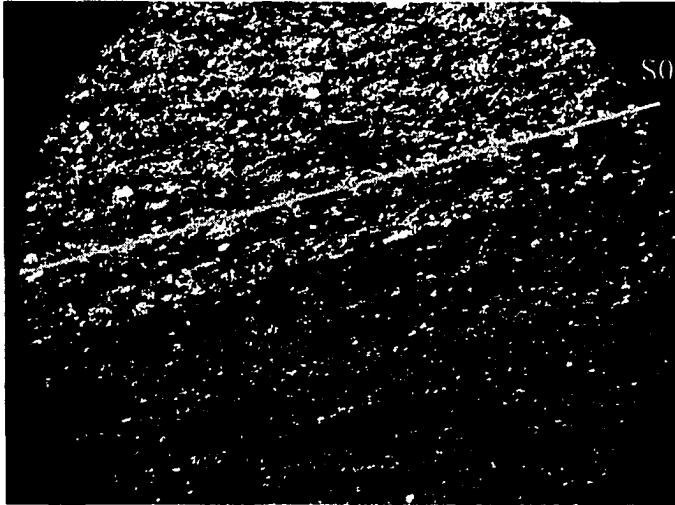
### A.8.c Whole rock argon spectrum



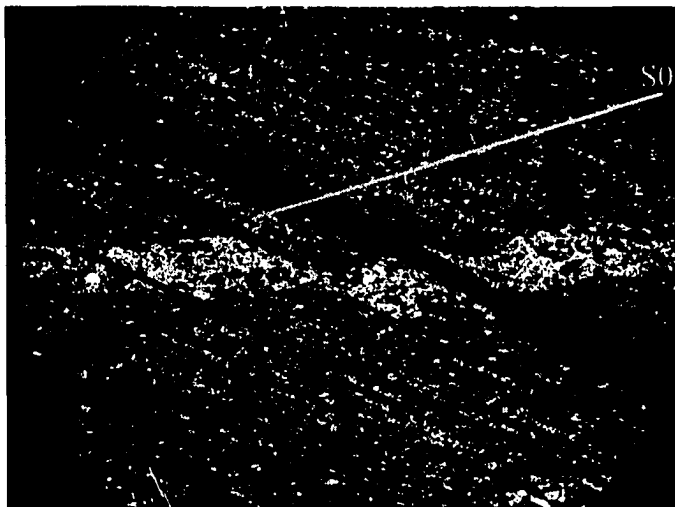
## ***A.9 HV123A***

### **A.9.a Description**

This sample is a green slate. A coarser grained bed 1 cm thick occurs within the thin section. Mineralogy within the bed is 40% quartz grains up to 0.2mm in diameter, 55% clay sized matrix, 2% chlorite, <1% muscovite grains, <1% zircon, 3-5% opaques. Finer grained beds have approximately 20% grains to 80% matrix.



Thin section photo taken under crossed polars. Planar bedding is shown as well as S2 slightly clockwise to it.

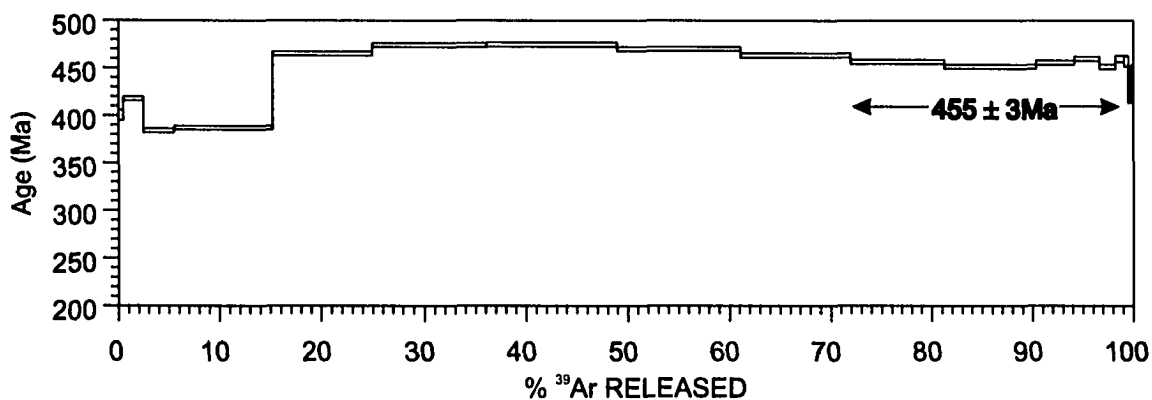


Thin section photo taken under crossed polars. S2 is observed to significantly offset bedding in this photo. Elsewhere total bed separation is achieved. Separation is due to pressure solution associated with crenulation.

### A.9.b Whole Rock Argon Summary

T°C	<sup>39</sup> Ar(mV)	<sup>39</sup> Ar(%)	AGE(Ma)±1σ	% ATM	<sup>37</sup> Ar/ <sup>39</sup> Ar	<sup>36</sup> Ar/ <sup>40</sup> Ar	<sup>39</sup> Ar/ <sup>40</sup> Ar	% IIC
450	17	0.4	400 ± 5	1.1	0	0.000037	0.009593	0
500	71.3	1.9	417 ± 2	0.7	0	0.000026	0.009175	0
525	110.8	3	384 ± 1	0.5	0	0.000018	0.010097	0
550	349.1	9.6	387 ± 1	0.3	0	0.000013	0.01003	0
575	350.8	9.7	465 ± 2	0.2	0	0.000007	0.008173	0
600	401.8	11.1	474 ± 2	0.2	0	0.000008	0.007995	0
625	462.7	12.8	474 ± 2	0.3	0	0.00001	0.007979	0
650	438.9	12.1	470 ± 2	1.3	0	0.000046	0.007981	0
675	390.3	10.8	463 ± 2	0.4	0	0.000015	0.008192	0
700	335.1	9.2	456 ± 2	0.4	0	0.000015	0.008329	0
750	327.9	9	451 ± 2	0.5	0	0.000019	0.008427	0
800	136.8	3.7	455 ± 2	1.6	0.01	0.000055	0.008248	0
850	90.7	2.5	459 ± 2	1.7	0.02	0.00006	0.008157	0
900	56.2	1.5	451 ± 2	2.9	0.05	0.0001	0.008226	0
950	31.5	0.8	459 ± 3	6.6	0.11	0.000223	0.007753	0.01
1000	14.9	0.4	457 ± 5	12.8	0.31	0.000433	0.007283	0.04
1100	10.3	0.2	421 ± 8	25.3	1.4	0.000857	0.006827	0.18
1450	7.8	0.2	439 ± 14	50	2.87	0.001695	0.004364	0.37
TOTAL GAS AGE = 454 ± 4 Ma								
J = .00241 ± .0000121								

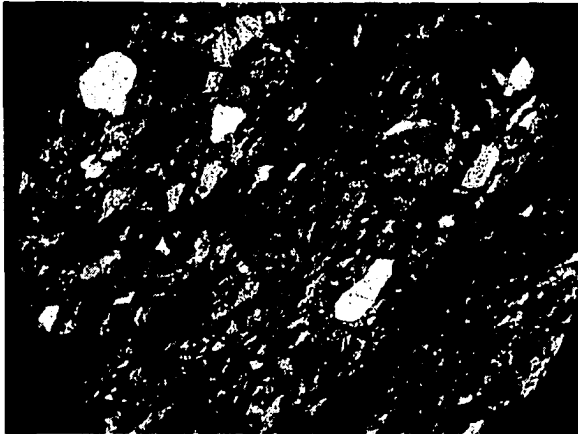
### A.9.c Whole rock argon spectrum



## A.10 HV134A

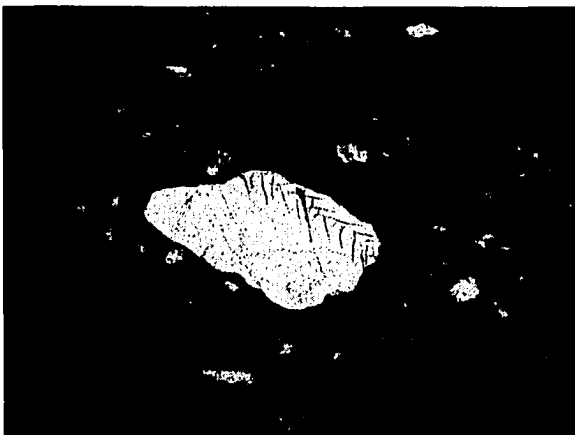
### A.10.a Description

This sample is a slate of the Summerside formation. Sedimentary detrital grains compose 40-50% of the sample, clay sized matrix and a muddy fabric compose the rest of the sample. The grains range from 0.05 mm to 0.75 mm (mud to coarse sand) and are rounded to subrounded. 35-40% of the grains are quartz; 10% are twinned feldspars, some of which show partial degradation, as a result of weathering or alteration processes; and 5-10 percent are detrital muscovite and chlorite. There is a large vein in this sample composed of 75-80% sugary textured chlorite, 20% quartz, and minor calcite.



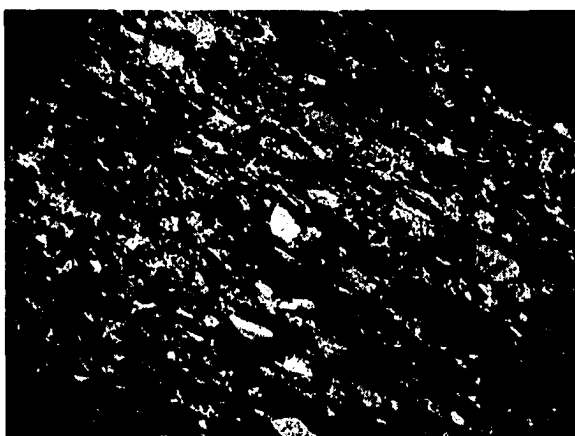
Thin section photo under crossed polars showing the detrital nature of this sample. However, there is a fabric present in this slightly coarser grained rock (top right to bottom left). This fabric is interpreted as S2.

1mm



Thin section photo under crossed polars. The S2 fabric is shown in this sample. slight dissolution of the larger quartz clast is observed on the upper boundary.

1mm



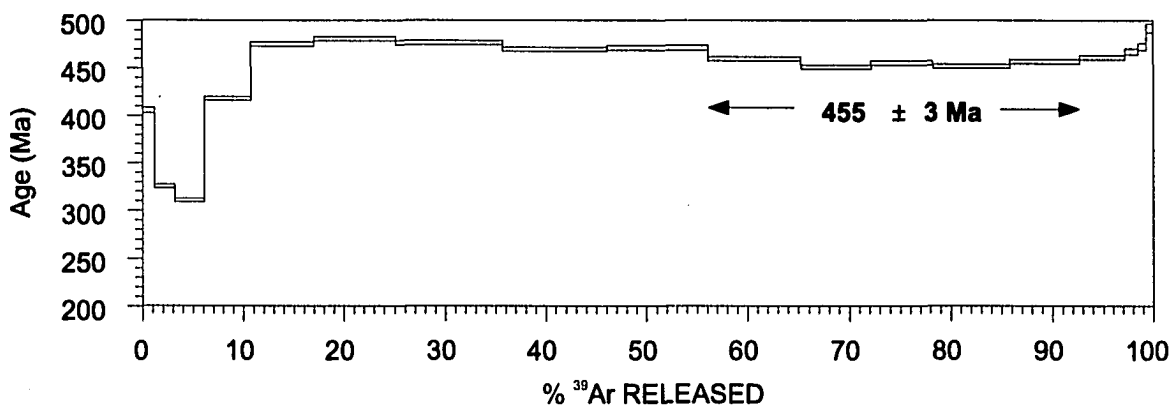
Thin section photo under crossed polars. This photo shows the S2 fabric in this sample. However, at this slightly higher magnification the highly birefringent oriented nature of the matrix of this sample is apparent.

0.5 mm

### A.10.b Whole Rock Argon Summary

T°C	<sup>39</sup> Ar(mV)	<sup>39</sup> Ar(%)	AGE(Ma)±1σ	% ATM	<sup>37</sup> Ar/ <sup>39</sup> Ar	<sup>36</sup> Ar/ <sup>40</sup> Ar	<sup>39</sup> Ar/ <sup>40</sup> Ar	% IIC
450	42.2	1.1	405 ± 2	10.6	0	0.000359	0.008516	0
500	75.3	2	324 ± 1	5.9	0	0.0002	0.011433	0
525	110	2.9	310 ± 1	2.5	0	0.000086	0.012454	0
550	171.3	4.6	417 ± 1	1.1	0	0.000039	0.0091	0
575	236.2	6.3	475 ± 2	0.5	0	0.000017	0.007921	0
600	300.6	8	480 ± 2	0.2	0	0.000009	0.00783	0
625	394.5	10.5	476 ± 2	0.2	0	0.000009	0.007911	0
650	386.8	10.3	469 ± 2	0.2	0	0.000007	0.008048	0
675	372.6	10	471 ± 2	3	0	0.000103	0.00779	0
700	340.9	9.1	459 ± 2	0.2	0	0.000009	0.008246	0
725	256.2	6.8	450 ± 2	0.2	0	0.000007	0.008431	0
750	226.5	6	454 ± 2	0.2	0	0.000007	0.008343	0
800	282.8	7.5	451 ± 2	0.3	0	0.000013	0.008398	0
850	256.7	6.8	456 ± 2	0.6	0.01	0.00002	0.008274	0
900	166.7	4.4	460 ± 2	1.3	0.03	0.000045	0.008128	0
950	49.1	1.3	467 ± 2	5.5	0.23	0.000186	0.007665	0.03
1100	30.7	0.8	472 ± 3	14.1	0.49	0.000478	0.00688	0.06
1450	24.9	0.6	492 ± 4	18	0.97	0.000611	0.006266	0.11
TOTAL GAS AGE = 454 ± 4 Ma								
J = .002399 ± .000012								

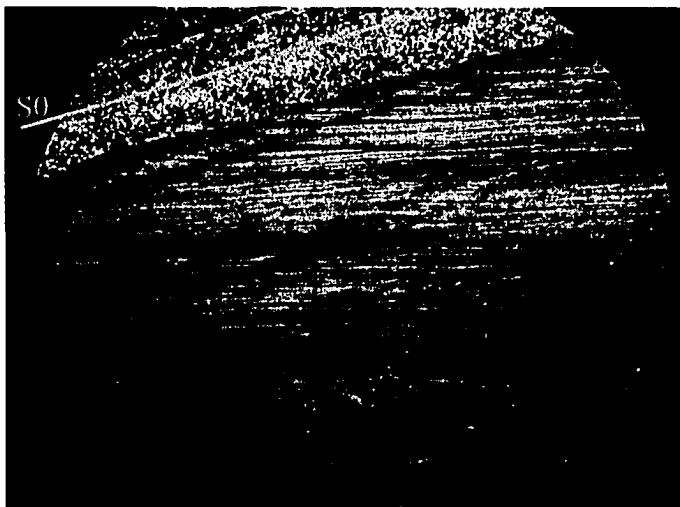
### A.10.c Whole rock argon spectrum



## **A.11 HY056A**

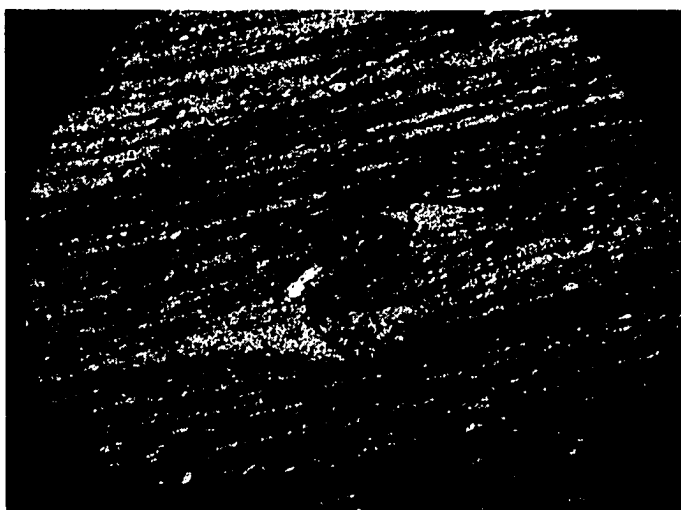
### **A.11.a Description**

This sample is a green slate. There is a single set of laminations in this thin section that are composed mainly of quartz grains averaging 0.01 mm in diameter. The majority of the sample, though, is very fine-grained. Bulk extinction and high birefringence indicate that the fine-grained portion of the thin section is relatively high in aligned muscovite and/or clay minerals. There is < 5% identifiable chlorite in slightly larger grains as well as some very fine chlorite, interpreted on the basis of the green colour of the section under plane polarized light.



Thin section photo under crossed polars. This thin section shows the bedding and across cutting fabric interpreted as S2.

5 mm



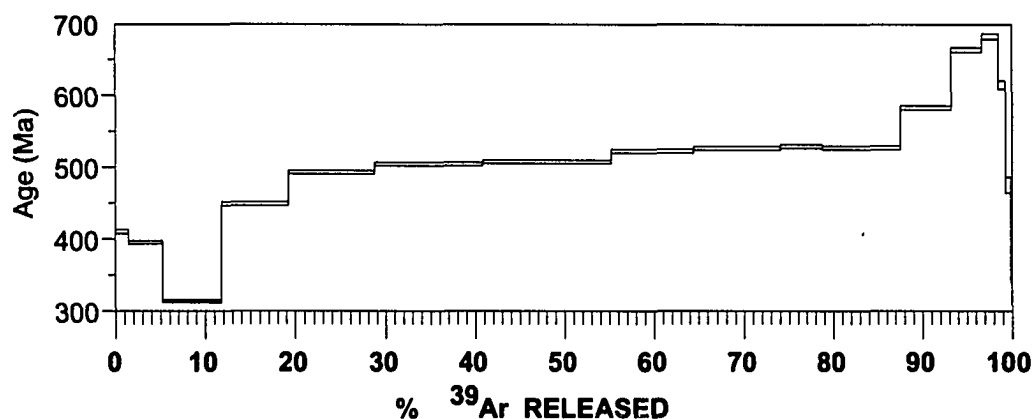
Thin section photo under plane polarized light. Deflection around a competent piece of the fine grained matrix indicates some shortening attributed to the development of this S2 fabric.

0.5 mm

### A.11.b Whole Rock Argon Summary

T°C	<sup>39</sup> Ar(mV)	<sup>39</sup> Ar(%)	AGE(Ma)±1σ	% ATM	<sup>37</sup> Ar/ <sup>39</sup> Ar	<sup>36</sup> Ar/ <sup>40</sup> Ar	<sup>39</sup> Ar/ <sup>40</sup> Ar	% HC
450	31.1	1.4	410 ± 2	2.8	0	0.000097	0.009161	0
500	83.6	3.8	395 ± 1	1.4	0	0.000049	0.009686	0
525	143.1	6.5	313 ± 1	0.8	0	0.000028	0.012574	0
550	161.2	7.4	448 ± 2	0.3	0	0.00001	0.008495	0
575	206.1	9.4	492 ± 2	0.2	0	0.000008	0.007648	0
600	264	12.1	504 ± 2	0.2	0	0.000009	0.007447	0
625	313.3	14.3	507 ± 2	0.2	0	0.000009	0.007392	0
675	200.6	9.2	522 ± 2	0.5	0	0.000017	0.007134	0
700	209	9.5	526 ± 2	0.3	0	0.000011	0.007085	0
700	103.3	4.7	528 ± 2	0.3	0	0.000012	0.007038	0
750	191.1	8.7	526 ± 2	0.3	0	0.000011	0.007075	0
800	123.2	5.6	582 ± 2	0.5	0	0.000018	0.006281	0
850	76.1	3.4	663 ± 3	1.6	0.01	0.000054	0.005325	0
900	39.7	1.8	682 ± 3	2.3	0.03	0.000079	0.005112	0
950	16.1	0.7	614 ± 5	8	0.12	0.000273	0.005454	0.01
1100	13.1	0.6	475 ± 10	35.4	0.96	0.001199	0.005158	0.12
1420	2.5	0.1	374 ± 34	46.8	1.44	0.001586	0.005534	0.2
TOTAL GAS AGE = 503.5 ± 4.6 Ma								
J = .002408 ± 2.408E-05								

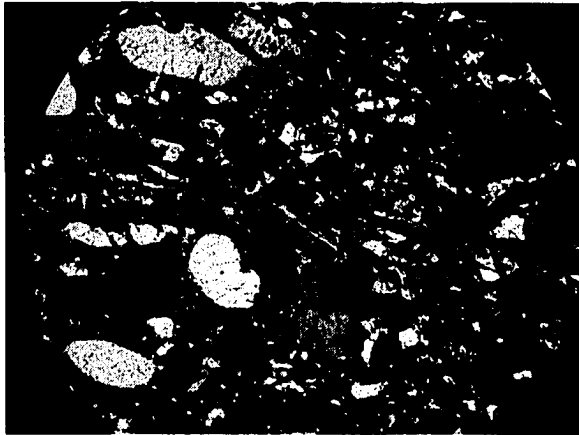
### A.11.c Whole rock argon spectrum



## A.12 HQ092A

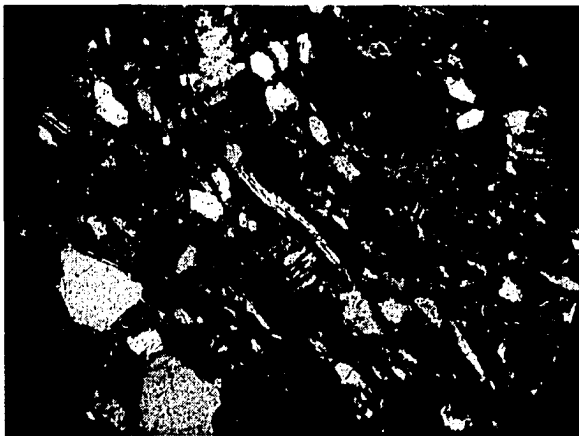
### A.12.a Description

This is a poorly sorted medium sandstone with subangular to rounded clasts. The grain size variation is from 0.1 to 1.8 mm (fine sand to granule). The rock consists of 50-60% quartz, 2-5% feldspar, 2% chlorite, and 2% muscovite. The matrix (30%) is composed of very fine-grained mica and clay. Most of the clasts in this rock have irregular dissolved-looking boundaries.



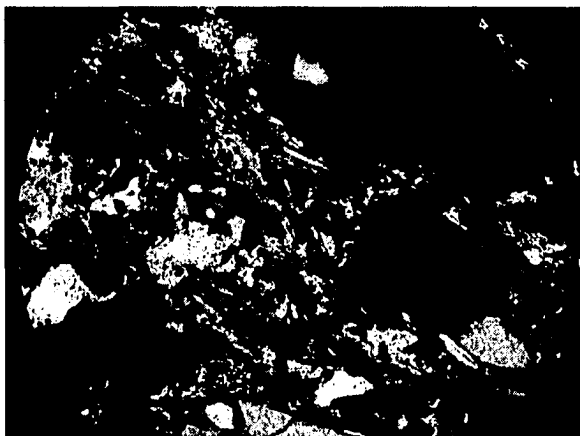
Thin section photo under crossed polars. this thin section shows a mixture of opaques, quartz, chlorite, and matrix, that have a very poorly sorted detrital texture.

1mm



Thin section photo under crossed polars. This shows a large muscovite crystal that appears to be detrital.

1mm



Thin section photo under crossed polars. This thin section is at slightly higher magnification and shows more very fine grained micas in the matrix and surrounding large clasts. It is difficult to determine if these are tectonic or sedimentary. It is very possibly that they have been simply reoriented rather than crystallized during deformation.

0.5 mm

### A.12.b Whole Rock Argon Summary

T°C	<sup>39</sup> Ar(mV)	<sup>39</sup> Ar(%)	AGE(Ma)±1σ	% ATM	<sup>37</sup> Ar/ <sup>39</sup> Ar	<sup>36</sup> Ar/ <sup>40</sup> Ar	<sup>39</sup> Ar/ <sup>40</sup> Ar	% IIC
500	79.1	5.5	468 ± 2	0.8	0	0.000029	0.008022	0
525	107.4	7.4	410 ± 2	0.4	0	0.000015	0.009358	0
550	129.1	8.9	477 ± 2	0.2	0	0.000008	0.007903	0
575	129.2	8.9	501 ± 2	0.1	0	0.000006	0.007476	0
600	140.2	9.7	515 ± 2	0.3	0	0.000011	0.007248	0
625	141.4	9.8	520 ± 2	0.3	0	0.000011	0.007163	0
650	113.1	7.8	520 ± 2	9.8	0	0.000333	0.006477	0
675	123.7	8.6	497 ± 2	0.8	0	0.000028	0.007495	0
700	110.3	7.6	500 ± 2	0.4	0	0.000013	0.007488	0
725	80.6	5.6	518 ± 2	0.4	0	0.000013	0.007189	0
750	59.5	4.1	547 ± 2	0.4	0	0.000013	0.006742	0
800	68.6	4.7	662 ± 3	0.4	0	0.000016	0.005385	0
850	67.5	4.6	833 ± 3	0.7	0.01	0.000025	0.00406	0
900	39.7	2.7	933 ± 4	1.1	0.02	0.00004	0.003504	0
950	23	1.6	1011 ± 6	2.1	0.06	0.000071	0.003126	0
1100	18.7	1.3	1038 ± 6	5	0.35	0.00017	0.002931	0.03
1420	6.4	0.4	2047 ± 18	22.3	1.12	0.000757	0.000883	0.08
TOTAL GAS AGE = 564.2 ± 5 Ma								
J = .002403 ± 2.403E-05								

### A.12.c Whole rock argon spectrum

